ETHANOL INHIBITION OF CONTINUOUS ANAEROBIC YEAST GROWTH

BY

GERHARD KLAUS HOPPE

Submitted to the University of Cape Town in fulfillment of the requirements for the degree of Master of Science in Engineering.

August 1981

ABSTRACT

The growing interest in fermentation and fermentation technology as a means to produce chemicals has led to the investigation of different aspects of many fermentations. In this work, the inhibitory effects of the product ethanol on the yeast Saccharomyces cerevisiae ATCC 4126 have been studied during the conversion of the substrate glucose.

Continuous culture techniques under anaerobic conditions (the medium was not deaerated) were used where high concentrations of ethanol were produced by the yeast itself. This was in contrast to previous studies in the literature where ethanol was added to the culture. The fermentations were carried out at 30°C, pH = 4,0 using a semi-defined glucose, salts medium at three glucose feed concentrations of 20, 100 and 200 $g l^{-1}$ and for dilution rates from 0,013 h^{-1} to 0,50 h^{-1}.

A growth function of the form

$$\mu = \hat{\mu} \cdot \frac{C_s}{C_s + K_s} \cdot \frac{K_p}{K_p + C_p}$$

was used to describe the observed data with

$\hat{\mu} = 0,64 \quad h^{-1}$
$K_s = 3,3 \quad g l^{-1}$
$K_p = 5,2 \quad g l^{-1}$
$C_p = 0,43 \ (C_{sf} - C_s) \quad g l^{-1}$

as the values of the kinetic parameters. The fit of the data to the model was reasonable with the exception of the data of the 200 $g l^{-1}$ glucose feed concentration at low dilution rates. Data of other workers has also been found to fit the model.

From the data and model it was evident that very low dilution rates were necessary to achieve high conversions in the region of product limited growth. This

suggested that cell recycle, ethanol removal or some other means of improving the ethanol tolerance would be essential if continuous ethanol fermentation were to become economically viable.

The use of micro-aerobic conditions for the 100 gl^{-1} glucose feed, created by air sparging for a dissolved oxygen level of 0,4 mgl^{-1} (0,5% saturation), appeared to enhance the ethanol tolerance of the yeast. In the model, the value of K_p increased to 16,0 gl^{-1}, representing a greatly reduced degree of inhibition. This was also reflected in the operating conditions where at a dilution rate of 0,1 h^{-1}, the degree of substrate utilisation increased from 58% to 98% and the ethanol productivity from 2,5 to 4,0 $gl^{-1}h^{-1}$ with an increased cell mass concentration of 7,3 gl^{-1} compared to 2,3 gl^{-1}.

ACKNOWLEDGEMENTS

To Professor G.S. Hansford for his encouragement, guidance and patience for the duration of the work.

To all the members of the Chemical Engineering Department for their support, friendliness and technical advice.

To the CSIR and the Cooperative Scientific Programmes (National Materials Programme - Bagasse to Ethanol) for its financial support.

To Stephanie Gilinsky for the competent typing.

And to my wife, who never knew me without "the thesis".

CONTENTS

Page No.

NOMENCLATURE

C_{sf}	-	substrate feed concentration, glucose - gl^{-1}
C_s	-	substrate concentration, glucose - gl^{-1}
C_x	-	cell mass concentration, yeast - gl^{-1}
C_p	-	product concentration, ethanol - gl^{-1}
D	-	dilution rate - h^{-1}
F	-	flowrate to and from fermenter - lh^{-1}
K_s	-	substrate saturation constant - gl^{-1}
K_p	-	product inhibition constant - gl^{-1}
Y_{xs}	-	cell mass yield coefficient - (g cell mass)(g substrate)$^{-1}$
Y_{ps}	-	Product yield coefficient - (g product)(g substrate)$^{-1}$
m	-	specific maintenance rate - (g substrate)(g cell mass)$^{-1}$
u	-	specific growth rate - h^{-1}
$\hat{u}$, u_o	-	maximum specific growth rate - h^{-1}
α	-	growth associated Luedeking and Piret product formation constant
β	-	non-growth associated Luedeking and Piret product formation constant
A,B,C	-	Other product inhibition model constants

LIST OF FIGURES

LIST OF TABLES

1. INTRODUCTION

There is again an increasing and renewed interest in fermentations and fermentation technology. Many chemicals and chemical feedstocks such as acetone, butanol and ethanol were produced by fermentation before the 1950's when there was the advent of synthetic processes using cheap petrochemicals e.g. oil. This is however a finite source and with its cost increasing, there is a strong awareness for the need of other sources and preferably renewable sources. South Africa is well endowed with or has the capacity to produce the renewable sources such as sugar, starches and cellulosic materials. These can then be hydrolysed to various sugars and be further fermented to produce a product such as ethanol.

The aim of this study has been to use continuous laboratory fermentations to study the kinetics of the common glucose to ethanol fermentation using yeast. For large scale production, the use of continuous processes has been recognised as essential even though disadvantages still exist, see Table 1.1. In the

TABLE 1.1 ADVANTAGES AND DISADVANTAGES OF CONTINUOUS FERMENTATIONS.

ADVANTAGES	DISADVANTAGES
1. Higher throughput - with resultant lower capital investment.	1. Possibility of infection.
2. Ability and simplicity of control.	2. Possibility of mutation.
3. Reduced operating costs.	3. Lack of knowledge of dynamic behaviour.
4. Uniform product.	
5. Uniform demand on ancillaries - eg. cooling water, power.	

laboratory, continuous culture techniques also provide the best method for controlling microbial growth and environmental conditions at constant values. Batch experiments represent a dynamic state where the system is continually changing. The kinetics of this fermentation have been well studied, especially the inhibitory effect of the product ethanol. However the studies have often involved batch experiments and have considered the effect of exogenous ethanol, i.e. ethanol added to the system. This study therefore takes a closer look at the kinetics of the ethanol inhibition in a continuous system and with ethanol produced by the yeast cells themselves. This data would then be used to model the kinetics. Such a model may then be applied to other ethanol fermentation systems, be used to develop design functions and also be used to indicate where a process may be advantagously changed or improved.

2. LITERATURE REVIEW

2.1 Ethanol Inhibition Studies

The effects of ethanol on the kinetics of the alcoholic fermentation of yeast have been continuously studied since the turn of the century.

Rahn [1] reanalysed extensive experiments performed by Rubner in 1912 on alcoholic sucrose fermentations. Rubner had studied the reactions using the heats of fermentation. Rahn converted these to sugar equivalents and deduced that the rate of fermentation was unaffected by the sugar concentration but was decreased by the increasing ethanol concentration. He postulated a linear relationship and assuming the existence of a limiting ethanol concentration above which growth ceased (10,2% ethanol, obtained from a 20% batch sucrose fermentation which took 88 h to ferment to completion), found this to apply reasonably well. The equation postulated was

$$-\frac{dC_s}{dt} = \text{const}\ (1 - C_p/C_{pm})$$

where C_{pm} = limiting ethanol concentration.

From further batch data where ethanol was added to the medium the rate of fermentation was found to be a linear function of the ethanol concentration added to the medium initially. However, at additions equivalent to the limiting ethanol concentration, the rate of fermentation was slow but still noticeable provided the number of fermenting cells was large.

Similar linear relationships were also obtained by Hinshelwood with batch cultures of Bacterium lactis aerogenes and by Holzberg et al [2] in continuous culture with high sugar concentration grape juice (20% glucose) using Saccharomyces cerevisiae var. ellipsodeus.

Holzberg et al [2] added ethanol to the feed and kept the ethanol concentration in the fermenter similar to that in the feed by increasing the dilution rate so as to prevent ethanol accumulation by the yeast. By following the yeast population with respect to time, he calculated μ from

$$\frac{d(\ln N)}{dt} = \mu - D$$

Hence they described the decrease in the specific growth rate with increasing ethanol concentration by

$$\mu = \mu_m (1 - 0{,}235 (Cp - 2{,}6))$$

which implied that a threshhold ethanol concentration of 2,6% had to be exceeded before linear inhibition occurred and that growth ceased above an ethanol concentration of 6,85%. Batch data did not fit the above relationship in both the exponential and stationary phases. This was suggested to be because of nutritional deficiencies in the medium.

Égamberdiev and Ierusalimskii [3] studied the effect of ethanol on the rate of growth of Saccharomyces vini also in a grape liquor with a sugar content of 17,5%. By adding ethanol to a young active culture in the exponential growth phase which had not yet started to form large amounts of ethanol, the added ethanol became the main limiting factor determining the rate of growth. The following relationship resulted.

$$\mu = \mu_o \frac{K_p}{K_p + C_p}$$

where μ_o = specific growth rate when $C_p = 0$

K_p = constant

= C_p at $\mu = \mu_o/2$

This is similar to that of non-competitive inhibition of enzyme reactions. The authors reported the following values for the constants, Table 2.1.

TABLE 2.1 GROWTH AND ETHANOL INHIBITION CONSTANTS DETERMINED BY EGAMBERDIEV AND IERUSALIMSKII [3]

	AEROBIC	ANAEROBIC
μ_o (h^{-1})	0,36	0,31
K_p (vol %)	2,8	2,6
(gl^{-1})	22,1	20,5

The relationship was found to hold for ethanol concentrations up to 14 vol % (103 gl^{-1} in a 17,5% sugar solution). At higher concentrations the growth rate decreased more rapidly than predicted.

A similar type of non-competitive inhibition was also observed by Aiba and Shoda [4] , in a reassessment of data from Aiba et al [5] , where the inhibition had been described by an exponential function. In both cases they described the inhibition in batch and continuous fermentations by similar functions and upon both the specific growth rate and the specific rate of ethanol production. Different values for the constant were obtained for the batch versus the continuous system and for specific rates of growth and product formation. The functions and the values of the constants are summarised in Table 2.2.

The continuous experiments were conducted using a respiration deficient mutant of a baker's yeast in a 1 or 2% synthetic glucose medium at 30°C under conditions where one component, namely glucose, was the "limiting nutrient" i.e. its concentration remained below 0,1%. This is in contrast to the batch experiments where the glucose is not strictly "limiting" until the glucose concentration decreases to 1-2% (at this level, the

TABLE 22 ETHANOL INHIBITED GROWTH AND PRODUCT FORMATION FUNCTIONS

Aiba et al [5]	Aiba and Shoda [4]
$\mu = \mu_o . e^{-k_1 C_p} \cdot \frac{C_s}{C_s + K_s}$	$\mu = \mu_o \cdot \frac{1}{1 + C_p/K_p} \cdot \frac{C_s}{C_s + K_s}$
k_1 = 0,028 (B) 0,016 (C) $g\ell^{-1}$ K_s = 0,22 $g\ell^{-1}$	K_p = 16,0 (B) 55,0 (C) $g\ell^{-1}$ K_s = 0,22 $g\ell^{-1}$
$\nu = \nu_o e^{-k_2 C_p} \cdot \frac{C_s}{C_s + K_s'}$	$\nu = \nu_o \cdot \frac{1}{1 + C_p/K_p'} \cdot \frac{C_s}{C_s + K_s'}$
k_2 = 0,015(B) 0,029 (C) $g\ell^{-1}$ K_s' = 0,44 $g\ell^{-1}$	K_p' = 71,5 (B) 12,5 (C) $g\ell^{-1}$ K_s' = 0,44 $g\ell^{-1}$

NOTE: B = Batch C = Continuous

specific growth rate decreased appreciably). In the continuous experiments, ethanol was added to the feed medium in varying amounts, it being produced by the cells in the batch runs.

Aiba and Shoda [4] pointed out that the dual assessment of the results was possible because of the narrow range of ethanol concentrations observed, namely C_p = 0 to 60 $g1^{-1}$. Examination of the values of K_p and K_p' showed that for growth, batch operation was less favourable than continuous operation, but that the reverse applied for product formation so that the mode of operations changed the association of ethanol with the respective enzymes for growth and fermentation.

Comparison of the functions with their respective constants shows them not to be very compatible eg. the non-competitive term with K_p = 16,0 $g1^{-1}$ is 20% more

inhibitory than the exponential term with k_1 = 0,028 gl^{-1} at an ethanol concentration of 10 gl^{-1}, ie. the specific growth rate is depressed by a factor of 0,60 compared to 0,75 for the exponential case.

Kunkee and Amerine [6] presented a formula for complete yeast inhibition based on wine stabilisation studies by Delle in 1911 which related the inhibition to both the sugar and ethanol concentrations. The equation was as follows:

$$DU = a + 4,5.C$$

where

DU = Delle Units and varies from 75 to 85
a = sugar concentration - % w/v
c = ethanol concentration - % v/v

This gave complete inhibition at either 18% ethanol or 80% sugar concentration, with ethanol 4,5 times more inhibitory than sugar.

Bazua and Wilke [7] using Saccharomyces cerevisiae ATCC No. 4126 and a limiting 1% glucose substrate, used batch and continuous experiments at 30°C to establish second order inhibition functions incorporating two or three constants. Initial batch experiments, where ethanol of different concentrations was added to the medium, established some growth for an initial ethanol concentration of 80 gl^{-1} but no growth at 100 gl^{-1}. In further batch experiments ethanol was added after 5,5 h, when the cells were in the logarithmic phase of growth. A similar result was obtained. From subsequent continuous fermentations with added ethanol it was deduced that the inhibition produced by the ethanol was of a non-competitive type. The effect of the ethanol on both the specific rate of growth and ethanol production was then modelled by two parabolic functions

as given in Table 2.3. The three constant functions gave, of course, a better fit. Some of the data presented by the authors was however suspect. Ethanol concentrations were achieved above those theoretically possible from the feed sugar concentrations given ie. the yield of ethanol per gram of glucose was greater than 0,511.

TABLE 2.3: ETHANOL INHIBITION FUNCTIONS DETERMINED BY BAZUA AND WILKE[7]

FUNCTION 1	FUNCTION 2
$\mu_{max} = \mu_o(1+C_p/C_{pmax})^{\frac{1}{2}}$	$\mu_{max} = \mu_o - aC_p/(b-C_{pmax})$
$\nu_{max} = \nu_o(1+C_p/C_p'_{max})^{\frac{1}{2}}$	$\nu_{max} = \nu_o - a'C_p/(b-C_p'_{max})$
$\mu_o = 0,448\ h^{-1}$	$\mu_o = 0,428\ h^{-1}$ $\quad \nu_o = 1,802\ h^{-1}$
$\nu_o = 1,913\ h^{-1}$	$a = 0,182$ $\quad a' = 0,506$
$C_{pmax} = 93,6\ g\ell^{-1}$	$b = 133,78\ g\ell^{-1}$ $\quad b' = 119,25\ g\ell^{-1}$
$C_p'_{max} = 99,0\ g\ell^{-1}$	$C_{pmax} = 93,84\ g\ell^{-1}$ $\quad C_p'_{max} = 93,1\ g\ell^{-1}$

Ghose and Tyagi[8] considered the effects of ethanol on a fermentation of bagasse hydrolysate (reducing sugar content of 20 $g\,l^{-1}$) using Saccharomyces cerevisiae NRRL-Y-132. Inhibition was also determined by the method of addition of varying concentrations of ethanol to the feed medium to a continuous culture. A non-competitive type of inhibition was obtained with the following relationships for the specific rate of growth and product formation.

$$\mu = \mu_m\ (1-C_p/C_{pm})$$
$$\nu = \nu_m\ (1-C_p/C'_{pm})$$

where μ_m = maximum specific growth rate = 0,4 h^{-1}

C_{pm} = maximum ethanol concentration for growth = 87 gl^{-1}

ν_m = maximum specific ethanol production rate = 1,43 h^{-1}

C'_{pm} = maximum ethanol concentration for ethanol production = 114 gl^{-1}

These relationships are similar to those of Holzberg et al[2] and Bazua and Wilke [7] in predicting the upper ethanol limits for both growth and ethanol production compared to the open ended limits inherent in the non-competitive enzyme inhibition function by Aiba and Shoda[4] and Égamberdiev and Ierusalimskii [3]

The foregoing investigations have all considered the effect of additional ethanol added to the system together with that produced by the yeast or the systems have been operated such that only the "added" ethanol existed in the system. However, as shown in the following recent publications, the ethanol produced by the yeast itself may have the same type of effect but to a differing degree.

Nagodawithana and Steinkraus [9] studied the influence of the rate of ethanol formation and accumulation on the viability of Saccharomyces cerevisiae in "rapid batch fermentations". Rapid fermentations were classified as those which were complete in 2,5 to 3 h at 30°C using clover honey solutions of 25% sugar content. Using high initial cell concentrations, 3 h fermentation times were achieved at a 98% loss in viability. A lower temperature (15°C and hence lower fermentation rate) or a lower initial cell concentration (1/10 of that used previously) meant a 6 h fermentation but with little or no loss in viability. It was therefore postulated that at 30°C the ethanol was produced so rapidly that it could not diffuse out of the cell and that this contributed to the high cell death rate.

Experiments where ethanol was added to the medium also showed that, internally produced ethanol proved much more lethal (after three hours, had a 33% viability level for a 13,8% w/v ethanol addition to the medium compared to a 15% viability level for a 9,4% w/v self produced ethanol concentration).

The lower temperature would correlate with the postulation that at elevated temperatures the ethanol cannot escape sufficiently rapidly from within the cell but a lower initial cell concentration does not alter the specific growth rate of the cells present and hence substrate consumption and ethanol production would still be at the same level. However for a low inoculum. the growth and substrate consumption would be low initially and sufficient time would be available for new cells to adapt to the environment and consume the remaining substrate.

Strehaiano et al [10] studied the interrelationship between the initial glucose concentration, ethanol concentration and the specific rates of growth and ethanol production in batch fermentations. The specific rate of ethanol production reduced to a unit sugar basis, was found to be a linear function of the specific growth rate on a log-log basis, with the maximum specific rate of ethanol production occurring when the specific growth rate was a maximum i.e. when the inhibition by the glucose and the ethanol was the weakest.

However even at the low initial glucose concentration and the correspondingly low ethanol concentrations (less than 0,05 $d^{o}GL$ or 0,4 gl^{-1}) the growth rate decreased very rapidly. The authors evaluated inhibition constants and found them, even at the 20 gl^{-1} glucose level to be very small 0,05 $d^{o}GL$ or 0,4 gl^{-1}. compared to orders of magnitude of 2,5 $d^{o}GL$ or 20 gl^{-1} as given by Aiba and Shoda [4] and Yarovenko and Nakhmanowich [11].

This the authors said was in agreement with the observations of Nagodawithana and Steinkraus [9] , the ethanol was produced internally faster than it was excreted into the medium and therefore caused growth inhibition.

Navarro and Durand [12] using Saccharomyces carlsbergensis and 120 gl^{-1} saccharose medium in batch fermentations, measured the degree of inhibition as a function of the culture temperature and of the ethanol produced by the yeast cells, both in the medium and within the cells themselves. Increasing the culture temperature was found to accentuate the inhibition action of the ethanol. The production of ethanol continued after the cessation of growth for at 30°C. the ethanol concentration was only 26% of the final 52 gl^{-1} when the biomass concentration reached its maximum (50% of the final concentration at 20°C). The authors therefore concluded that the inhibition of growth cannot be only due to the extracellular alcohol. This observation of ethanol accummulation after growth had stopped was similar to that by Holzberg et al [2] in his batch experiments, where the authors however concluded that the further accummulation of the ethanol was due to a nutritional deficiency for growth. The rate of ethanol production increased with temperature. the maximum occurring just before the cessation of growth. again at the low ethanol concentrations given previously. The authors therefore put forward the hypothesis that when the temperature increased, the rate of formation of alcohol increased faster than the rate of excretion of the ethanol from the cells. Measurements of the internal cell ethanol concentrations showed these also to peak with cessation of growth and maximum ethanol production rates and with very much higher concentrations e.g. 300 gl^{-1} at 30°C compared to 13 gl^{-1} externally and 170 gl^{-1} at 20°C compared to 25 gl^{-1} externally.

Linear correlations were found for the specific ethanol production rate with respect to the various ethanol concentrations.

$$\frac{1}{C_x}\frac{dC_p}{dt} = B(C_{pm}-C_p)$$

and

$$\frac{1}{C_x}\frac{dC_p}{dt} = k(C_{pc}-C_p)$$

where

B,k = constants

C_{pm} = maximum ethanol concentration in the medium

C_{pc} = maximum ethanol concentration in the cells

The first relationship was comparable to that of Holzberg et al [2] and the second was comparable to that representing mass transfer at an interface. By using the Arrhenius equation, an activation energy was found for the second equation the order of those found for diffusion phenomena. Therefore it was concluded that the accummulation of ethanol within the cells, was due to the resistance to transfer of alcohol from the cell to the medium. Also the internal ethanol was more inhibiting as supported by the much lower inhibition constant of Strehaiano et al [10] compared to those by Aiba et al [5] and Égamberdiev and Ierusalimskii [3], who added ethanol to the medium.

2.2 Effect of Oxygen

The effect of oxygen has also been considered because recent work by Thomas, Hossack and Rose [13] has shown that the viability of yeast cells, subject to the toxic effect of ethanol in the medium, may be influenced by the composition of the cell membrane. Enrichment of the membrane with unsaturated sterols and fatty acids

rather than the corresponding saturated compounds increased the viability of Saccharomyces cerevisiae cells when these were suspended in a 1M ($46\ g\ l^{-1}$) ethanol buffer, by resisting the penetration of the ethanol to the inner cell. The increases in the viability level were very significant, going from 0-5% to 80-85% viability after 10 hours in the ethanol buffer.

The value of unsaturated fatty acids and sterols in anaerobic nutrition had been shown twenty four years earlier by Andreason and Stier [14] without knowledge of their function. Very restricted growth was observed when these compounds were not present. Work previous to theirs had suggested that air, namely the oxygen in the air, was necessary for cellular growth directly or for the formation of compounds which then allowed growth to occur. Recently, Larue et al [15] established that unsaturated fatty acids and sterols were necessary for fermentation to continue after yeast growth had ceased, expecially with high glucose concentrations. These compounds allowed resting cells to maintain their viability and hence their fermentative ability.

Kunkee and Amerine [6] and Cysewski [16] both found that micro-amounts of oxygen stimulated fermentation. Cysewski [16] found that the amount of oxygen needed for optimum fermentation rates was very small. An oxygen tension of 0,07 mm Hg was sufficient after an initial adaptation period of 3 weeks at 0,7 mm Hg oxygen tension. Hence it could be said that since the initial metabolic pathways are similar for both anaerobic and aerobic growth, oxygen stimulated yeast growth but was insufficient for complete respiration and hence the ethanol formation route was still followed i.e. anabolic processes rather than catabolic processes were affected.

The effect of oxygen is also very interrelated with the level of the glucose in the medium, both controlling

the degree of respiration or of fermentation. Moss et al [17] showed that when the glucose concentration was low, between 0,02 to 1,5 gl^{-1}, glucose metabolism was sensitive to the oxygen concentration. At low dissolved oxygen concentrations, glucose was utilised for ethanol fermentation whereas when the dissolved oxygen concentration was high, aerobic metabolism resulted. For glucose concentrations between 27 and 43 gl^{-1}, metabolism was mainly by ethanolic fermentation, even when the dissolved oxygen concentration was very high i.e. up to saturation. The second phenomenon is often referred to as the Crabtree effect or glucose repression and yeast cells in this state are described as repressed. Sufficient energy appears to be available to the yeast even by fermentation due to the high glucose concentration.

2.3 Substrate Inhibition.

A brief comment is made on substrate inhibition because in considering the effect of ethanol in the medium produced by the yeast cells, lower than maximum concentrations of ethanol will be produced when there is incomplete utilisation of the substrate. However, for the alcoholic yeast fermentation, inhibition due to glucose has been generally accepted to be a minor effect compared to the inhibition of the ethanol produced. Ough [18] stated that concentrations of 1% to 15% w/v sugar had little or no effect, whereas above 17½% w/v sugar, the high osmotic pressure began to have an inhibiting effect. Where yeast inhibition has been tested, Ghose and Tyagi [8] , Pironti [19] and Jackson and Edwards [20], it has been done using the relationship analogous to competitive enzyme inhibition.

$$\text{i.e. } \mu = \hat{\mu} \frac{C_s}{K_s + C_s + C_s^2/K_i}$$

where K_i = inhibition saturation constant, gl^{-1}

Pironti [19] using glucose found a value of ω of 1120 assuming $K_s = 0,58\ g\,l^{-1}$ (i.e. $K_i = 708\ g\,l^{-1}$) and Ghose and Tyagi [8] using bagasse hydrolysate obtained ω equal to 427,5 (the lower value is probably due to unfermentable sugars and celladextrins in the hydrolysate). A high value of ω is indicative of a low degree of inhibition.

3. THEORY

This section considers an extension of the simple continuous culture theory using Monod growth kinetics to include the effect of product inhibition. In modelling culture cell concentrations, the concept of a maintenance energy will also be applied.

Section 2.1 showed that many models have been used to describe ethanol inhibited growth kinetics. All investigations recognised a non-competitive type of inhibition and hence the traditional non-competitive inhibition of enzyme kinetics relationship (Aiba, Humphrey and Millis [21]) was used. It can be shown that, when the different growth inhibition models are given by their Taylor series expansion, consideration of the major terms shows the models to be the same.

Figure 3.1 shows the fermentation system and the notation used to describe the various variables/concepts. Classical continuous fermentation theory (Aiba, Humphrey and Millis [21]) shows that under steady state operation, the dilution rate is equivalent to the specific growth rate of the organisms. Therefore, substituting for the inhibited specific growth rate relation, Equation (3.1) results.

$$D = \mu = \hat{\mu} \cdot \frac{C_s}{C_s+K_s} \cdot \frac{K_p}{K_p+C_p} \qquad (3.1)$$

If the efficiency of substrate utilisation for product formation, namely ethanol, can be characterised by a constant yield coefficient, Y_{ps}, then

$$C_p = Y_{ps} (C_{sf} - C_s) \qquad (3.2)$$

and substitution for C_p in the growth rate equation, allows the substrate concentration C_s to be obtained as a function of the dilution rate (see Appendix I).

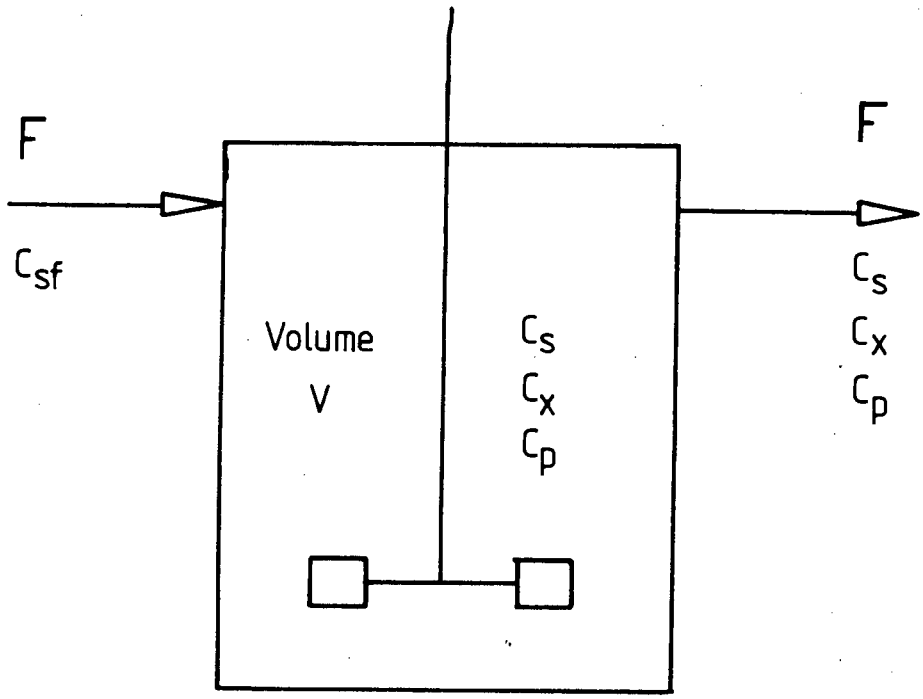

At Steady State:

Dilution Rate	=	D	= F / V
Ethanol Concentration	=	C_p	= $Y_{ps}.(C_{sf} - C_s)$
Ethanol Productivity	=	$D.C_p$	
Specific Ethanol Productivity	=	$D.C_p / C_x$	

FIGURE 3.1 : FERMENTER AND ASSOCIATED SYMBOLISM

When the value of K_s, the substrate saturation constant, is very much less than the substrate concentration, the Equation (3.1) may be approximated by

$$D = \hat{\mu} \cdot \frac{K_p}{K_p + C_p} \qquad \text{when } C_s \gg K_s$$

Rearranging

$$\frac{1}{D} = \frac{1}{\hat{\mu}} + \frac{1}{\hat{\mu} K_p} \cdot C_p \qquad (3.3)$$

Using Equation (3.3) it is possible to obtain both $\hat{\mu}$ and Kp. Plotting the reciprocal of the dilution rate versus the ethanol concentration should yield a straight line of slope $1/\hat{\mu}Kp$ and intercept $1/\hat{\mu}$. All three constants in Equation (3.1) could also be obtained by using a simplex method for function minimisation on a computer.

The cell mass concentration in the fermenter is obtained by a substrate balance over the fermentation system. Substrate is mainly converted to energy (from the production of ethanol) and some is used for cell mass production. The observed utilisation of substrate for cell mass does not always remain constant. Pirt [22] suggested that the change in the "observed" cell mass yield coefficient was due to an energy of maintenance, described as the energy or substrate consumed for functions other than the production of new cell material ie. growth. Such functions may be the maintenance of solute gradients, turnover of macromolecules and motion. Therefore, the growth rate is not altered but the substrate available for growth is decreased. By introducing the factor m, the specific rate of substrate consumption for maintenance, a substrate balance will yield Equation (3.4) for the biomass concentration

$$C_x = \frac{Y_{xs} \cdot D \cdot (C_{sf} - C_s)}{(D + Y_{xs} \cdot m)} \qquad (3.4)$$

Note that Y_{xs} is now the "true" yield of cell mass per unit substrate consumed. As m tends to zero, Equation (3.4) will revert to the case of a constant observed cell mass yield coefficient, equivalent to the true yield.

Equation (3.4) may be rearranged to give

$$\frac{(C_{sf} - C_s)}{C_x} \cdot D = m + \frac{D}{Y_{xs}} \qquad (3.5)$$

This shows that the observed biomass yield coefficient $(C_{sf}-C_s)/C_x$ is not a constant but a function of the dilution rate. Equation (3.5) may be used to determine the true cell mass yield coefficient, Y_{xs}, given by the slope of the straight line of the specific substrate utilisation rate versus dilution rate, the intercept giving the specific maintenance rate m.

A product balance, incorporating the ethanol produced from the maintenance function gives

$$C_p = \frac{C_x . Y_{ps}}{D} \cdot \left(m + \frac{D}{Y_{xs}}\right)$$

The product yield coefficient used in the balance equation for the maintenance process need not be the same as for synthesis as has been assumed here, but since m is small compared to μ/Y_{xs} for higher growth rates, the influence will not be significant.

Rearranging the equation for the product concentration will give the rate of product formation

$$\frac{DC_p}{C_x} = mY_{ps} + D.\frac{Y_{ps}}{Y_{xs}} \qquad (3.6)$$

Equation (3.6) may be compared to the Luedeking and Piret model for production formation which was applied by Aijar and Luedeking [23] to the ethanol fermentation using Saccharomyces cerevisiae.

i.e. $\nu = \beta + \alpha\mu$

= rate of product formation

where $\nu = DC_p/C_x$

$\beta = mY_{ps}$

= nongrowth or maintenance associated product formation rate

$\alpha = \frac{Y_{ps}}{Y_{xs}}$

= growth associated product formation rate.

4. EXPERIMENTAL PROCEDURE

4.1 Organism

The organism used in this study was Saccharomyces cerevisiae, ATCC 4126. This yeast was chosen because several recently published works [7,16] have used it, making comparison of data possible.

From the stock culture, slopes, containing Wickerham medium as in Table 4.1, were subcultured every two months and stored at 15 - 20°C. These slopes were used for making inocula for the fermentations.

TABLE 4.1 WICKERHAM MEDIUM FOR SLOPE CULTURES [24].

Component	Concentration $g l^{-1}$
Malt extract	3
Yeast extract	3
Peptone	5
Glucose	10
Agar	20
Distilled Water	to 1 l

4.2 Medium

4.2.1 Composition

The composition of the medium used was that given by Cysewski[16] and was chosen because of its relative simplicity in the number of components and because it had been optimised for this particular yeast. It is semi-defined (i.e. its composition is not completely known) because of the inclusion of yeast extract and tap water. Trace organic and inorganic elements were assumed to be supplied in sufficient quantities by the yeast extract and the tap water. Analyses of yeast extract and tap water are given in Appendix F,G. The pH of the medium was adjusted to a 4,0

by the addition of citric acid and sodium citrate. The total medium composition is given in Table 4.2, all components being reagent grade.

TABLE 4.2 FERMENTATION MEDIUM

Component	Concentration $g l^{-1}$
Glucose monohydrate (dextrose)	110,0
Yeast Extract (Difco)	8,5
NH_4Cl	1,32
$MgSO_4.7H_2O$	0,11
$CaCl_2$	0,06
Citric Acid	1,5
Sodium citrate	0,2
Antifoam	0,01 ml
Tap water to	1 l

4.2.2 Preparation

The medium was prepared to two portions. The glucose was made up in 60% of the final volume with the remainder of the components in 40% of the final volume. This allowed separate sterilisation of the two solutions and prevented adverse reactions taking place between the glucose and the other components. Sterilisation was at 121°C (or 105 kPa.g) in a 120l vertical autoclave. 1l volumes were kept at temperature for 15 minutes and larger volumes, namely 5l, 10 l and 20l, were kept at temperature for 30 minutes. Medium reservoirs for the continous fermentation were prepared less than 24 hours prior to usage and were mixed on a magnetic stirrer before being cooled to room temperature.

No attempt was made to deaerate the medium and oxygen levels in the medium were in the range 3 - 4 $mg l^{-1}$, increasing for decreasing sugar concentrations. For different glucose feed concentrations, the other components in the medium were increased or decreased in proportion to the glucose concentration.

4.3 Inoculum

The inoculum was prepared by placing a loopful of yeast from the agar slopes, into 50 ml of sterile medium in a 250 ml Erlenmeyer flask. The flask containing the medium had been stoppered with cotton wool and covered with foil during sterilisation at 121°C for 15 minutes. The inoculum was then incubated at 34°C under semi-aerobic conditions in an incubator without shaking for 20 hrs before being transferred to the continuous fermenter.

4.4 Apparatus and Anaerobic Operation

The system for the continuous fermentations is shown in Fig. 4.1. It consisted of a 1ℓ Gallenkamp modular fermenter incorporating the following modules:

(i) a basic 1ℓ Quickfit, flanged, glass, culture vessel with a multiple port head plate

(ii) a magnetic stirrer with continuous speed control, acting on a four bladed turbine (plastic covered steel follower)

(iii) a temperature controller consisting of a themistor probe actuating either a heater element or a water cooling coil; the water flow rate was adjustable with an on/off control using a solenoid valve

(iv) a pH controller, incorporating pH probe, pH indicator and set point controller operating separate acid (4N HCl) and base (4N NaOH) pumps.

(v) a feed-harvest pump module consisting of two concentrically mounted peristaltic pumps with a variable speed control

(vi) a sterilisable dissolved oxygen monitoring probe and oxygen meter.

The magnetic stirrer, pH and oxygen probes were all-
by [illegible] to operation. The [illegible] was closed
[illegible] diameter in a [illegible] sieve through
the [illegible] plate. The feed-inlet to the fermentor was controlled
by a [illegible] pipette [illegible] and the feed
stream [illegible] by hose [illegible] fermentor, removed
to "the [illegible]" from the culture by [illegible] and a condenser
on the exit gas stream reduced the loss of water vapour and
entrained ethanol.

The system was sterilized initially as a "closed system"
in a vertical autoclave. The fermentor was completely
assembled, including temperature, pH and oxygen probes, flow
measuring pipette and all feed and harvest lines (made
silicone rubber) and sterilized for 15 minutes at 121°C.
The fermentor vessel contained water during sterilization
so that the probes were in contact with a solution but not
the medium (sterilization [illegible] of
membranes and porous plugs).
[illegible]
reservoirs and subsequently fill[illegible]
by virtue
[illegible] strength of
[illegible]
[illegible] in water in the vessel was replaced
by medium and flow [illegible] started and set to the operating
conditions as given in Table 4.3.

TABLE 4.3 OPERATING CONDITIONS FOR CONTINUOUS FERMENTATIONS

PARAMETER	SET VALUE
Temperature -	30,0 ± 0,5
pH	4,0 ± 0,
Agitation -	300 ± 30

When the medium had reached [illegible] the fermentor
was inoculated with the 50 ml of propagated inoculum. The
inoculum was introduced through a septum by means of a sterile

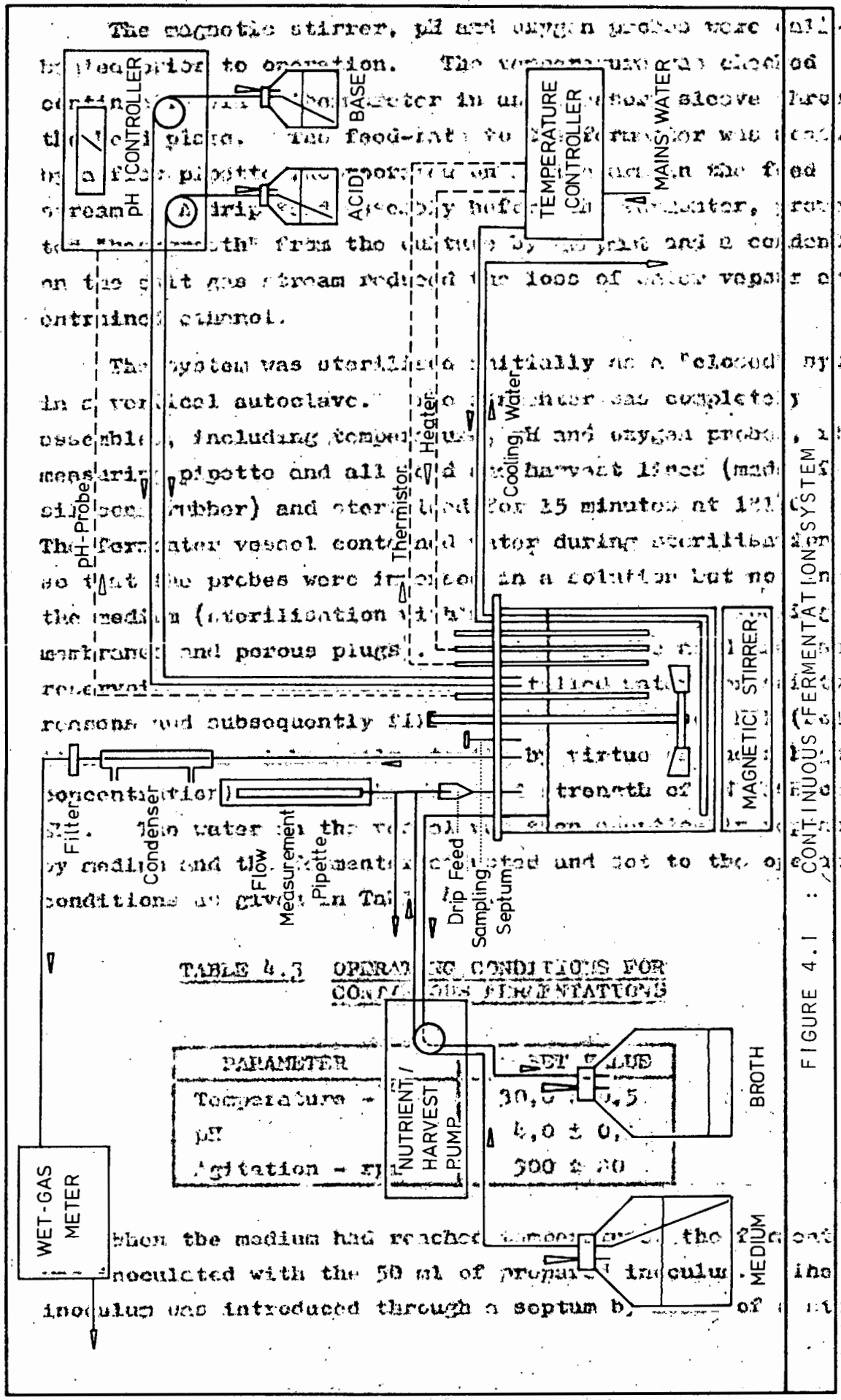

FIGURE 4.1 : CONTINUOUS FERMENTATION SYSTEM

syringe. Batch growth was allowed to proceed until the glucose had been reduced to approximately 50% of its starting concentration before feed was introduced. The flow was set to a predetermined level and continuously checked by timing a particular volume using the side arm mounted flow pipette. Adjustment was made by changing the speed of the peristaltic feed-harvest pump. A constant level was maintained by setting the harvest tube at the desired level in the fermenter and applying a withdrawal rate greater than the feed rate. This was achieved by using a larger size tubing than on the feed line. Any adjustments in feed rate were therefore always in the same proportion to the withdrawal rate because the two pumps were mounted in tandem on the same shaft. Hence the excess withdrawal rate was determinable, assumed to be carbon dioxide and added to the carbon dioxide leaving via the gas port. The carbon dioxide produced was vented to the atmosphere via the condenser, a 0,45 m Millipore filter and its flow rate measured by means of a Wet Gas meter (Alexander Wright & Co. (Westminster) Ltd.).

Samples, nominally 10 ml, were drawn through a septum by a sterile syringe, being taken one to three times during a residence time. Steady state generally occurred three to five residence times after a step change in the flow rate and was assumed to have been achieved when concentrations of biomass and glucose remained constant for one or more residence times. Samples were analysed for biomass, glucose and ethanol concentrations. Recordings of temperature, pH, and carbon dioxide produced were also recorded at the time of the sample.

During the fermentation, the feed reservoir was replaced as needed. Once a steady state had been established and sufficiently well defined, the flow-rate was changed and a new steady state established. A set of steady states was obtained for three different feed glucose concentrations - 20, 100 and 200 $g l^{-1}$.

4.5 Micro-aerobic operation

A set of steady states was also obtained for the 100 gl^{-1} feed glucose concentration under micro-aerobic conditions. These conditions were achieved by sparging air, previously filtered and demisted, through a 0 - 1 l rotameter with needle control valve and a further 0,45 µm Millipore filter, into the fermenter. The air entered through the hollow agitator shaft and was dispersed by the blade turbine. The dissolved oxygen concentration in the fermenter was controlled at an estimated 0,04 mgl^{-1} by adjusting the air flow rate (nominally 0,5vvm) and observing the dissolved oxygen content on the oxygen meter. The meter displayed in units of percentage of air-saturation for the medium at the operating temperature. The control value therefore represented 0,5% of air-saturation. This value for the dissolved oxygen content in the medium was found to be the optimum when changing from anaerobic to aerobic metabolism for this particular yeast [16].

4.6 Analyses

Samples removed from the fermenter were immediately prepared for analysis. The content of the sampling syringe was gently released into a glass vial from which volumes of broth were pipetted into volumetric flasks to give the desired dilutions, depending on the analysis to be performed. The dilutent was water for biomass and glucose concentrations because these were measured immediately. Ethanol samples were prepared by diluting the broth with saturated benzoic acid. This did not affect the subsequent analysis for ethanol but helped to prevent growth and extend storage life, even when held at 2 - 4 °C. Ethanol concentrations were usually analysed in blocks.

Samples for glucose and ethanol were also centrifuged to remove the yeast cells before being analysed or stored respectively. Centrifuging at 4000 rpm for 15 minutes, using an MSE Super Minor Centrifuge, was found to give a

supernatent of 100% transmittance on the photometer used for biomass measurements.

The following analysis procedures were adopted.

4.6.1 Cell Mass Concentration

The yeast concentration was determined using a Beckmann Photometer, Model 1211, with a green filter of nominal 580 nm. Measurements of percentage transmission, measured relative to a standard of distilled water (this having been found equivalent to the solution without the yeast cells because of the generally high degree of dilution necessary for the operational range), were converted to dry weight equivalent using a previously determined calibration curve (see Appendix E). The usual working range was 50 to 200 mgl^{-1}, resulting in a dilution of 10-20X. Reproducibility was better than ± 3%.

4.6.2 Glucose concentration

The glucose concentration was measured using a Beckmann Glucose Analyser 2 with a measuring range of 100 to 4500 mgl^{-1}. The analyser is calibrated at a value of 1500 mgl^{-1} and hence samples were diluted so as to be in the region of this value. The analyser measures the rate of oxygen utilisation from an oxygen-saturated solution of glucose oxidase when 10 µl of glucose sample are placed into 1 ml of the enzyme in a controlled reaction cup. The maximum rate of oxygen consumption was directly proportional to the concentration of glucose in the sample. Reproducibility was better than ± 2%.

4.6.3 Ethanol Concentration

Ethanol concentration was determined by gas chromatography. Two chromatographs were used; initially a Hewlett Packard 5750 and later a Varian 1440 Aerograph. Both were operated isothermally and using flame ionisation detectors. Their operating conditions are given in Table 4.4.

TABLE 4.4 OPERATING CONDITIONS FOR THE GAS CHROMATOGRAPHS

VARIABLE	HEWLETT PACKARD 5750	VARIAN 1440
COLUMN TYPE	Glass 1500 mm x 3,2 mm Chromosorb 101, 80-100 mesh	Stainless Steel 1500 mm x 3 mm 1,5% OV-101 Chromosorb G HP 100/120
TEMPERATURES:		
Injection Port	210°C	145°C
Column	150°C	60°C
Flame Detector	210°C	245°C
GAS PRESSURES:		
*Oxygen] Detector	270 kPag	300 kPag
*Hydrogen] Detector	205 kPag	300 kPag
*Nitrogen - Carrier	270 kPag	300 kPag

* "Medical Air" was used for oxygen and high purity nitrogen as the carrier.

Results from the Hewlett Packard 5750 were determined by use of a calibration curve for the area under the chromatogram versus concentration. The Varian was connected to a CDS 411 integrator and samples were analysed directly using n-butanol (0,5 $g\,l^{-1}$) as an internal standard. For both methods the ethanol was diluted to less than 1,5 $g\,l^{-1}$ using the saturated benzoic acid. The volume injected was 2 µl.

5. RESULTS AND DISCUSSION

The results are presented in two main sections covering the anaerobic fermentations and one micro-aerobic fermentation. For each type of fermentation the following have been considered: the general time course of the experiments, the primary steady state variables obtained, namely the glucose, cell mass and ethanol concentrations, and the secondary steady state variables such as the observed cell mass and ethanol yield coefficients and the ethanol productivities. This data has then been applied in modelling the growth kinetics and used to predict operating concentrations and ethanol production rates. The primary data has also been used to check the "mass balance" at any steady state and examined more closely for any anomolies. Finally an estimate and discussion of the experimental and systematic errors in the experiments has been presented.

5.1 ANAEROBIC FERMENTATION

5.1.1 Time Course of the Continuous Fermentations

The typical time course for a fermentation from start-up through to several steady states is given in Figure 5.1. From the concentration profiles it is evident that following a step change in the dilution rate, approximately three residence times were necessary to achieve the new steady state. A further three residence times were generally observed to give a representative steady state value. Using the distribution of residence times for a chemostat, and considering only the effect of mixing, 5% of the original material would remain after three residence times had elapsed.

The steady states were obtained in a random manner rather than in an ascending or descending order for the

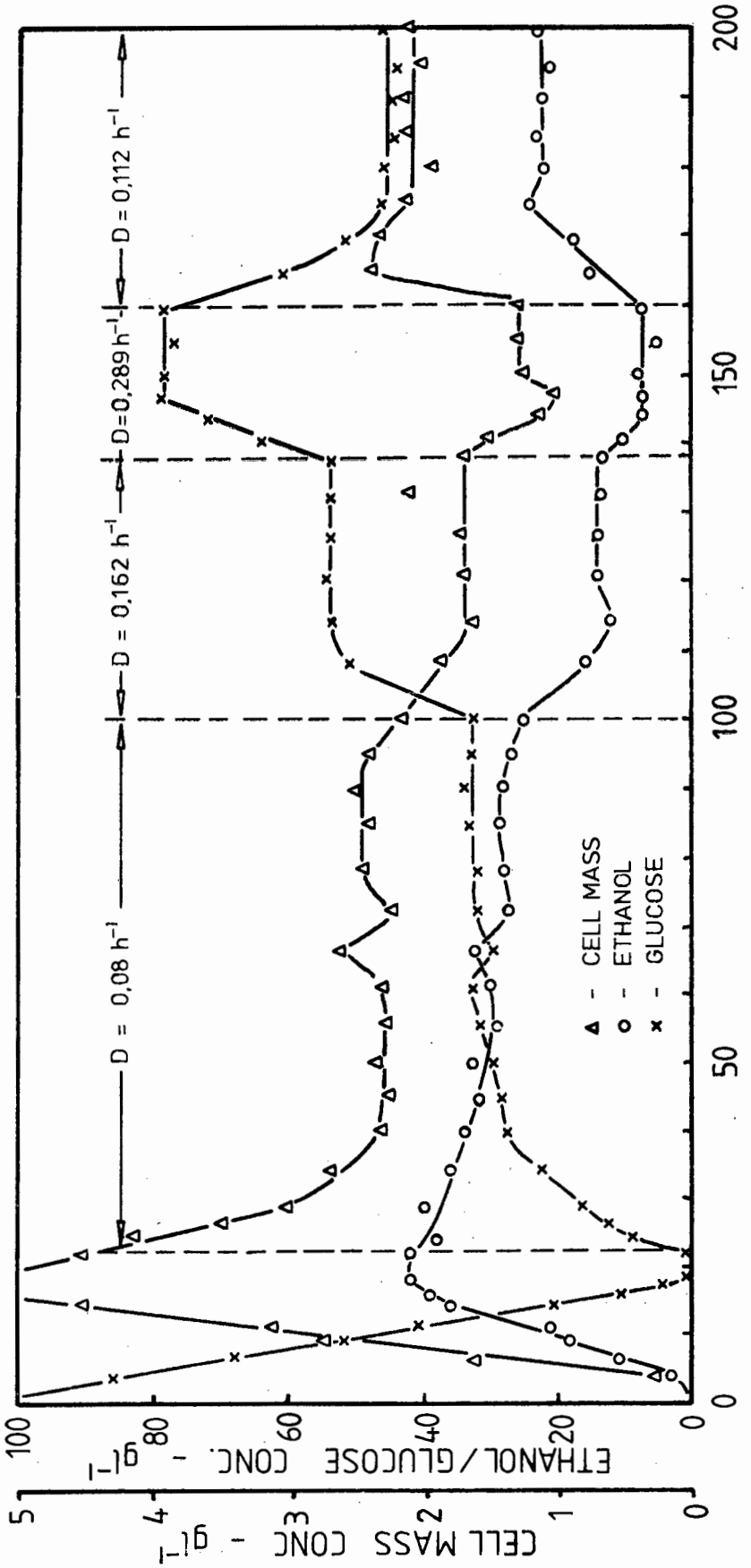

FIGURE 5.1 : OPERATING TIME COURSE FOR FERMENTATION GF-8C-79 FOR THE PERIOD 0-200 h (pH = 4,0 ± 0,1, t = 30,0 ± 0,5°C)

dilution rates. This was to minimise any effects due to adaption.

Fermentations of up to 1500 hours duration were achieved with no visible signs of contamination. Experiments were however generally shorter, around 600 hours.

5.1.2 The Steady State Concentrations and Yields

The steady state parameters as a function of the dilution rate and the feed glucose concentration are given in Figures 5.2 to 5.4. The different parameters are considered separately. They will be discussed in greater detail when considering the model. In Figure 5.3, for the 100 gl^{-1} glucose feed concentration, data from Cysewski [16] has been included, because it was obtained under very similar conditions (only the temperature was higher at 35°C).

(a) Glucose Concentration: This increased very rapidly with increasing dilution rate. The lower the feed glucose concentration and the lower the dilution rate, the better was the ability of the yeast to ferment the glucose completely. This can be seen most clearly in Figure 5.5 where the substrate consumed is given as a function of the dilution rate and feed substrate concentration. For the 200 gl^{-1} feed glucose concentration, the conversion was still 37% incomplete at a dilution rate of 0,013 h^{-1} (residence time of 77 hours) and complete utilisation of the glucose would appear to have been unattainable. At a dilution rate of 0,1 h^{-1}, the respective conversions were 95, 57 and 32% for the 20, 100 and 200 gl^{-1} glucose feed concentrations. The data of Cysewski [16] followed a similar pattern. Although the concentration was considerably higher at lower dilution rates (27 gl^{-1} compared to 10 gl^{-1} at 0,04 h^{-1}), the difference decreased with increasing dilution rate. From 0,23 h^{-1} onwards, the glucose concentrations were lower and

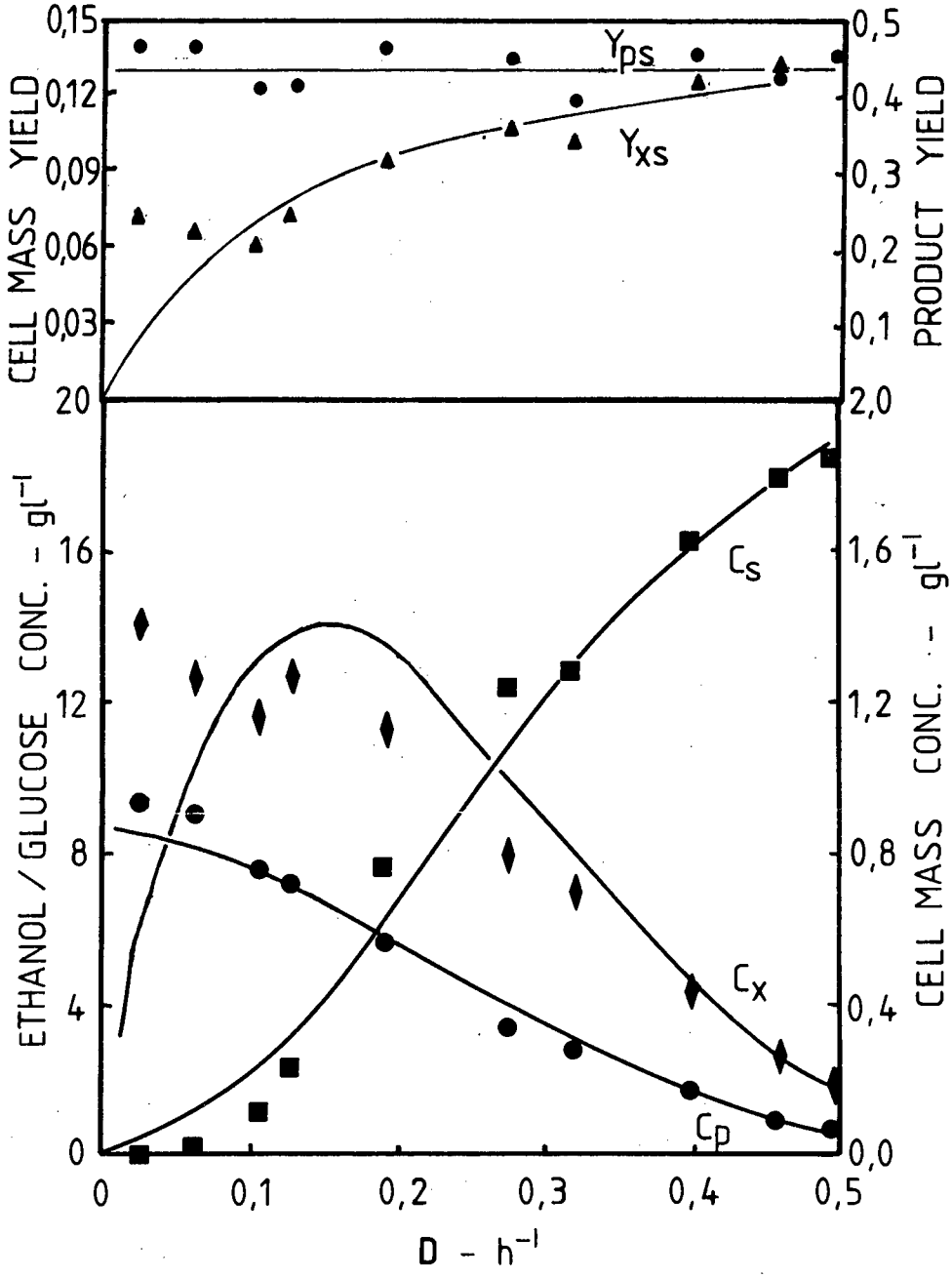

FIGURE 5.2 : PROCESS VARIABLES, EXPERIMENTAL AND PREDICTED AS A FUNCTION OF THE DILUTION RATE - ANAEROBIC WITH 20 gl^{-1} FEED GLUCOSE CONCENTRATION

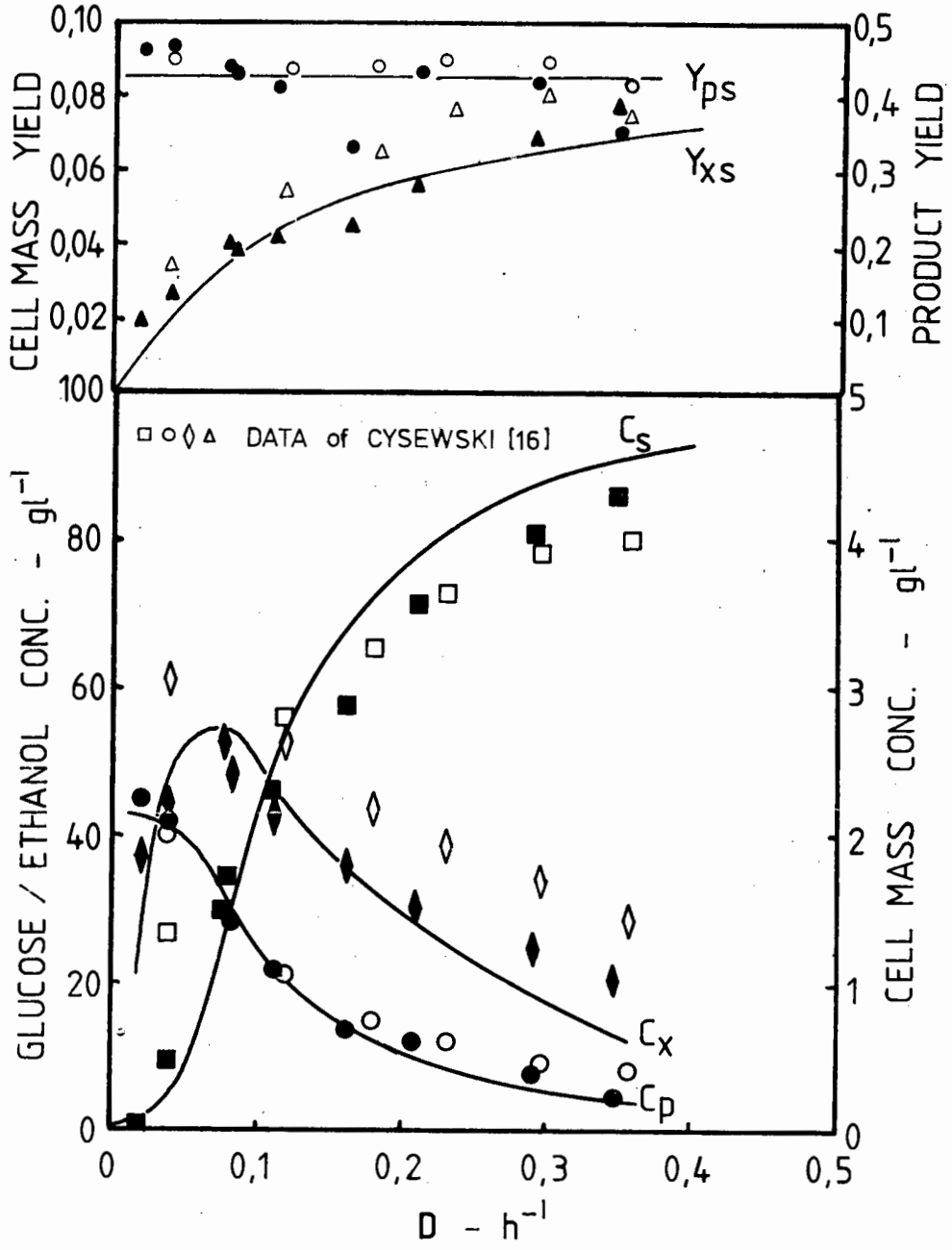

FIGURE 5.3 : PROCESS VARIABLES, EXPERIMENTAL AND PREDICTED AS A FUNCTION OF THE DILUTION RATE - ANAEROBIC WITH 100 $g\ell^{-1}$ FEED GLUCOSE CONCENTRATION

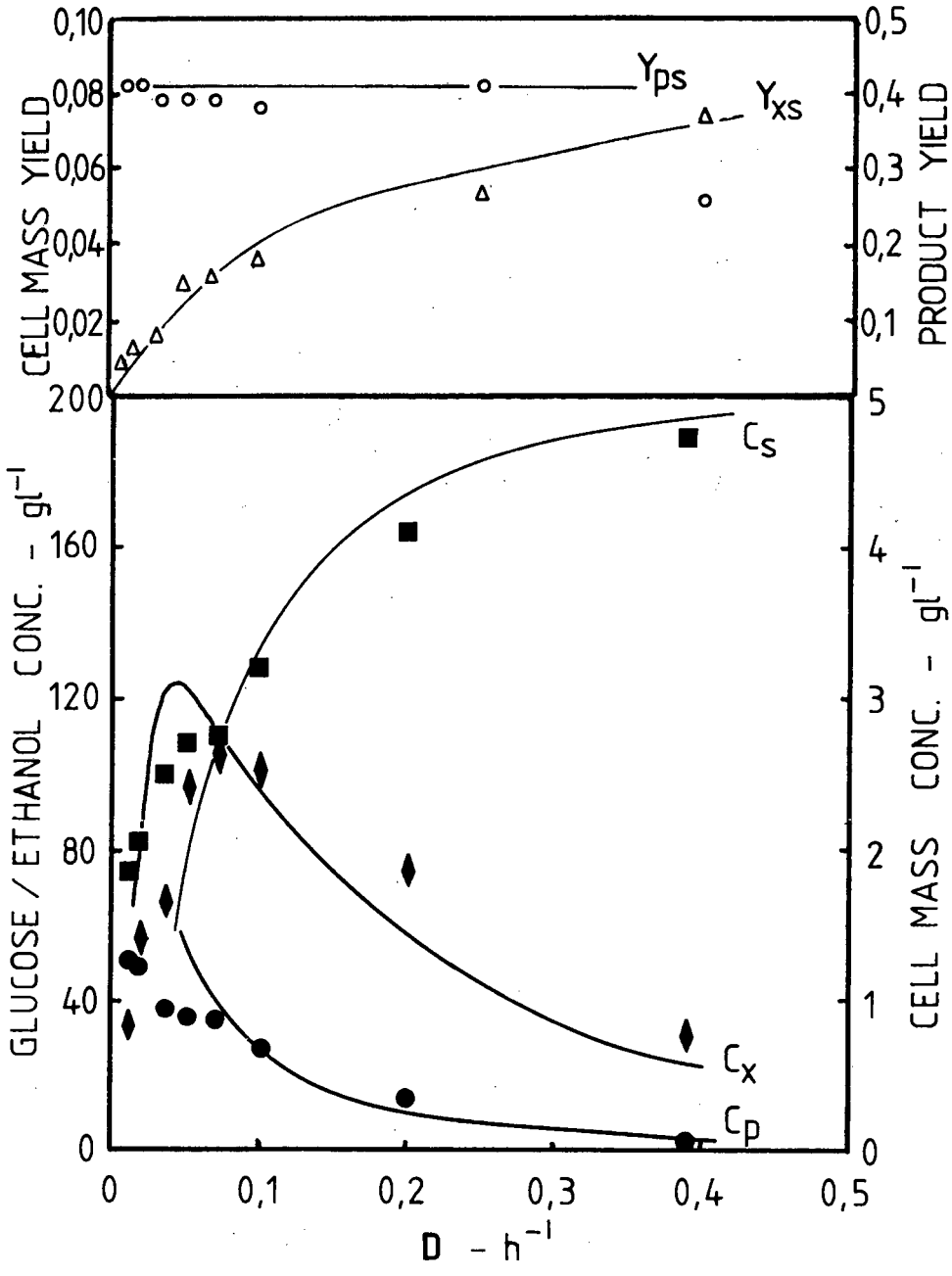

FIGURE 5.4 : PROCESS VARIABLES, EXPERIMENTAL AND PREDICTED AS A FUNCTION OF THE DILUTION RATE - ANAEROBIC WITH 200 $g\ell^{-1}$ FEED GLUCOSE CONCENTRATION

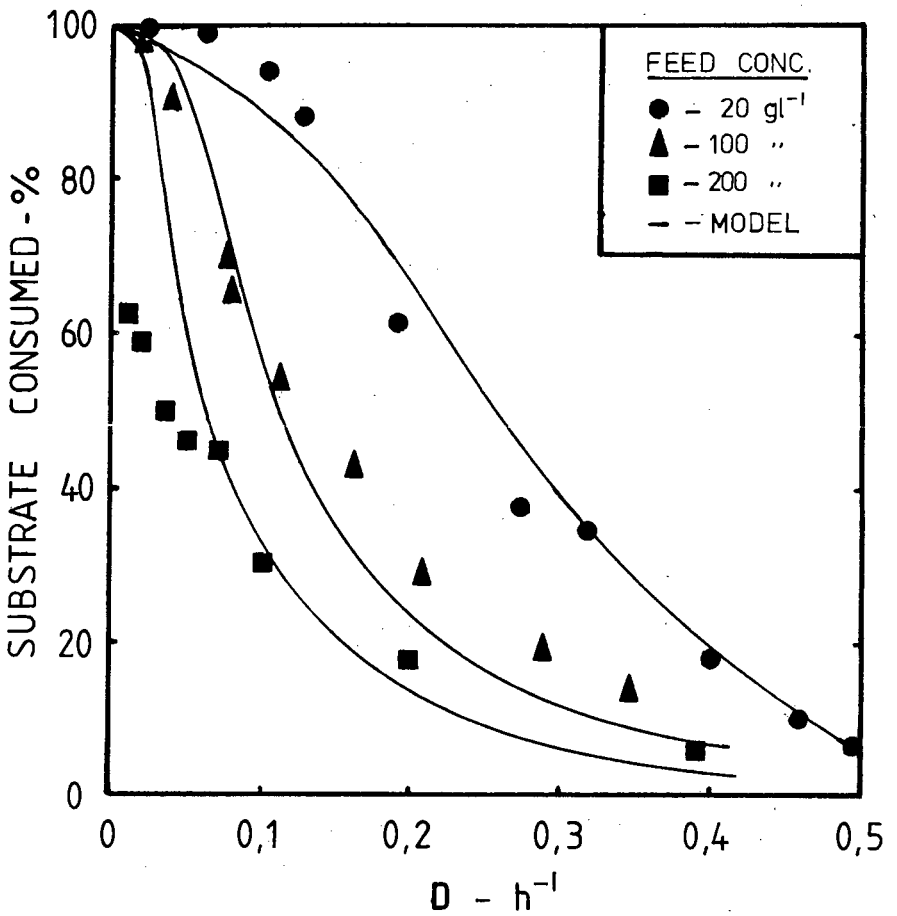

FIGURE 5.5 : PERCENTAGE SUBSTRATE CONSUMED AS A FUNCTION OF THE DILUTION RATE FOR VARIOUS FEED CONCENTRATIONS

increased less rapidly compared to those in this work.

(b) Ethanol Concentration/Ethanol yield: All the ethanol concentrations decreased with increasing dilution rate, due to the lower utilisation of substrate. The fraction of glucose converted to ethanol, i.e. the ethanol yield coefficient remained approximately constant with dilution rate. For the 100 and 200 gl^{-1} glucose feed concentrations, the yield appeared to drop above a dilution rate of 0,3 h^{-1}. This may have been due to the greater rate of oxygen supply (from the dissolved oxygen in the medium) at the high dilution rates and therefore caused a shift of some of the fermentative to respiratory metabolism. However, because of the low cell mass concentration, there could have been only a small amount of glucose diverted, which would therefore not have had the desired effect on the yield coefficient. A linear regression for ethanol concentration as a function of the glucose consumed, gave a decreased yield coefficient for the 200 gl^{-1} glucose feed concentration, i.e. 0,4 (g ethanol) (g glucose)$^{-1}$ compared to 0,44 for the two lower feed concentrations. The data of Cysewski [16] was consistant with the data found here except that the value of the ethanol concentration reported for the dilution rate of 0,04 h^{-1} would have given a yield coefficient of 0,55 which was beyond that theoretically possible. It was most probable that the substrate concentration was at the level found in this work (10 gl^{-1} not 27 gl^{-1}), which would also have given a consistent yield coefficient. The yield coefficient was also 0,44 and Pironti[19] working with anaerobic glucose fermentations of feed concentrations of 20 to 180 gl^{-1} found values in the range 0,45 to 0,47.

(c) Cell Mass Concentration/Cell Mass Yield: The cell mass concentration and the cell mass yield showed the the same trend for all three feed glucose concentrations except for the 20 gl^{-1} feed concentration at

low dilution rates. At the higher feed concentrations, the cell mass concentration increased to a maximum (approximately 2,7 gl^{-1} at 0,08 h^{-1} for both feed concentrations) and then rapidly decreased. The initial decrease towards low dilution rates was due to the energy of maintenance forming the major portion of the substrate consumed whereas the latter decrease, as the dilution rate increased was due to ethanol inhibition. This inhibition effect diminishes as the dilution rate increases because of the decreasing ethanol concentration. For the two higher feed concentrations, the cell mass yield increased rapidly initially due to the decrease in the maintenance effect and then slowly increased with increasing dilution rate. The yield coefficient is usually assumed constant (after the initial rise) and independent of dilution rate. This slow increase may have been caused by a maintenance rate which is not constant but also growth dependent; or as previously stated, the increasing rate of oxygen supply for the cell mass present may cause a shift in the metabolism and hence an increase in the yield coefficient.

For the 20 gl^{-1} feed concentration, the cell mass concentration was still increasing at the lowest dilution rate measured, 0,024 h^{-1}, although it had showed signs of decreasing at a dilution rate of 0,12 h^{-1}. The increase at even low dilution rates would have been the result of a very low or negligible maintenance rate. Similarly the yield coefficient had not decreased and was significantly higher than for the other two feed glucose concentrations. This would have seemed to indicate a nutritional deficiency between the 20 gl^{-1} feed concentration and the higher feed levels. Since all constituents of the medium were changed proportionately, the only parameter which has not decreased proportionately was the inherent oxygen content (was actually higher for the 20 gl^{-1} feed concentration due to the lower salt and sugar content). This phenomenon will be discussed again in Section 5.2 in relation

to the micro-aerobic fermentation. The data of Cysewski [16] showed a higher cell mass concentration and followed a pattern similar to that for the 20 gl^{-1} feed concentration data found here, namely, that the cell mass concentration did not decrease at lower dilution rates.

5.1.3 Ethanol Productivity

The ethanol productivities for the three glucose feed concentrations are given in Figure 5.6. Immediately evident was the similarity of the productivity curves for the 100 and 200 gl^{-1} feed concentration. Whereas the productivity for the 20 gl^{-1} feed curve rose gradually and decreased again immediately at a lower rate, the productivity for the two higher concentrations rose rapdily, remained at a plateau, i.e. from 0,08 to 0,28 h^{-1}, and decreased again rapidly. In all three cases the maximum occurred at a dilution rate of approximately 0,20 h^{-1}. However, the productivities at the 100 and 200 gl^{-1} feed concentrations were only 2,4 and 2,7 times higher respectively than at the 20 gl^{-1} feed concentration level compared to feed concentration increases of 5 and 10 fold respectively. This was because of the poorer substrate utilisations for the higher feed concentrations. However, at the onset of the plateau for the two higher feed concentrations, productivities were 94% of their maximum with only 40% of the optimum dilution rate, but the substrate utilisation had doubled from 32 to 65% and 18 to 37% for the 100 and 200 gl^{-1} feed concentrations respectively. This would be of economic importance because of the high substrate costs.

By comparing the productivity curves with the biomass concentration profiles, especially for the 100 and 200 gl^{-1} feed concentrations, the onset of the maximum productivity plateau corresponded to the maximum cell mass concentration. Such a correspondence was not evident for the lowest feed concentration.

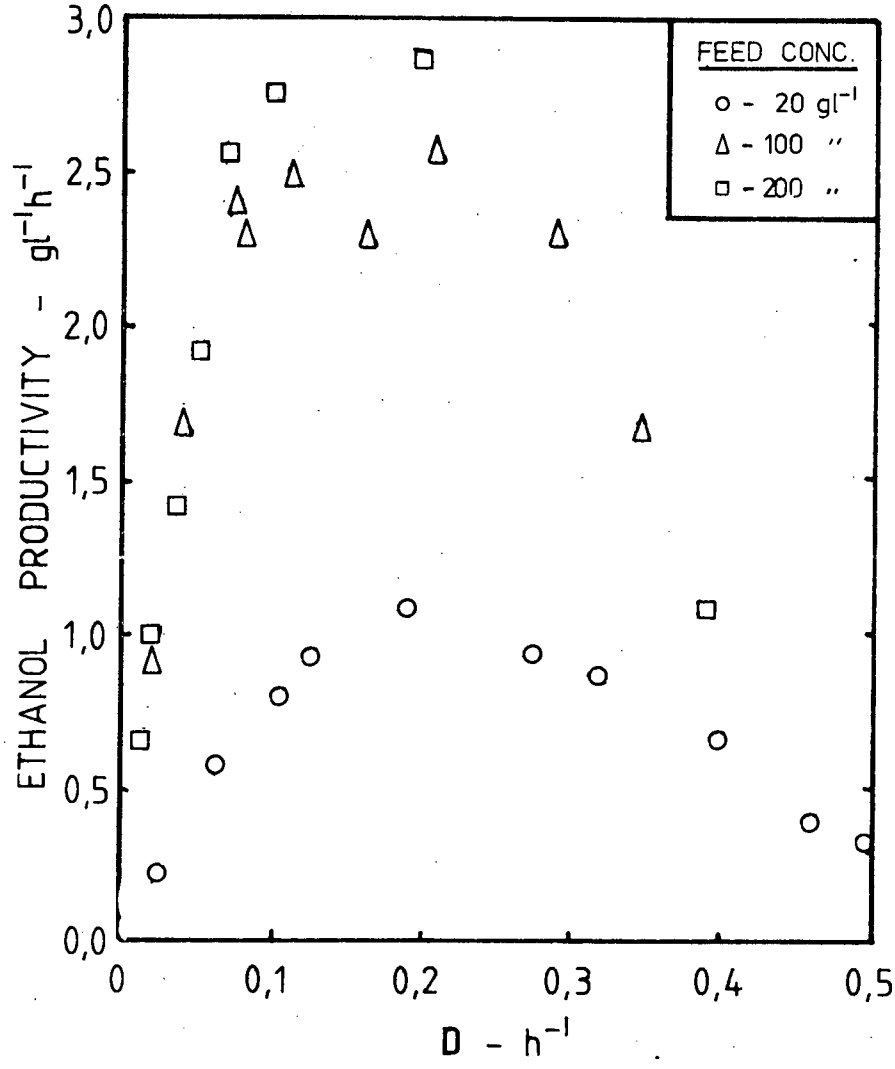

FIGURE 5.6 ETHANOL PRODUCTIVITY AS A FUNCTION OF THE DILUTION RATE FOR VARIOUS FEED CONCENTRATIONS

The maximum ethanol productivities achieved compared favourably with those from literature obtained under similar conditions, see Table 5.1.

TABLE 5.1 MAXIMUM ETHANOL PRODUCTIVITIES

Source	Feed Conc. (gl^{-1})	Max. Eth. Prod. ($gl^{-1}h^{-1}$)	D (h^{-1})	Substrate Utilised (%)
Bazua & Wilke [7]	9,4	1,28	0,27	96
Pironti [19]	20,0	2,0	0,22	99,8
This Work	20,0	1,1	0,19	62
Pironti [19]	90,0	3,5	0,14	60
Cysewski [16]	100,0	2,9	0,32	20
This Work	100,0	2,6	0,21	29
Pironti [19]	180,0	2,4	0,048	66
This Work	200,0	2,9	0,200	18

5.1.4 Growth Curve - Experimental and Model

The experimental growth curves for this particular microbial system for different glucose feed concentrations are given in Figure 5.7. For comparison, a Monod growth curve with arbitrary constants was also depicted. This immediately showed that the experimental growth curves were far removed from those that would be predicted by the Monod equation. Because glucose has been shown to have little effect on the growth kinetics for the range of glucose concentrations considered here (Section 2.3), the inhibition due to the ethanol is considerable and must therefore be allowed for in a model describing the growth. A form, as given by Equation (3.1), has been used to model the experimental results. By means of a Nelder-Mead [25] minimisation routine on a UNIVAC 1106 computer, the following values for the constants were determined in the model.

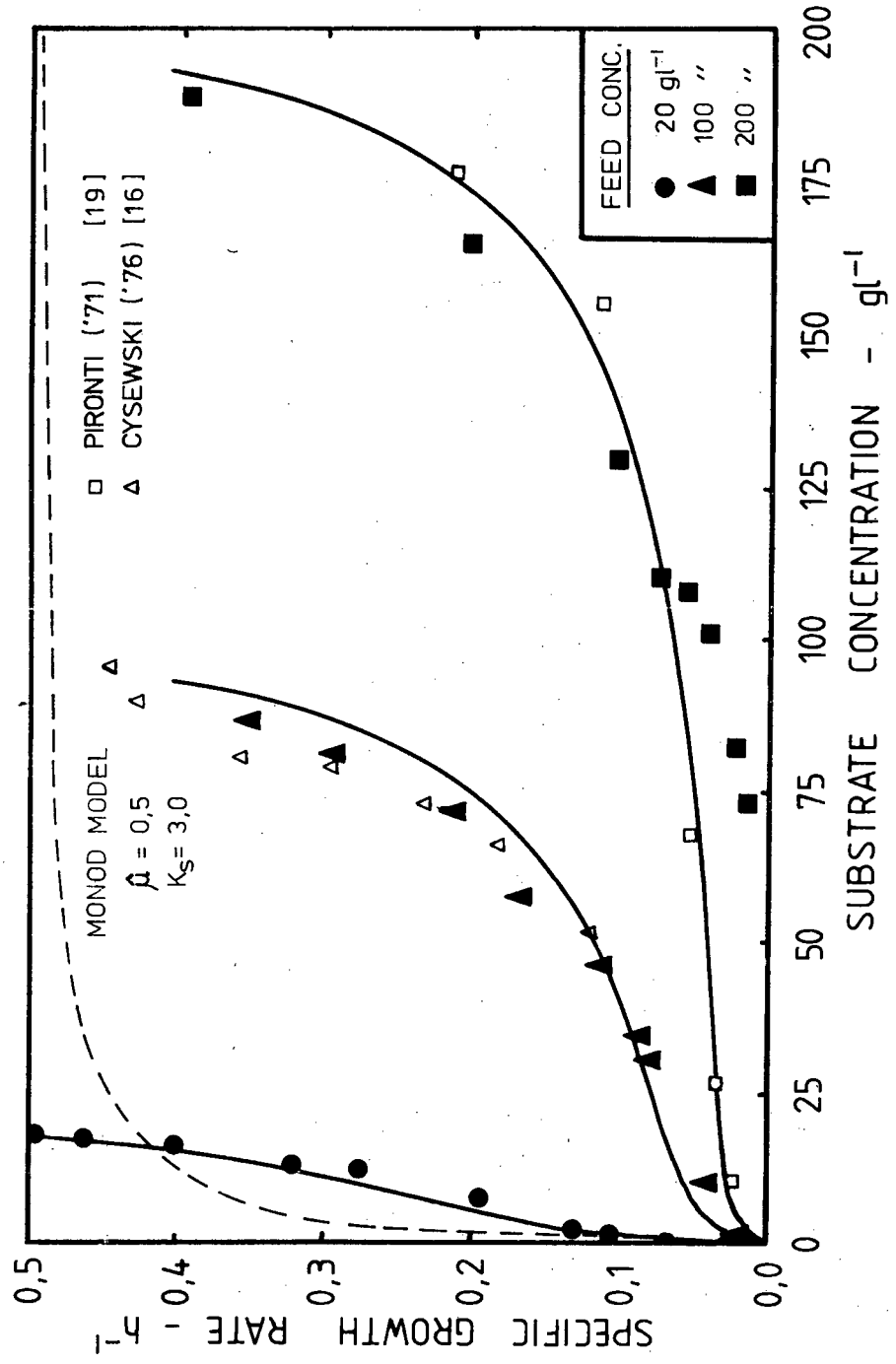

FIGURE 5.7 : SPECIFIC GROWTH RATE, EXPERIMENTAL AND PREDICTED, FOR DIFFERENT FEED CONCENTRATIONS

$$\text{MODEL:}\quad \mu = \hat{\mu} \cdot \frac{C_s}{C_s+K_s} \cdot \frac{K_p}{K_p+C_p}$$

where $\hat{\mu} = 0{,}64\ h^{-1}$

$K_s = 3{,}3\ g l^{-1}$

$K_p = 5{,}2\ g l^{-1}$

The complete data from all the fermentations (i.e. for all the steady states of the three feed glucose concentrations) was used. The model had been generalised further. Instead of using the experimentally determined ethanol concentrations, these were all combined to give an overall ethanol yield coefficient, equal to 0,43 (g ethanol)/(g glucose consumed) (see Figure 5.8). The following substitution was therefore possible:

$$C_p = Y_{ps}(C_{sf} - C_s) = 0{,}43\ (C_{sf} - C_s)$$

and allowed the specific growth rate to be determined at any glucose concentration for any given glucose feed concentration. An "operating profile" could therefore be determined, given a particular feed concentration.

The specific growth rate curve as predicted by the model for the three different glucose feed concentrations was also shown in Figure 5.8. The fit was good except for the low dilution rates of the 200 $g l^{-1}$ feed concentration. However, the following points need to be made concerning the modelling of the three overall fermentations as a single unit:

(i) that the same conditions be applied to each fermentation, both environmental and nutritional - the concentration of oxygen (considered as a nutrient or growth factor) available to the cells was lower for the higher sugar concentration because of the inherent lower oxygen concentration in the medium and because of the higher concentration

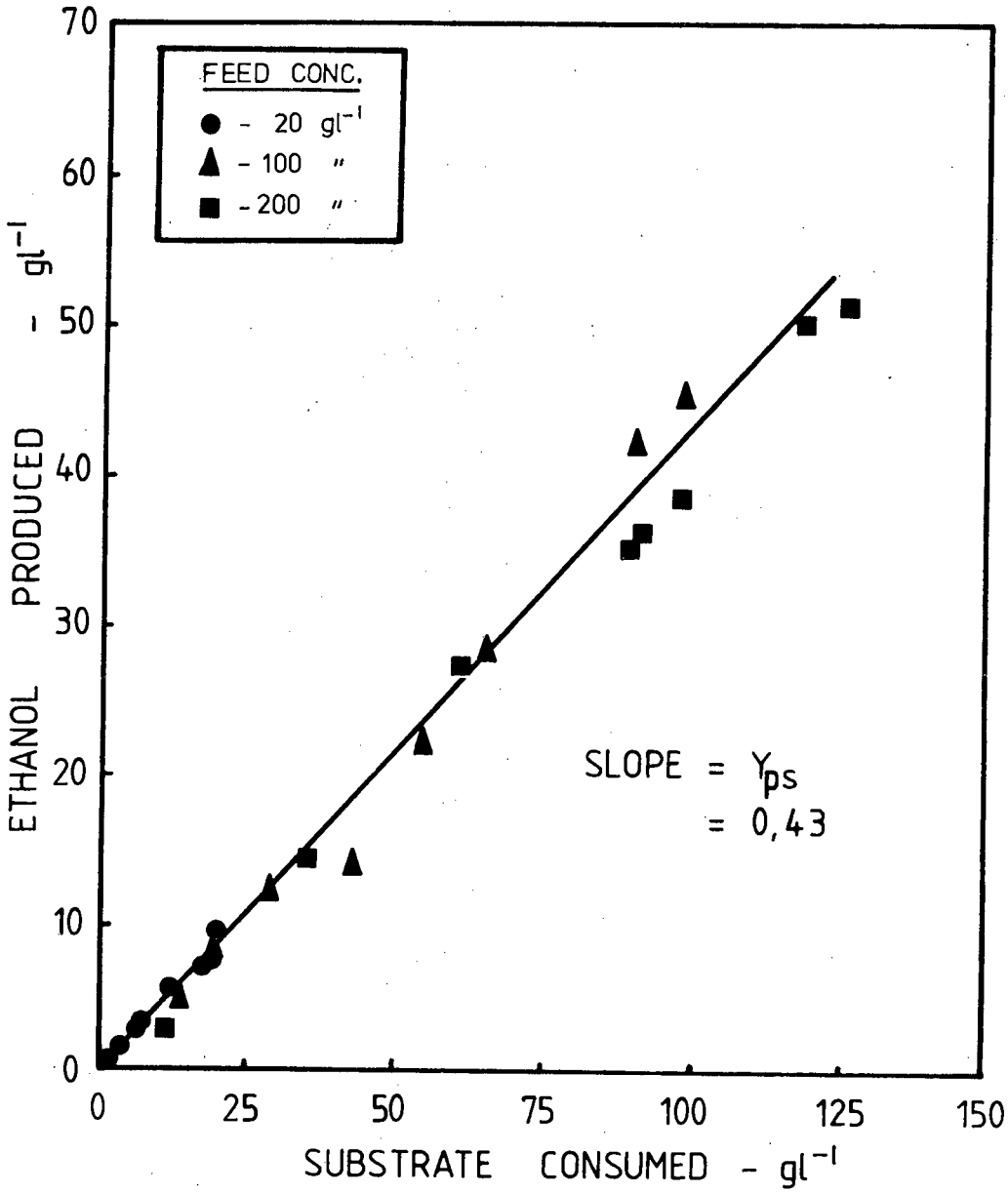

FIGURE 5.8 : ETHANOL PRODUCED AS A FUNCTION OF THE SUBSTRATE CONSUMED FOR DIFFERENT FEED CONCENTRATIONS

of cells - this may or may not have had a significant effect.

(ii) during the 20 gl^{-1} fermentation, substrate limiting growth was experienced plus inhibition by ethanol whereas at the higher feed concentrations the growth was limited by the effect of ethanol only - this implied that the variable K_S which was important at low glucose concentrations should have been determined preferentially by the 20 gl^{-1} feed concentration data, i.e. K_S was very insensitive on the form of the growth curve for the 200 gl^{-1} feed concentration (see also section 5.4 for a sensitivity analysis on the model).

(iii) the Nelder-Mead [25] minimisation routine (based on the simplex method for function minimisation) needed to be used with care as it was able to give different results for different minimisation parameters and initial conditions.

The modelling of the individual growth curves was also attempted and the results are given in Table 5.2 and shown graphically in Figures 5.9 and 5.10.

In order to improve the fit of the 20 gl^{-1} data, it was necessary to use a lower value, 0,5 gl^{-1} for the saturation constant K_S. The ethanol inhibition constant decreased because the lowering of the value of K_S required a greater degree of inhibition, i.e. the greater the value of K_S, the lower the Monod curve.

For the two higher feed concentrations, a wide variation was obtained for all the constants in the model. The very high maximum specific growth rates appeared to be beyond those found in the literature, and therefore for the 100 gl^{-1} feed concentration, this parameter was forced to a constant value. The increased

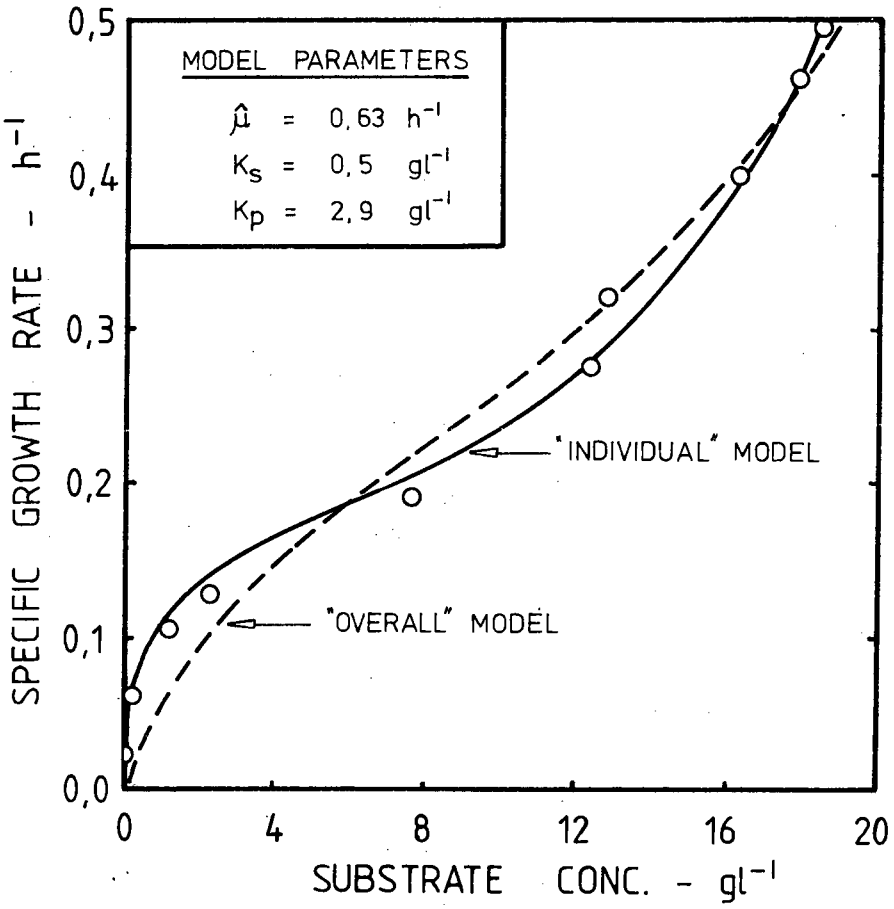

FIGURE 5.9 : OVERALL AND INDIVIDUAL GROWTH MODELS FOR THE 20 $g\ell^{-1}$ GLUCOSE FEED CONCENTRATION FERMENTATION

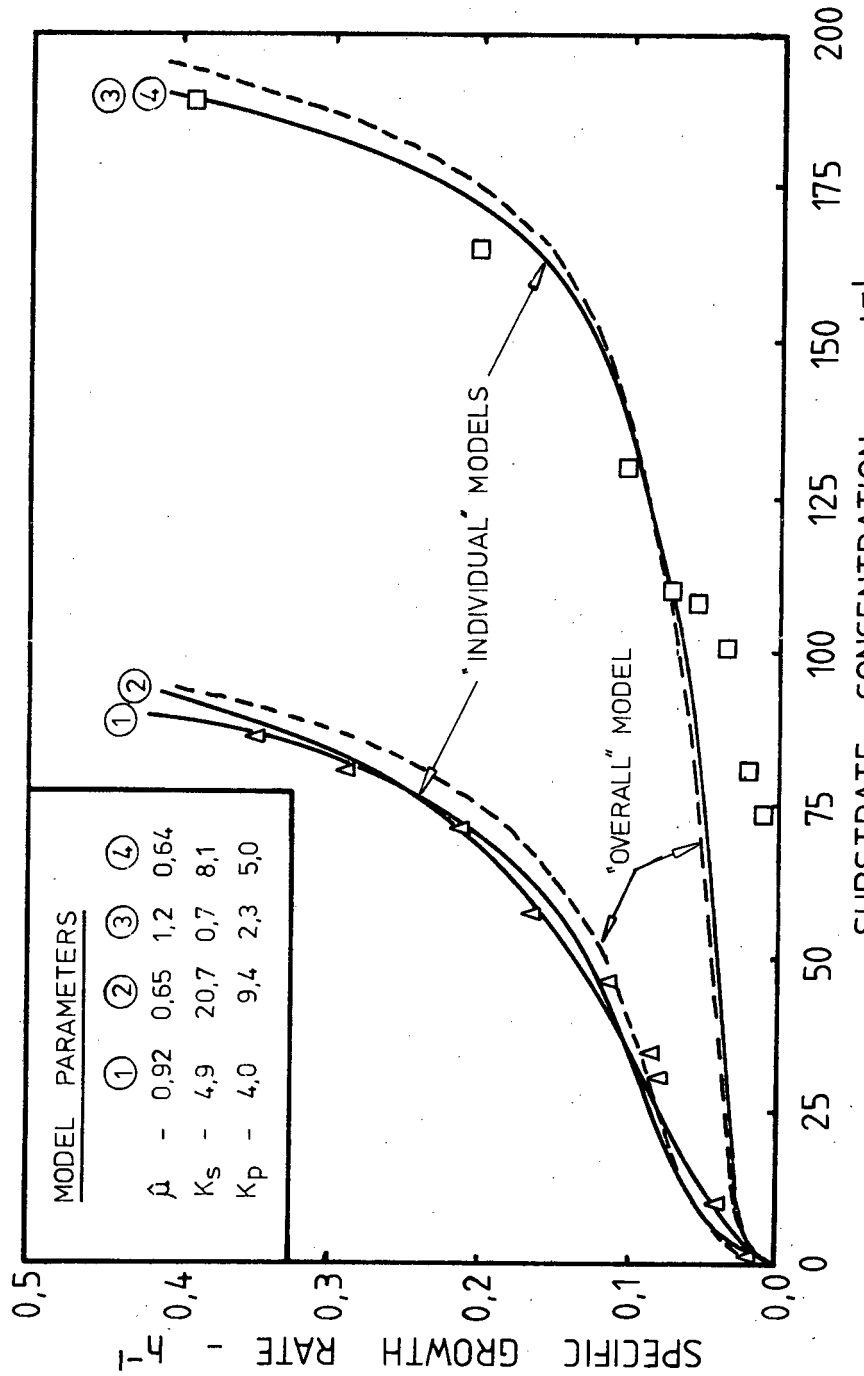

FIGURE 5.10 : OVERALL AND INDIVIDUAL GROWTH MODELS FOR THE 100 AND 200 gl^{-1} GLUCOSE FEED CONCENTRATION FERMENTATIONS

value of K_s therefore also increased the value of K_p, i.e. decreased the degree of inhibition. The same occurred for the 200 gl^{-1} feed concentration. The good fit for model four (see Figure 5.10), which had very similar values for the constants to those in the overall model, was because of the use of experimentally obtained ethanol concentrations. The experimental value at the highest dilution rate was very much lower than that predicted by the yield coefficient, i.e. 2,8 gl^{-1} compared to 4,7 gl^{-1}, and this decreased the inhibition effect of the ethanol, increasing the predicted growth rate.

TABLE 5.2 MODELLING OF THE INDIVIDUAL GROWTH CURVES COMPARED WITH VALUES FOR THE COMPOSITE DATA.

Model Parameter / Feed Concentration (gl^{-1})	$\hat{\mu}$ (h^{-1})	K_s (gl^{-1})	K_p (gl^{-1})	Y_{ps} (gg^{-1})
20	0,63	0,5	2,9	0,44
100	0,92 0,65*	4,9 20,7	4,0 9,4	0,44 0,44
200	1,2 0,64	0,7 8,1	2,3 5,0	0,43 Exp C_p
20, 100, 200	0,64	3,3	5,2	0,43

*This value for $\hat{\mu}$ was forced for comparison.

The model parameters could also have been derived directly from the experimental results. With the assumption that the saturation constant was much less than the substrate concentration, Equation (3.3) was applied. The resultant curve is given in Figure 5.11 and showed that for low concentrations of ethanol, corresponding to high concentrations of substrate glucose, a linear relationship existed between the

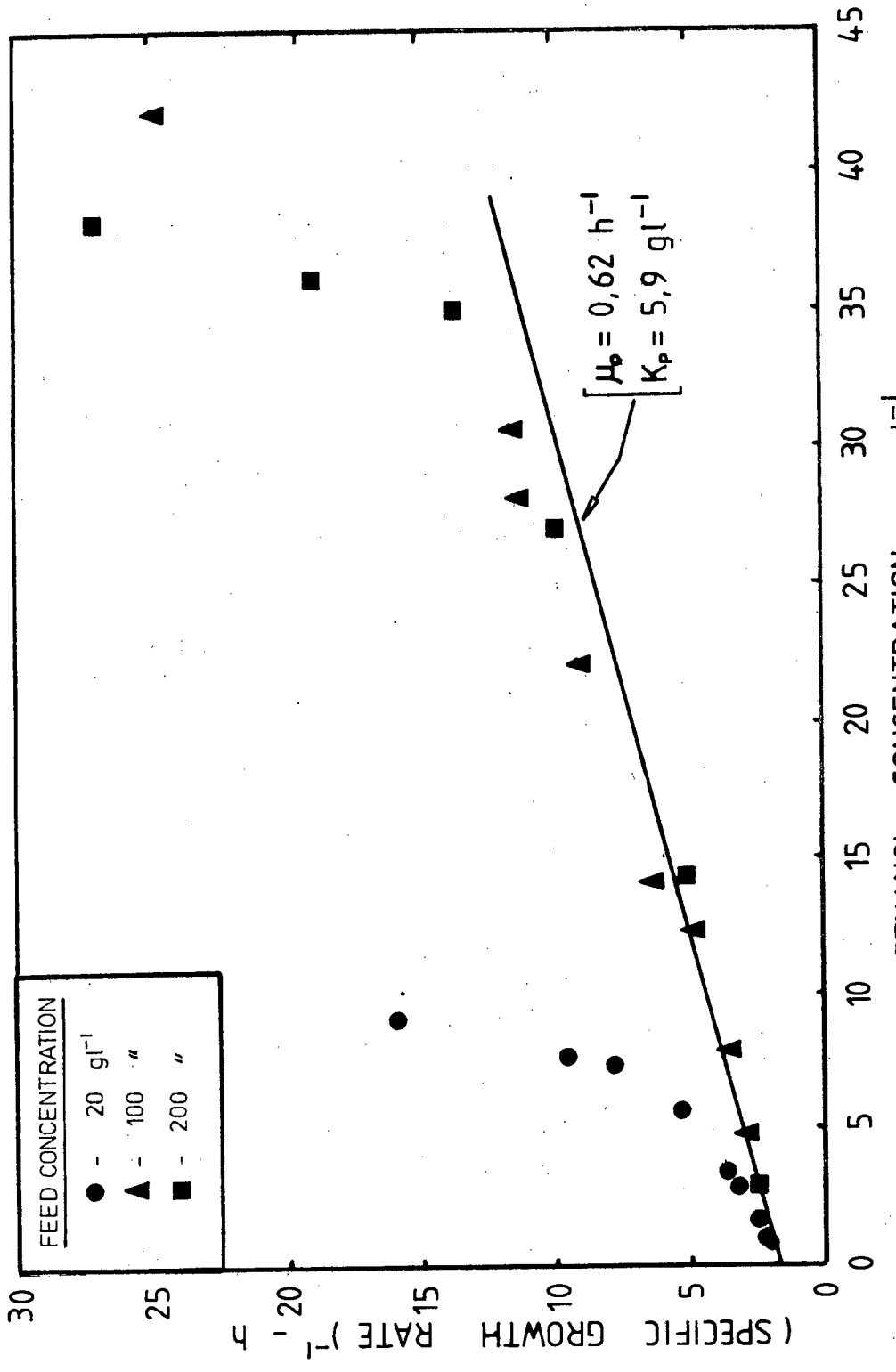

FIGURE 5.11 : INVERSE OF THE SPECIFIC GROWTH RATE AS A FUNCTION OF THE ETHANOL CONCENTRATION FOR DIFFERENT FEED CONCENTRATIONS

inverse of the specific growth rate and the ethanol concentration. The data was analysed for two cases:

(i) if the unknown K_s value was significant with respect to the substrate concentration values experienced during the bulk of the 20 gl^{-1} feed concentration fermentations, then the data from the higher feed glucose concentrations only would apply;

(ii) if the unknown Ks value was very much less than the substrate concentration levels encountered during the 20 gl^{-1} feed concentration fermentations, all sets of data could have been used, or at least both separately.

From Figure 5.11, it was possible to estimate two relationships. By linear regression on the lower six data points (100 and 200 gl^{-1} feed concentration data combined) the following equation was obtained

$$\frac{1}{\mu} = 1,60 + 0,27\ C_p$$

where

$$\frac{1}{\hat{\mu}} = 1,60 \quad \text{i.e.} \quad \hat{\mu} = 0,62\ h^{-1}$$

and

$$\frac{1}{\hat{\mu}K_p} = 0,27 \text{ i.e. } K_p = 5,9\ gl^{-1}$$

These are very similar to the overall values obtained by the optimisation routine. The first one or two points from the 20 gl^{-1} feed concentration could also have been incorporated in the analysis. However, a separate analysis on the first five points for the 20 gl^{-1} feed concentration gave the following values for the constants

$\hat{\mu}$ = 0,62 h^{-1}

K_p = 2,8 gl^{-1}

which again are very representative of the minimisation parameters obtained for that feed concentration.

The estimation of K_s was not possible because of insufficient data at very low substrate i.e. glucose, concentrations. However, as was stated in the above determination of the maximum specific growth rate and the ethanol inhibition constant, the relative magnitude of K_s could have been estimated. In Figure 5.11 the curves for the 20 gl^{-1} feed concentration very quickly departed from the curve for the two higher feed concentrations. Since the deviation from linearity in this form of plot would have been due to K_s, implies that K_s was significant at the glucose levels experienced in the 20 gl^{-1} feed concentration fermentations. This conclusion could also have been reached by considering the effect of ethanol on the specific growth rate directly, as in Figure 5.12. From the figure it was immediately evident that another factor had a decreasing effect on the specific growth rate. For the same ethanol concentration, different substrate levels existed dependent on the initial feed concentration. If K_s was insignificant to all these levels, then the specific growth rate would have been the same for all feed concentrations and a single relationship would have resulted. It must be noted that deviation from the single relationship would eventually have occurred for any feed concentration when the ethanol concentration reached the maximum possible for that feed concentration.

The variation of the values for the constants in the model with those found in the literature was considerable. The maximum specific growth rate was found to be higher as with the value for the substrate saturation constant. The value for K_p, the ethanol inhibition

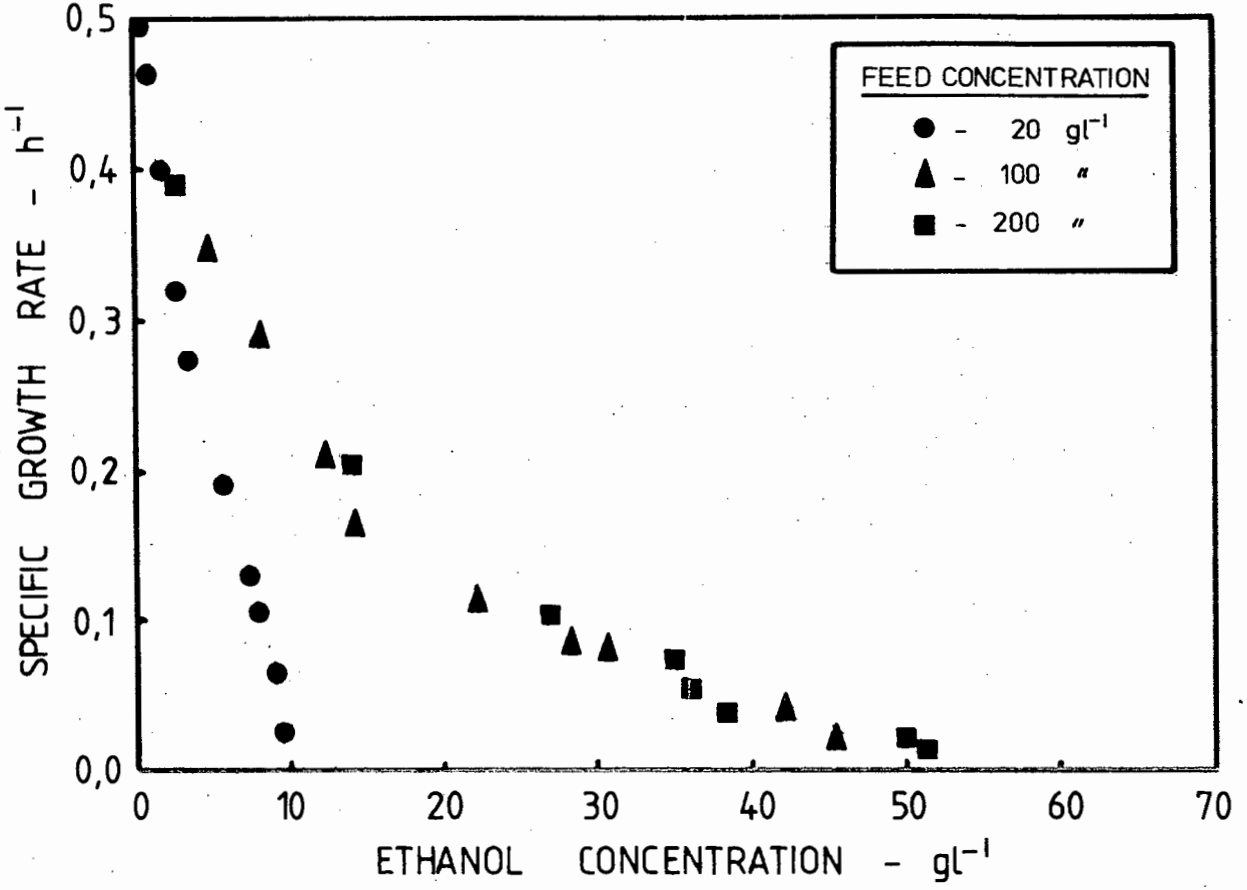

FIGURE 5.12 : SPECIFIC GROWTH RATE AS A FUNCTION OF THE ETHANOL CONCENTRATION FOR DIFFERENT FEED CONCENTRATIONS

constant, was lower which implied a greater degree of inhibition. Only Strehaiano et al [10] found a value considerably lower than was evaluated here. Table 5.3 presents the various literature values for $\hat{\mu}$, K_s and K_p, where it has been derived from a similar inhibition relationship. The effect of these different values for the inhibition constant on the specific growth rate is shown in Figure 5.13. The effects of other inhibition functions was also included. All the experiments in the literature evaluations were conducted by observing the effect of ethanol added to the feed stream whereas the ethanol was produced by the yeast in these experiments. This indicated that the ethanol produced by the cells was more toxic than that added to the medium. This supported the findings of Nagodawithana and Steinkraus [9] and Navarro and Durand[12], obtained from batch experiments.

5.1.5 Prediction of the Fermentation Concentrations

A further test for the growth model, was to use it to predict the concentration profiles for any continuous fermentation. Since the specific growth rate has been expressed as a function of the substrate concentration only, it was in effect also a statement of the substrate concentration as a function of the dilution rate, because the specific growth rate and the dilution rate are equivalent for a continuous stirred tank reactor. Hence the growth curve is also equivalent to the substrate concentration profile.

The ethanol concentration profile with respect to the dilution rate has also been fixed because a constant ethanol yield coefficient has been established. Both the predicted curves for the substrate (glucose) and ethanol concentrations have been shown in Figure 5.2 to 5.4 for the three different feed concentrations.

To evaluate the cell mass concentration using the model it was necessary to allow for the varying cell

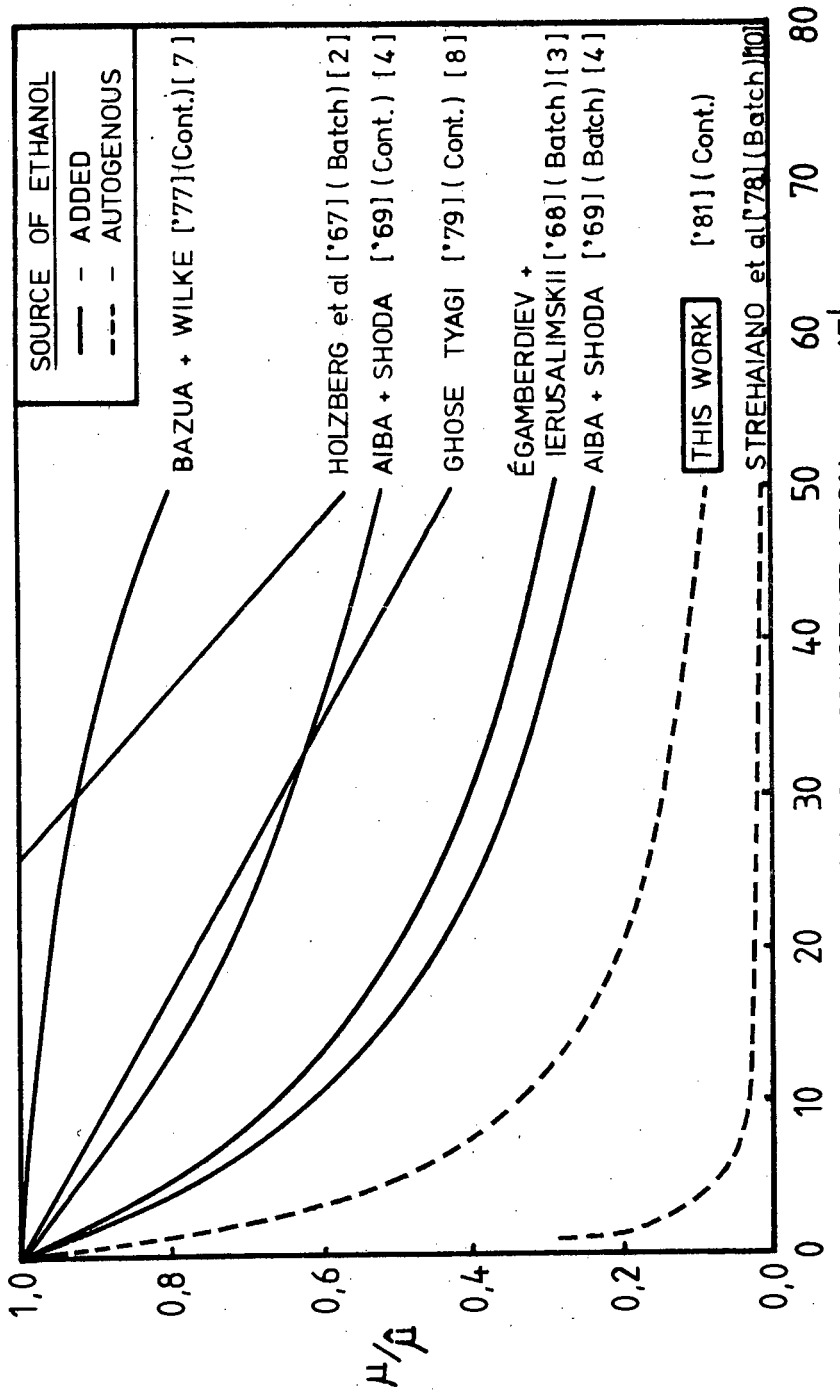

FIGURE 5.13 : COMPARISON OF THE EFFECT OF VARIOUS ETHANOL INHIBITION FUNCTIONS

TABLE 5.3 COMPARISON OF LITERATURE GROWTH MODEL PARAMETERS

SOURCE	$\hat{\mu}$ (h^{-1})	K_s (gl^{-1})	K_p (gl^{-1})	MODE OF OPERATION
Égamberdiev and Ierusalimskii [3]	0,31	-	20,6	Batch, 17,5% grape sugar
Aiba and Shoda [4]	0,28 0,43	0,22	16,0 55,0	Batch, 2% glucose Continuous, "
Bazua and Wilke [7]	0,45	0,24	-	Continuous, 1% glucose
Strehaiano et al [10]	-	-	0,4	Batch, 2,25% glucose
Yarovenko and Nakhmanovich [11]	0,12	-	15,8	Continuous, 2% wheat sugar
Leuenberger [26]	0,60	0,11	-	Continuous, 0,4% glucose

mass yield coefficient. This was done by introducing a specific maintenance rate which was determined using Equation (3.5). Figure 5.14 shows the substrate utilisation rate as a function of the dilution rate where the intercept of the straight lines at zero dilution rate represented the specific maintenance rate with the maximum cell mass yield coefficients being given by the slope of the lines. The data is summarised in Table 5.4 and showed that the specific maintenance rate increased with an increasing glucose feed concentration.

TABLE 5.4 SPECIFIC MAINTENANCE RATES AND MAXIMUM CELL MASS YIELD COEFFICIENTS

GLUCOSE FEED CONC (C_{sf} - gl^{-1})	SPECIFIC MAINTENANCE RATE (m - h^{-1})	MAXIMUM CELL MASS YIELD (Y_{xs})	CORRELATION COEFFICIENT
20	0,7	0,15	0,93
100	1,3	0,09	0,92
200	1,7	0,10	0,99

The maximum cell mass yield for the 20 gl^{-1} feed concentration was significantly greater than at the higher feed concentrations. The specific maintenance rates are very high compared to the literature, where values of 0,063 (g glucose)/(g cell mass.h) have been found (Pirt [22]). The values for the cell mass yield were typical (Cysewski [16], Aiba et al [5], Pironti [19]).

Closer examination of the data points showed that the data for the 20 and 100 gl^{-1} feed concentrations could also have been made to lie on non-linear curves which would have extrapolated through the origin, i.e. the specific maintenance maybe growth dependent as has been shown for a bacterium, Klebsiella aerogenes by Djavan and James [28]. For the two lower feed

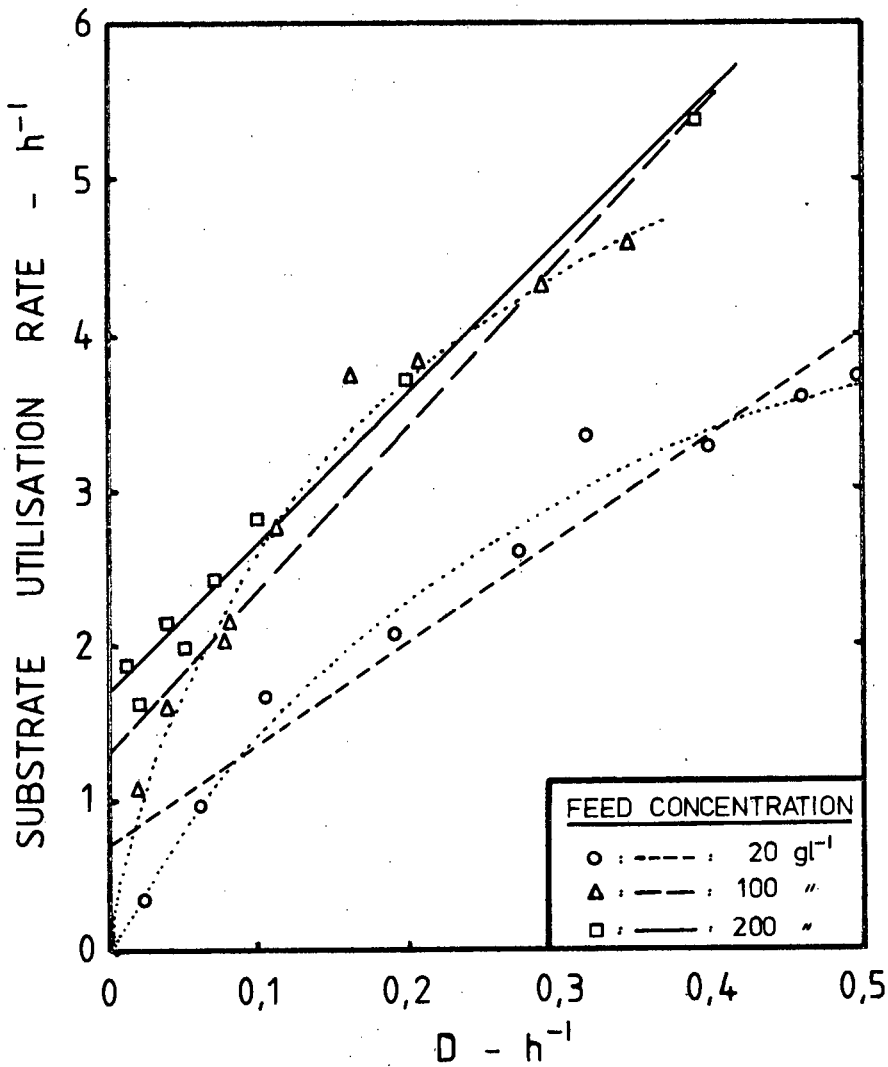

FIGURE 5.14 : SUBSTRATE UTILISATION RATE AS A FUNCTION OF THE DILUTION RATE FOR DIFFERENT FEED CONCENTRATIONS

concentrations the data point at the lowest dilution rate represented a substrate utilisation rate below the derived specific maintenance rate. This phenomenon will be discussed further in Section 5.5. At the higher dilution rates, the SUR increased less rapidly with an increase in the dilution rate.

The curves in Figure 5.14 represent an even distribution of the data points and give in regression therefore, equal weighting to the individual points. The points were also obtained in a random manner and not in an order of increasing or decreasing dilution rate. However, the specific maintenance rate and the maximum cell mass yield may also be derived from another similar plot which has however a bias towards the points at the lower dilution rates. It is derived by dividing Equation (3.5) by the dilution rate to give

$$\frac{(C_{sf}-C_s)}{C_x} = \frac{m}{D} + \frac{1}{Y_{xs}}$$

where the reciprocal of the observed yield is plotted against the reciprocal of the dilution rate. Reanalysis by this plot gave values of m and Y_{xs} as in Table 5.5. The results showed no consistent pattern, and were more irregular than those determined initially. For the 20 gl^{-1} feed concentration the lower two dilution rate states were excluded because of their very strong effect.

TABLE 5.5 REANALYSIS OF m AND Y_{xs}.

FEED CONC. (gl^{-1})	m - h^{-1}	Y_{xs}	CORRELATION COEFF.
20	1,06	0,18	0,98
100	0,79	0,07	0,94
200	1,68	0,11	0,98

Since no constant value was obtained for either the specific maintenance rate and the maximum cell mass yield, the initial individual values were used to predict the cell mass concentration as a function of the dilution rate. Although m and Y_{xs} could have been expressed as functions in terms of the feed glucose concentration, C_{sf}, e.g.

$$m = 0,22\ C_{sf}^{0,39} \qquad (r^2 = 0,996)$$

$$Y_{xs} = 0,142 - 0,00024\ C_{sf} \qquad (r^2 = 0,56)$$

it was felt that the three points did not make a representative sample. The cell mass concentration curves are also shown in Figure 5.2 to 5.4. They predicted a rise and gentle fall off as found with the experimental results except for the 20 gl^{-1} feed concentration where this had not been found experimentally. The agreement between predicted and experimental was fair.

Figure 5.15 shows data that has been calculated from literature results which were obtained from experiments performed under similar conditions. Their values for the specific maintenance rate and maximum cell mass yield are given in Table 5.6 and showed great variance in the specific maintenance rate with values which were very much lower. Only the results of Cysewski[16], whose experiments were performed closest to the conditions used in this study (although the temperature was higher at 35°C), showed an appreciable specific maintenance rate. Since Cysewski [16] had shown 35°C to be the optimum growth temperature, the specific maintenance rate could have been increased by the reduction of the temperature to 30°C as was used here. When comparing the maximum yield coefficients, these were very similar within any one feed concentration and followed the pattern observed in this study, namely a value of 0,140 at 20 gl^{-1} feed, decreasing to a constant value of 0,095 for 100 gl^{-1} feed concentrations and higher. These extra values for m and Y_{xs} did not

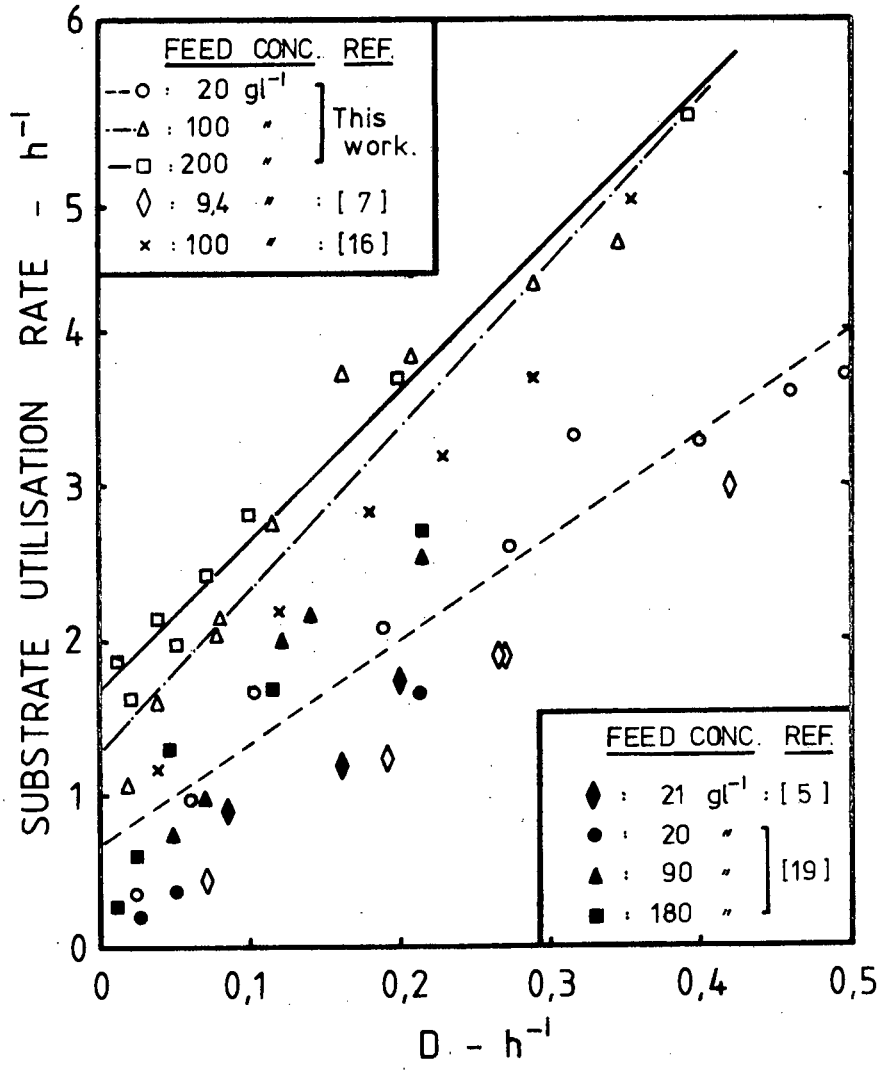

FIGURE 5.15 : LITERATURE SUBSTRATE UTILISATION RATES AS A FUNCTION OF THE DILUTION RATE COMPARED TO THOSE OF THIS WORK

improve the correlation with glucose feed concentration, C_{sf}.

TABLE 5.6 LITERATURE ESTIMATIONS OF m AND Y_{xs}

SOURCE	$C_{sf}(gl^{-1})$	m-(h^{-1})	Y_{xs}	r^2
Bazúa and Wilke [7]	9,4	0,00*	0,136	0,999
This work	20	0,70	0,151	0,94
Pironti [19]	20	0,00*	0,129	0,999
Aiba et al [5]	21	0,27	0,145	0,89
This work	100	1,30	0,094	0,92
Pironti [19]	90	0,33	0,089	0,91
Cysewski [16]	100	0,80	0,093	0,98
Pironti [19]	180	0,39	0,091	0,94
This work	200	1,68	0,104	0,99

*NB: where these values were negative, they were given the value zero.

5.1.6 Product Formation Rate

Ethanol productivity has been considered in the previous section, but this will be extended here to the specific ethanol productivity. This has been shown by Equation (3.6) to be related to the specific maintenance rate and the specific growth rate. Figure 5.16 shows the specific ethanol productivity to be a linear function of the dilution rate. However, at the higher feed glucose concentrations, the curves showed a maximum at approximately the same dilution rate of 0,3 h^{-1}. This appeared to be due to the very rapid decrease in the ethanol productivity at this point. For the 20 gl^{-1} feed concentration, both the ethanol productivity and the cell mass concentration decreased slowly.

Using the terminology of Section 3, namely α and β as the Luedeking and Piret [29] constants equivalent to

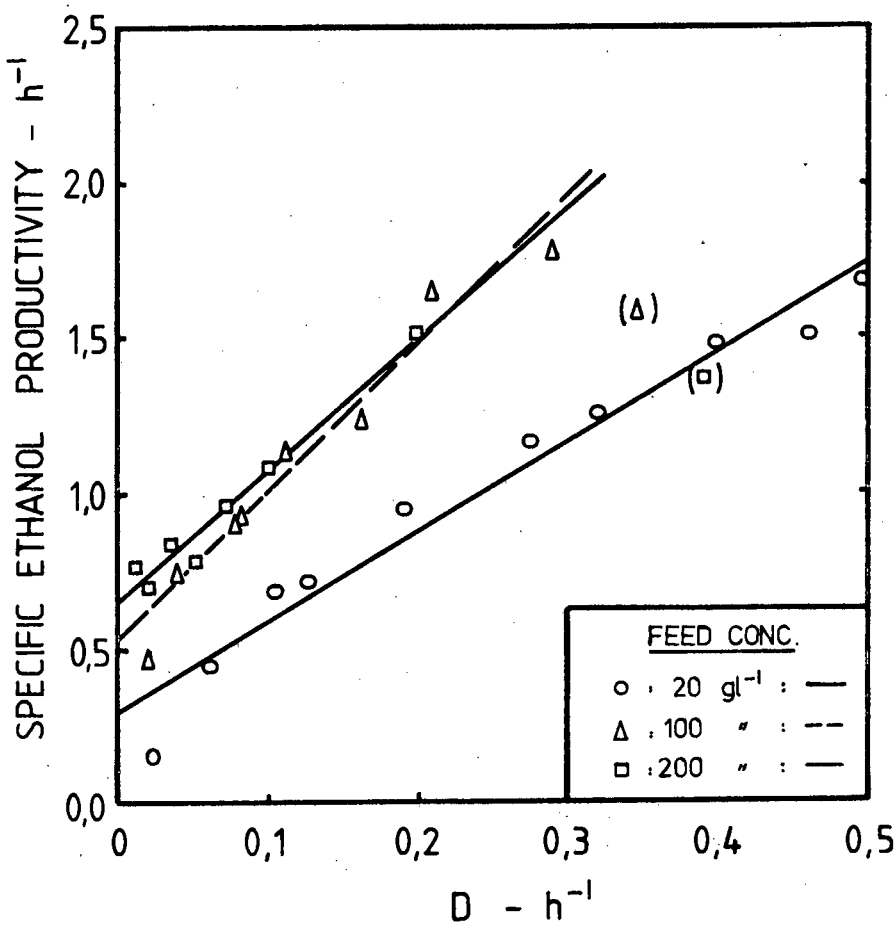

FIGURE 5.16 : SPECIFIC ETHANOL PRODUCTION RATE AS A FUNCTION OF THE DILUTION RATE FOR DIFFERENT FEED CONCENTRATIONS

Y_{ps}/Y_{xs} and mY_{ps} respectively, the value of the constants may be determined from Figure 5.16 and are given in Table 5.7. They have been compared to other constants derived from the literature. The values of β were high for this work due to the high specific maintenance rates. The values of α appeared consistent with those derived from the literature and increased with increasing feed concentration. Hence the productivity per unit of cell mass increased with increasing feed concentration.

The effect of ethanol inhibition on the specific ethanol productivity has also been examined. Figure 5.17 showed that the specific ethanol productivity was not a linear function of the ethanol concentration whereas an inverse relationship similar to non-competitive enzyme inhibition gave a better fit as in Figure 5.18 but was not conclusive. The two functions were as follows:

LINEAR: $\nu = \frac{DC_p}{C_x}$ = specific ethanol productivity

$= 1{,}69 - 0{,}022\ C_p \qquad (r^2 = 0{,}86)$

$= 0{,}022\ (75{,}9 - C_p) \quad$ cf. $\nu = B(C_{pm} - C_p)$

$= 1{,}69\ (1 - C_p/75{,}9) \qquad = A(1 - C_p/C_{pm})$

where A,B = constants

C_{pm} = maximum ethanol concentration in the medium

INVERSE: $\nu = 1{,}95 \cdot \frac{27{,}6}{27{,}6 + C_p}$ cf. $\nu = \nu_{max} \frac{K'_p}{K'_p + C_p}$

$(r^2 = 0{,}89)$ where ν_{max}, K'_p = constants

The linear form was similar to those expressed by Navarro and Durand [12] and Ghose and Tyagi [8] . Navarro and Durand [12] obtained a value for B of 0,00513 $lg^{-1}h^{-1}$ but gave no value for the maximum ethanol concentration that could be tolerated by the yeast

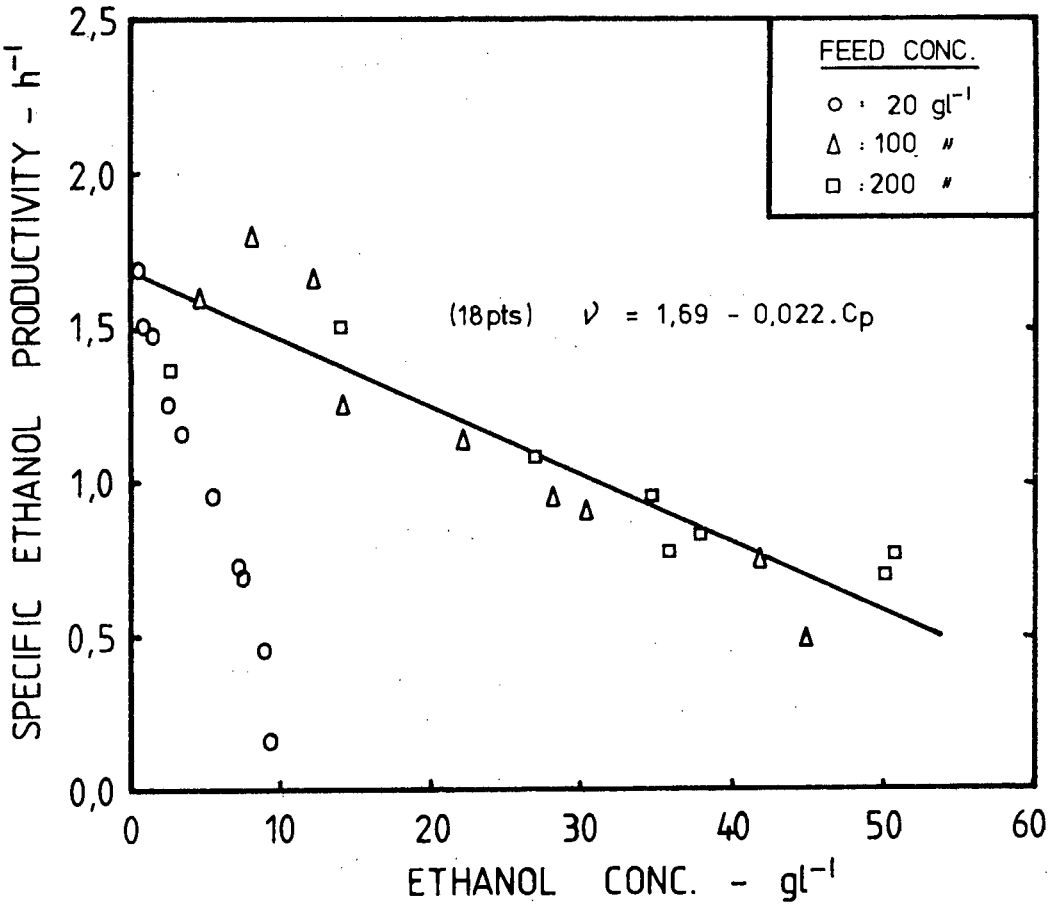

FIGURE 5.17 : SPECIFIC ETHANOL PRODUCTIVITY AS A FUNCTION OF THE ETHANOL CONCENTRATION FOR DIFFERENT FEED CONCENTRATIONS

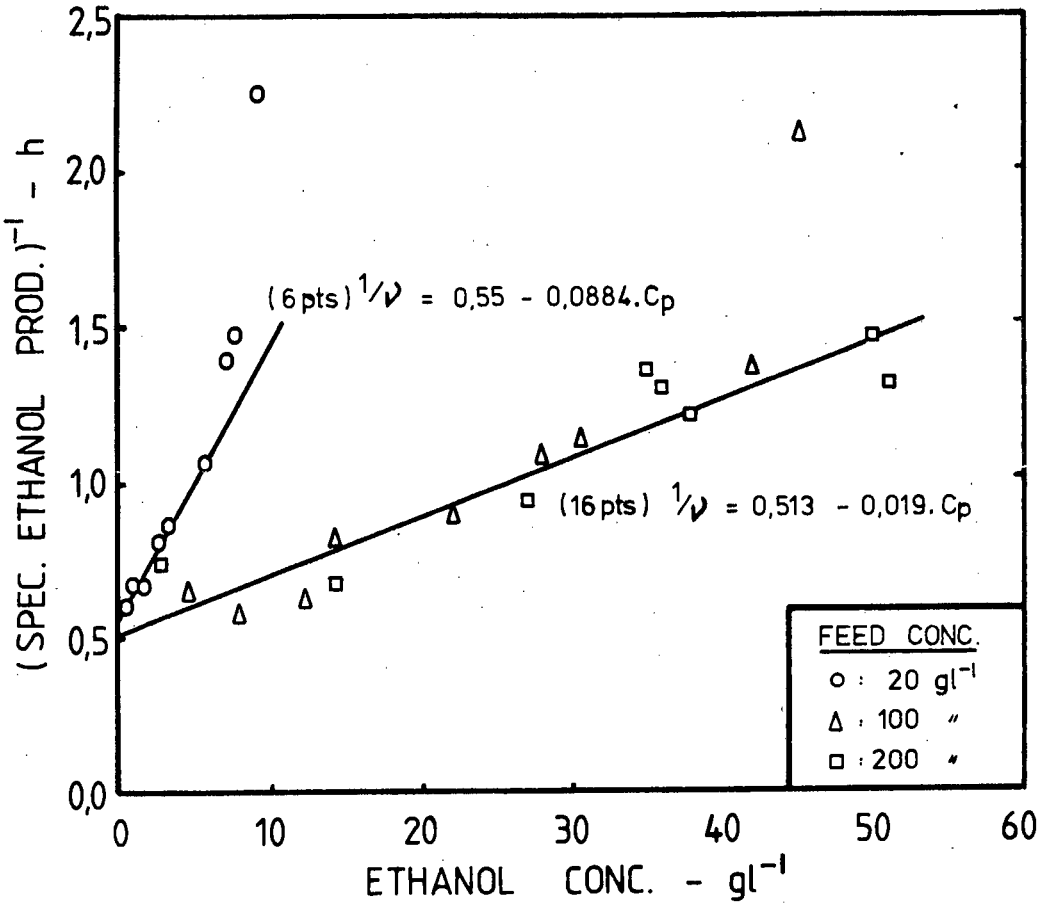

FIGURE 5.18 : INVERSE OF THE SPECIFIC ETHANOL PRODUCTIVITY AS A FUNCTION OF THE ETHANOL CONCENTRATIONS FOR DIFFERENT FEED CONCENTRATIONS

in the medium. Ghose and Tyagi [8] for their hydrolysate found a value of 1,43 h^{-1} for A (equivalent to the maximum specific ethanol productivity) but had a much higher C_{pm} of 114 gl^{-1}. This could be combined to give a value of 0,0125 $lg^{-1}h^{-1}$ for B. There existed therefore a considerable spread in the values.

The inverse relationship, although the fit was better, was similar to the relationship applied to the specific growth rate, assuming that the saturation constant was negligible compared to the substrate concentrations. Aiba et Shoda [4] obtained values for K'_p of 71,5 gl^{-1} for batch operation and 12,5 gl^{-1} for continuous operation. The value of 27,6 gl^{-1} obtained here implied less inhibition when compared to the continuous run of Aiba and Shoda [4], and when compared to the inhibition on the specific growth rate obtained in this work.

TABLE 5.7 SPECIFIC ETHANOL PRODUCTIVITY - LUEDEKING AND PIRET CONSTANTS

SOURCE	FEED CONC (gl^{-1})	$\alpha = Y_{ps}/Y_{xs}$	$\beta = mY_{ps}$ (h^{-1})	r^2
This work	20	2,89	0,29	0,96
" "	100	4,76	0,52	0,96
" "	200	4,27	0,64	0,97
Bazua and Wilke [7]	9,4	4,62/3,69+	0,0*	0,98
Aiba et al [5]	21	3,60	0,02	0,98
Cysewski [16]	100	4,43	0,39	0,99
Pironti [19]	20	3,14	0,11	0,91
"	90	5,70	0,10	0,95
"	180	4,27	0,33	0,90

NB: * A value below zero has been adjusted to zero

\+ The lower value was derived from ethanol concentrations adjusted to the theoretical yield constant since experimental values were greater than those theoretically possible.

From the trend of the 20 gl^{-1} feed concentration data in Figure 5.18, it appeared that the saturation constant, assuming similar kinetics for ethanol productivity, was considerable. On its own, the 20 gl^{-1} feed concentration data would have given the following values

$$\nu_{max} = 1,81\ h^{-1}$$
$$K'_p = 6,25\ gl^{-1}$$

The value for the inhibition constant appeared closer to those derived for growth inhibition than the inhibition constant for the higher feed concentrations.

5.2 MICRO-AEROBIC FERMENTATION:

Only one micro-aerobic fermentation was performed and at a feed concentration of 100 gl^{-1} glucose. It was a direct continuation of the 100 gl^{-1} anaerobic fermentation. Air was introduced into this fermentation after 355 hours of continuous fermentation without air and various steady states were obtained until the fermentation was terminated after a further 725 hours of operation. No contamination difficulties were experienced and steady states were again obtained randomly to minimise the effect of any adaptation. No oscillations or step changes were found within any one steady state.

5.2.1 Steady State Concentrations and Yields

The steady state concentrations and yield coefficients are given in Figure 5.19 as a function of the dilution rate. Also included was the data from Cysewski [16] corresponding to the conditions in this experiment. It was assumed that the air sparging in this work was equivalent to the continuous experiments of Cysewski [16] with ergosterol in the medium (10 mgl^{-1}). These two experiments then gave very similar results. Better results still had been obtained by Cysewski [16]

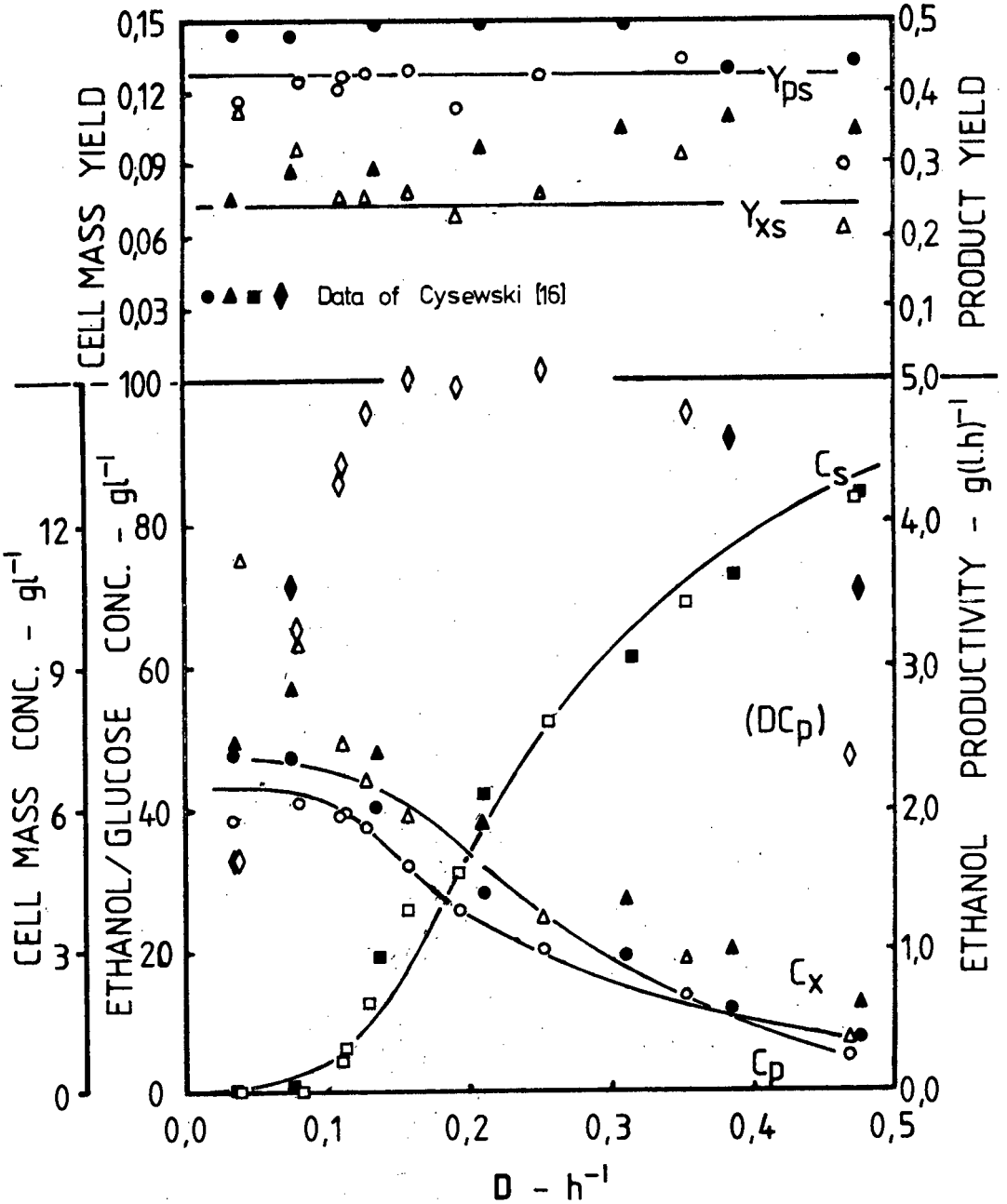

FIGURE 5.19 : PROCESS VARIABLES, EXPERIMENTAL AND PREDICTED, AS A FUNCTION OF THE DILUTION RATE - MICRO-AEROBIC WITH 100 $g\ell^{-1}$ FEED GLUCOSE CONCENTRATION

using oxygen sparging (oxygen tension of 0,07 mmHg) after an initial period of adaptation.

(a) Glucose Concentration: The glucose concentration remained very close to zero up to a dilution rate of 0,08 h^{-1}, but then increased very rapidly. This was in sharp contrast to the anaerobic fermentation at the same glucose feed concentration, where the glucose concentration rose almost immediately. This is also shown in Figure 5.20, considering the percentage of the substrate consumed as a function of the dilution rate. Incorporation of air sparging increased the conversion from 57% to 98% at a dilution rate of 0,1 h^{-1}, a 72% improvement. A comparison of the utilisations from the micro-aerobic and the 20 gl^{-1} anaerobic fermentations showed these to be very similar except at the higher dilution rates where the anaerobic fermentation was less efficient. This seemed to indicate a nutritional deficiency between the anaerobic 20 and 100 gl^{-1} glucose feed concentration fermentations (see Section 5.1.2). This may have been the oxygen supply which has been said to be necessary for yeast growth for the synthesis of lipids and sterols (Kunkee and Amerine [6] Andreason and Stier[14], Larue et al [15]. The dissolved oxygen content of the 100 gl^{-1} medium was therefore insufficient to support the possible yeast growth and fermentative ability.

(b) Ethanol Concentration/Ethanol yield: The ethanol concentration again decreased with increasing dilution rate i.e. as the utilisation of glucose decreased. The concentration peaked at a dilution rate of 0,08 h^{-1}, the dilution rate at which the glucose concentration began to increase rapidly. As the dilution rate decreased below 0,08 h^{-1}, the ethanol concentration also decreased with a corresponding decrease in the ethanol yield coefficient. The cell mass concentration increased at this point which seemed to show a shift towards respiratory metabolism and may

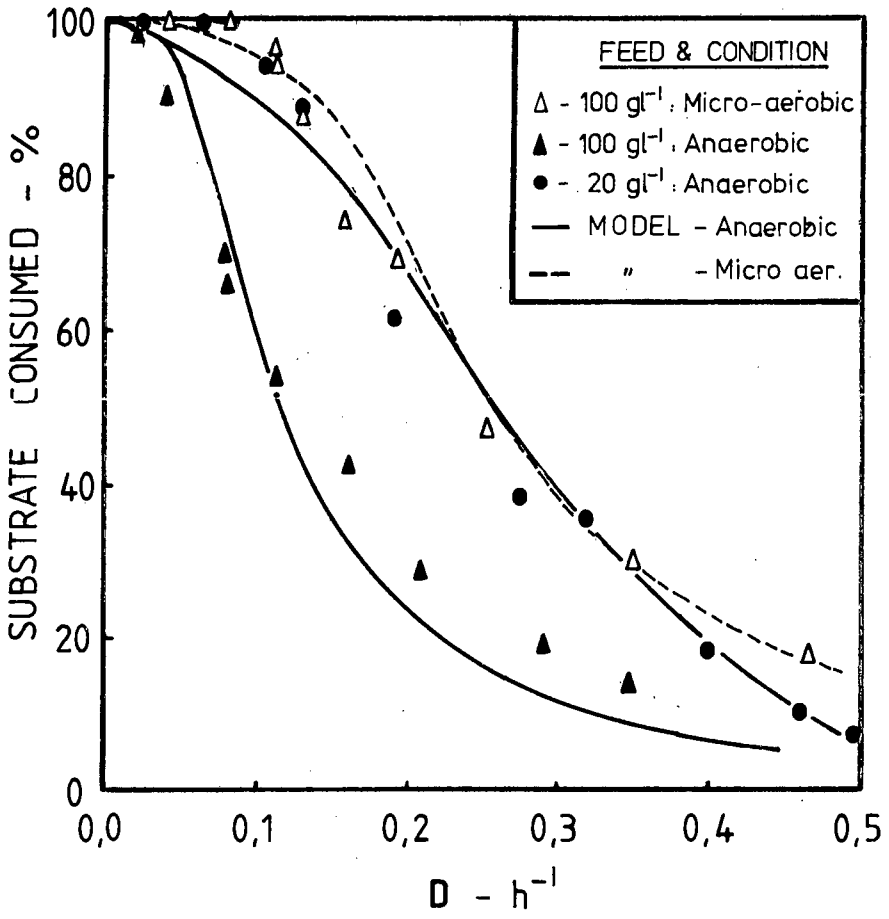

FIGURE 5.20 : PERCENTAGE SUBSTATE CONSUMED AS A FUNCTION OF THE DILUTION RATE UNDER ANAEROBIC AND MICRO-AEROBIC CONDITIONS

have indicated an excess supply of oxygen for the enhancement of the fermentative metabolism only. The average value of the ethanol yield coefficient had decreased to 0,41 (g ethanol)/(g glucose consumed) compared to 0,44 for the anaerobic case, a 7% decrease. This compared unfavourably to the results obtained by Cysewski [16] where the ethanol yield coefficient had increased to 0,48 from 0,44 even though the cell mass concentration had also increased. This implied that an increase in the efficiency of the conversion process had occurred with the introduction of ergosterol. The decrease in the conversion in this work could have been due to an excess sparging rate beyond that necessary for optimum conversion only or due to losses of ethanol entrained in the exit gas stream. It should be noted that a lower sparging rate was used for the steady state at a dilution rate of 0,04 h^{-1} and that the ethanol concentrations varied significantly within some of the steady states.

(c) Cell mass concentration/Cell mass yield: The level of the cell mass concentration was increased several fold compared to the anaerobic experiments, 3.7 times at a dilution rate of 0,08 h^{-1}. The cell mass concentration showed no maximum (for dilution rates of 0,04 h^{-1} and above), similar to the 20 gl^{-1} anaerobic fermentation and may be indicative of a very low maintenance rate. It may also have indicated a change in the metabolism as the ethanol concentration decreased also. Therefore the supply of oxygen exceeded that for stimulation of catabolic repression only and cell mass production increased for the loss of ethanol production. The cell mass yield coefficient remained fairly constant, except for the initial high in the region of complete glucose utilisation, and then decreased at the highest dilution rate considered, namely 0,466 h^{-1}. This could have indicated that the fermentation was nearing its washout condition.

5.2.2 Ethanol Productivity

The ethanol productivity increased significantly. The increase was two fold over the maximum anaerobic productivity of the 100 gl^{-1} feed glucose concentration and five fold for the 20 gl^{-1} feed concentration. The latter corresponded to the corresponding increase in the feed concentration, even with the greater concentration of ethanol. Hence the additional oxygen both increased conversion by greater cell mass growth and provided a greater ethanol tolerance. Reference to the specific ethanol productivity is made in Section 5.2.5. Maximum productivity was approached at approximately 80% substrate utilisation and at a dilution rate of 0,15 h^{-1} and remained constant until a dilution rate of 0,30 h^{-1} where it again fell rapidly. This trend corresponded to that for the anaerobic 100 and 200 gl^{-1} feed concentrations.

5.2.3 Growth Curve : Experimental and Simulated

The experimental growth curve was compared to that obtained by simulation in Figure 5.21, using the same model as for the anaerobic fermentations but with different values for the constants. The value of Cp was again replaced by the product of a constant yield coefficient and the glucose consumed. The yield coefficient had the value of 0,41 (g ethanol)/(g glucose consumed), determined by linear regression. Comparing the ethanol concentration - dilution rate data of the anaerobic and micro-aerobic fermentations, as in Figure 5.22, showed that the value of 0,43 obtained for the anaerobic data could also have applied for the micro-aerobic fermentation. Both yield coefficients were therefore used in the modelling and minimisation procedure and gave the following values for the constants in the model, Table 5.8. From Figure 5.12, it was evident that the three models gave very similar estimations of the data. The first two sets resulted again from different initial conditions in using the

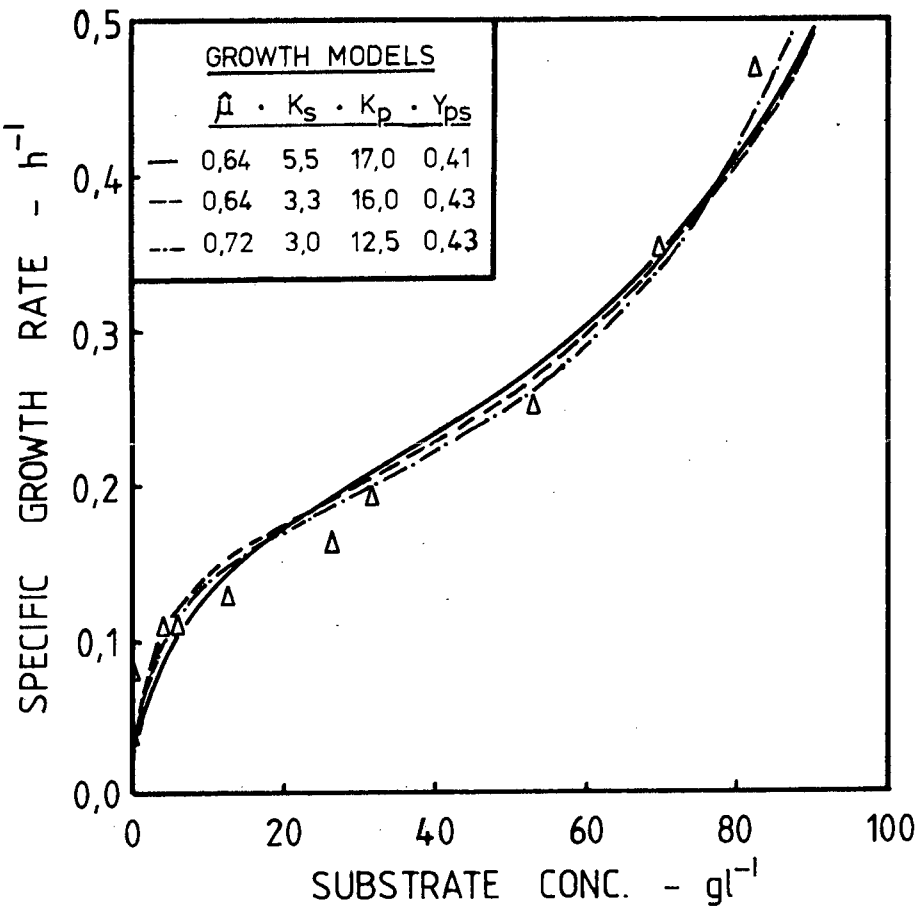

FIGURE 5.21 : VARIOUS SPECIFIC GROWTH RATE MODEL CONSTANTS FOR THE 100 $g\ell^{-1}$ FEED CONCENTRATION, MICRO-AEROBIC FERMENTATION

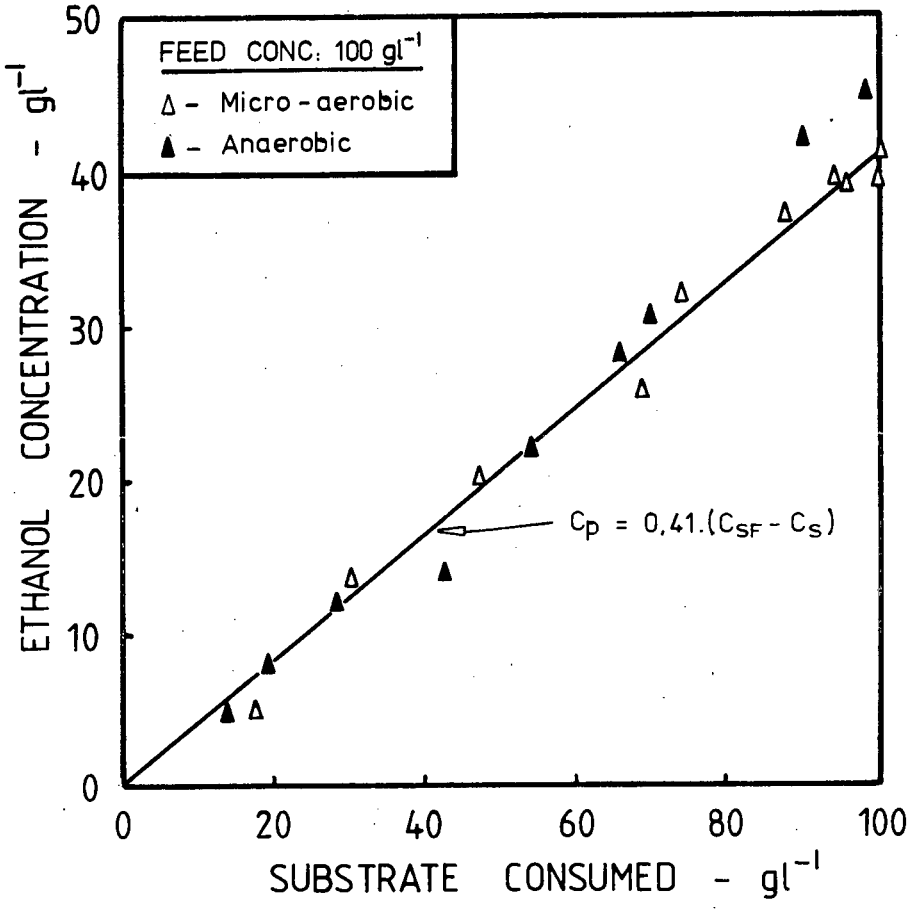

FIGURE 5.22 : ETHANOL CONCENTRATIONS AS A FUNCTION OF THE SUBSTRATE CONSUMED FOR THE 100 $g\ell^{-1}$ FEED CONCENTRATION FERMENTATIONS

Nelder-Mead minimisation routine. Of interest was the very close fit of the third set of constant values. These were equivalent to the anaerobic values except for a lower degree of ethanol inhibition i.e. the value of Kp had increased. Hence the ethanol tolerance of the yeast had increased or the ethanol tolerance had increased due to the greater amount of yeast present.

TABLE 5.8: VALUES FOR CONSTANTS IN MICRO-AEROBIC GROWTH MODEL

CONSTANT - VALUE	SET 1	SET 2	SET 3
$\hat{\mu}$ (h^{-1})	0,64	0,72	0,64
K_s (gl^{-1})	5,5	3,0	3,3
K_p (gl^{-1})	17,0	12,0	16,0
Y_{ps}	0,41	0,41	0,43

Estimation of $\hat{\mu}$ and Kp directly from the experimental results was also attempted, as given in Figure 5.23. Insufficient results were however available at the higher dilution rates and made estimation difficult. Two schemes were evaluated, namely the first two points and the first three points, and gave the following results:

First 2 pts: $\hat{\mu} = 0,58\ h^{-1}$ and $Kp = 21,5\ gl^{-1}$

3 pts: $\hat{\mu} = 0,69\ h^{-1}$ and $Kp = 12,3\ gl^{-1}$

An intermediate position was representative of the simulated values. The value of Kp now approached the values of some of the literature determinations, given in Table 5.3. Égamberdiev and Ierusalimskii [3] also determined an aerobic value by using shake flask tests and gave the value of Kp as increasing from 20,6 to 22,2 gl^{-1}. An increase was also observed in this work. The same authors also found the maximum specific growth rate to increase from 0,31 to 0,36 h^{-1}. Hence

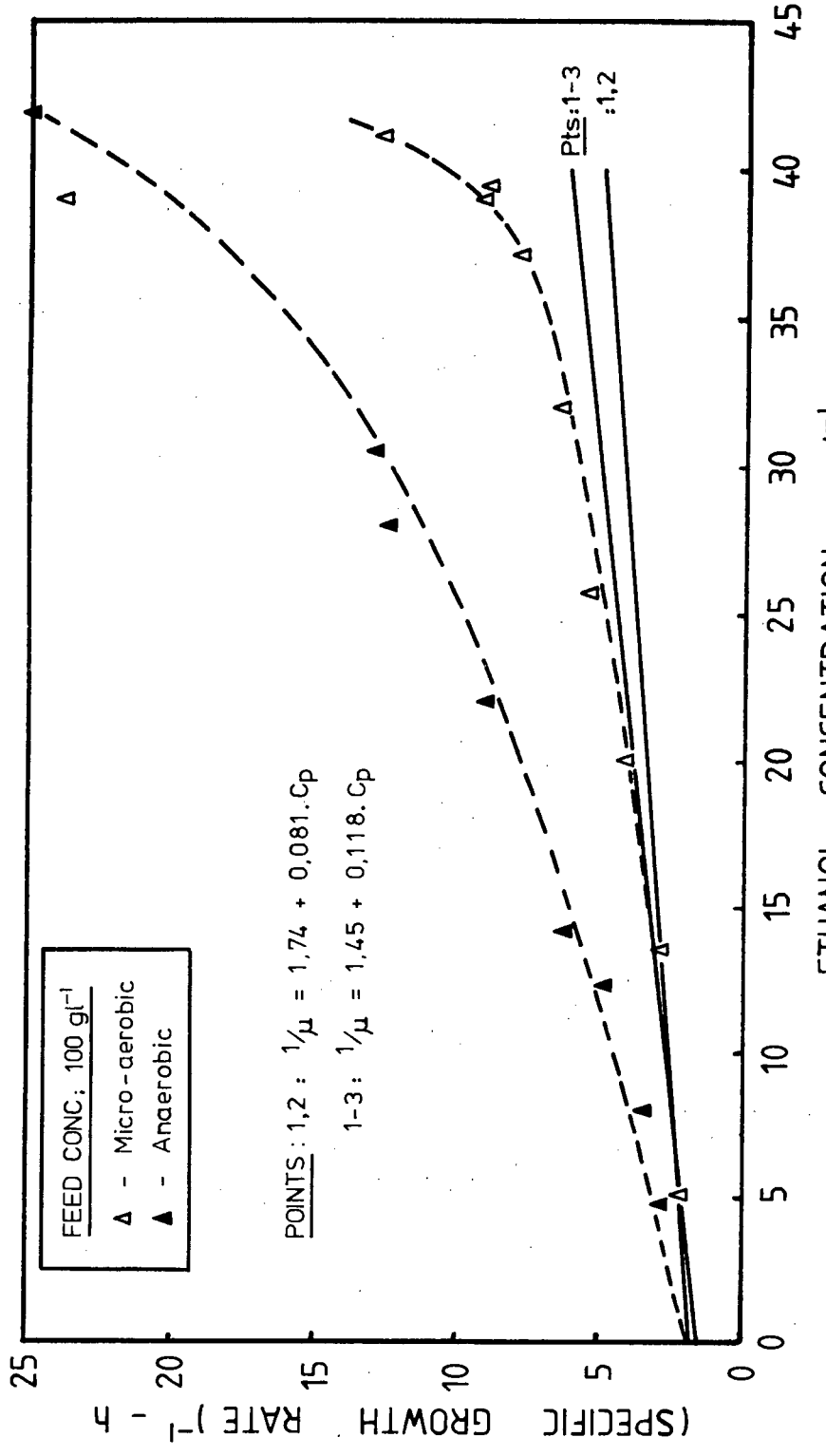

FIGURE 5.23 : INVERSE OF THE SPECIFIC GROWTH RATE AS A FUNCTION OF THE ETHANOL CONCENTRATION

the value of $\mu_{max} = 0,72\ h^{-1}$ as given in Figure 5.21 could very well also apply. Inspection of the model using it, shows a closer fit compared to the other model predictions.

The data of Cysewski [16] also showed that when ergosterol was added to the medium, the maximum dilution rate was increased.

5.2.4 Prediction of the Fermentation Concentrations

The concentration profiles predicted using the model are given in Figure 5.19. As before, the substrate and ethanol concentrations have already been derived. The predicted curves agreed very well with the experimental values and the use of 0,43 as the value for the ethanol yield coefficient and $0,72\ h^{-1}$ for the maximum specific growth rate seemed justified. Disagreement at the lower dilution rates in the region of complete utilisation of the glucose was probably due to excessive air sparging and a shift to a partial respiratory metabolism.

To predict the cell mass concentration, it was first necessary to check for the existence of a maintenance rate in consuming some of the glucose. Figure 5.24 examined the substrate utilisation rate as a function of the dilution rate and showed that the specific maintenance rate present for the anaerobic fermentation had completely disappeared or decreased to a level within the error limits of the determination. Several other literature fermentations using ergosterol, see Table 5.9, showed similar conclusions. Comparison of the initial portions of the anaerobic and micro-aerobic correlations showed that they increased at similar rates which implied that the cell mass yield coefficients had not significantly changed i.e. the maximum cell mass yield coefficient attained in the anaerobic fermentations was similar to the steady or average cell mass yield coefficient during the micro-aerobic fermentations. The two literature examples retained very

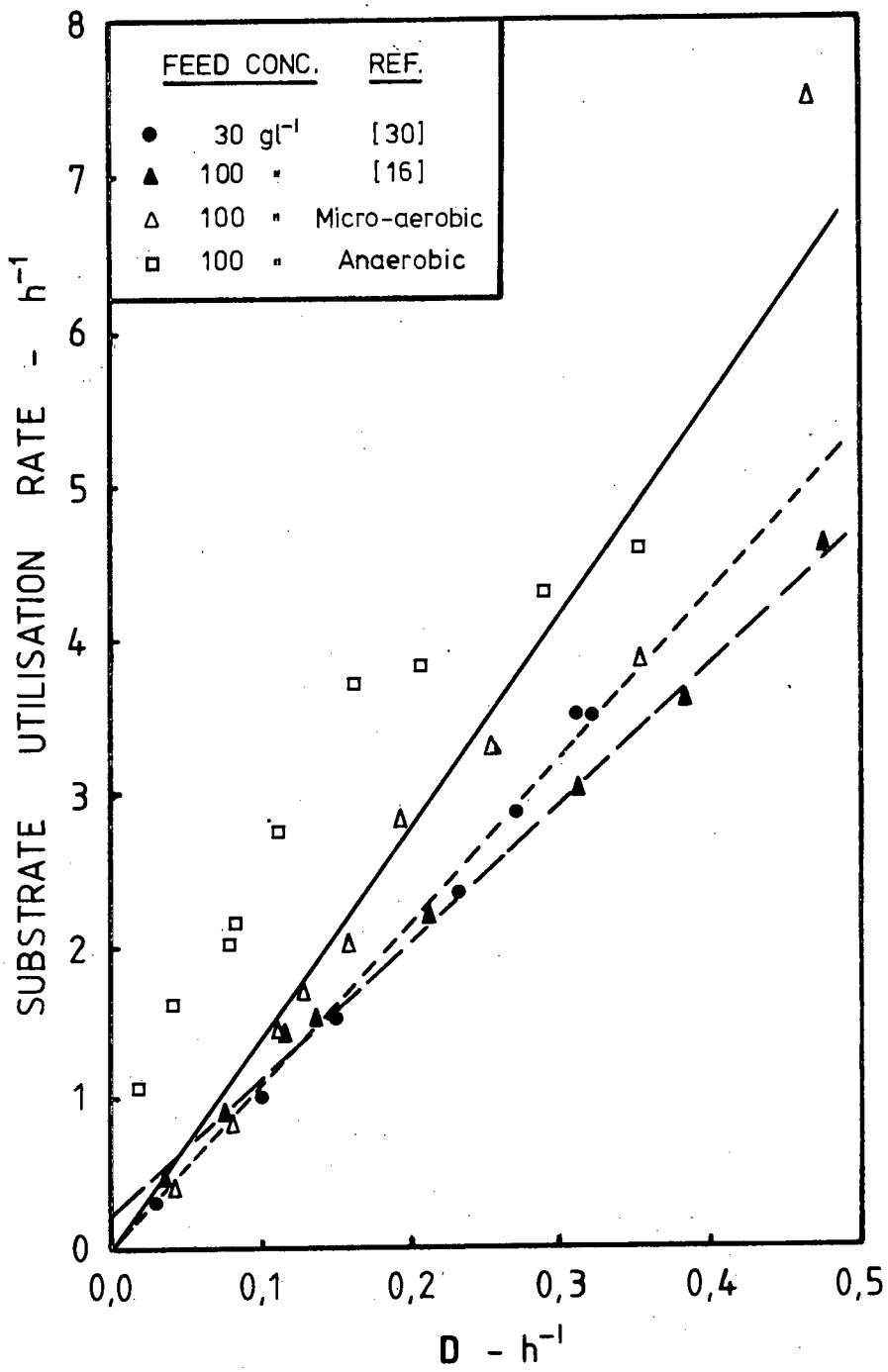

FIGURE 5.24 : SUBSTRATE UTILISATION RATE AS A FUNCTION OF THE DILUTION RATE

similar cell mass yield coefficients to those presented in Table 5.6. The cell mass concentration was therefore described by the product of the cell mass yield coefficient and the substrate consumed for growth and energy, and showed good agreement except at the low dilution rates i.e. in the region of complete glucose utilisation. Here the experimental cell mass concentrations increased steadily instead of leveling off at a maximum value. A possible explanation has been presented with respect to the change in the metabolic route for energy production.

TABLE 5.9 SPECIFIC MAINTENANCE RATES AND CELL MASS YIELD COEFFICIENTS

SOURCE	FEED CONC. (gl^{-1})	m (h^{-1})	Y_{xs}	r^2
This Work	100	0,0	0,072	0,94
Cysewski [16]	100	0,21	0,110	0,997
Schatzmann[30]	30	0,0	0,093	0,995

5.2.5 Product Formation Rate

The specific ethanol productivity increased linearly with the dilution rate i.e. it was directly growth related. This was shown in Figure 5.25. Since the specific maintenance rate was essentially zero, no product was formed due to maintenance processes i.e. the β coefficient in the Luedeking and Piret [29] product formation model was zero. This was shown by the offset of the micro-aerobic results compared to the anaerobic values. The specific ethanol productivity reached no maximum value as observed during the anaerobic fermentations of the 100 and 200 gl^{-1} feed concentrations. The maximum ethanol productivity predicted for the micro-aerobic

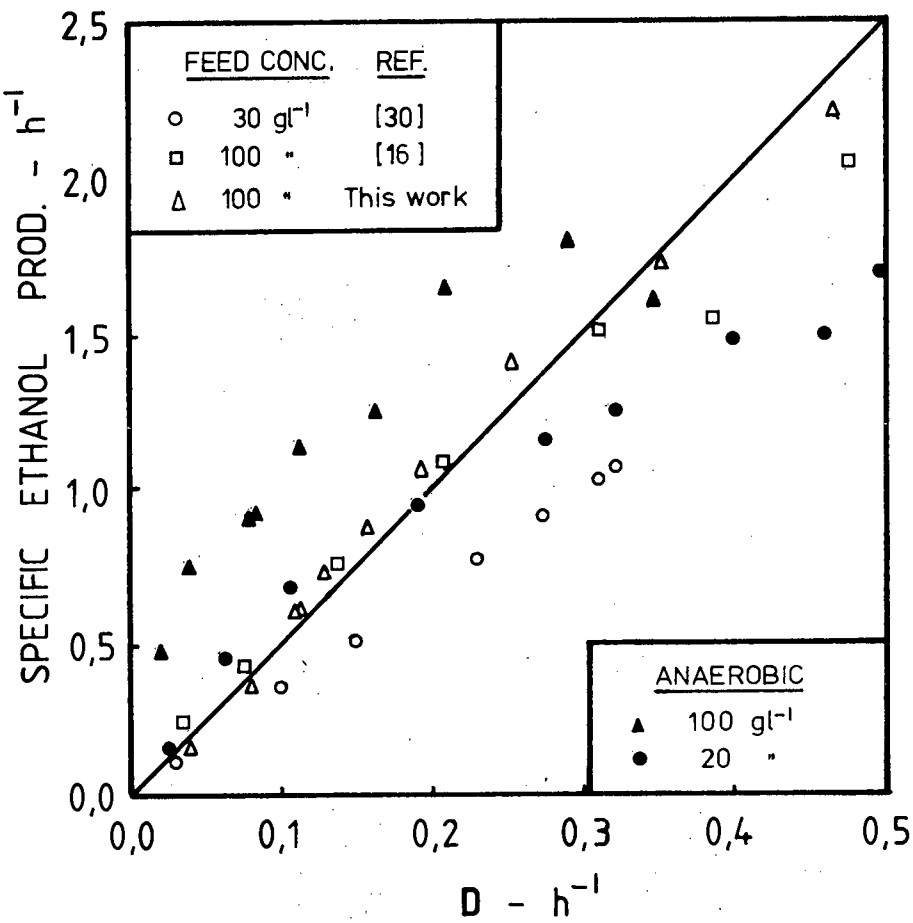

FIGURE 5.25 : SPECIFIC ETHANOL PRODUCTIVITY AS A FUNCTION OF THE DILUTION RATE

fermentation was 2,37 h^{-1}, (see Figure 5.26) representing a 22% increase. α, the Luedeking and Piret [29] constant had a value of 4,99, slightly higher than the corresponding anaerobic value.

An attempt was again made to determine the degree of the ethanol inhibition on the specific ethanol productivity. A linear dependence on the ethanol concentration is shown in Figure 5.26 and gave a much better fit than for the anaerobic case. The correlation coefficient was 0,985 and hence strongly supported a linear form of inhibition. The relationship determined was

$$\nu = 2,37 - 0,047\ Cp$$

which was also equivalent to

$$\nu = 0,047\ (50,8 - Cp) \quad \text{cf} \quad \nu = B(C_{pm} - C_p)$$

and $$\nu = 2,37\ (1 - Cp/50,8) \qquad \nu = A(1 - C_p/C_{pm})$$

The constants A, B and Cpm have been described in Section 5.1.6. The value for B of 0,047 $lg^{-1}h^{-1}$ was 100% higher than that determined for the anaerobic fermentations and was again very much higher than the literature values. A, the maximum specific ethanol productivity has been mentioned above and Cpm, the maximum ethanol concentration that could be tolerated was a very low 50,8 gl^{-1}. This low value should be viewed with scepticism and was well below levels of 80 to 110 gl^{-1} given in the literature. Analysis of the data of Cysewski [16] gave values of 0,036 $l(gh)^{-1}$ and 59,6 gl^{-1} for B and Cpm respectively, which were still beyond "normally" accepted levels. The maximum specific ethanol productivity, A, was a little lower at 2,16 h^{-1}.

An inverse relationship was also tested and a plot of the inverse of the specific ethanol productivity as a function of the ethanol concentration is given in Figure 5.27. No linear relationship was obtained. However, a similar relationship for the specific ethanol productivity as for the specific growth rate, namely

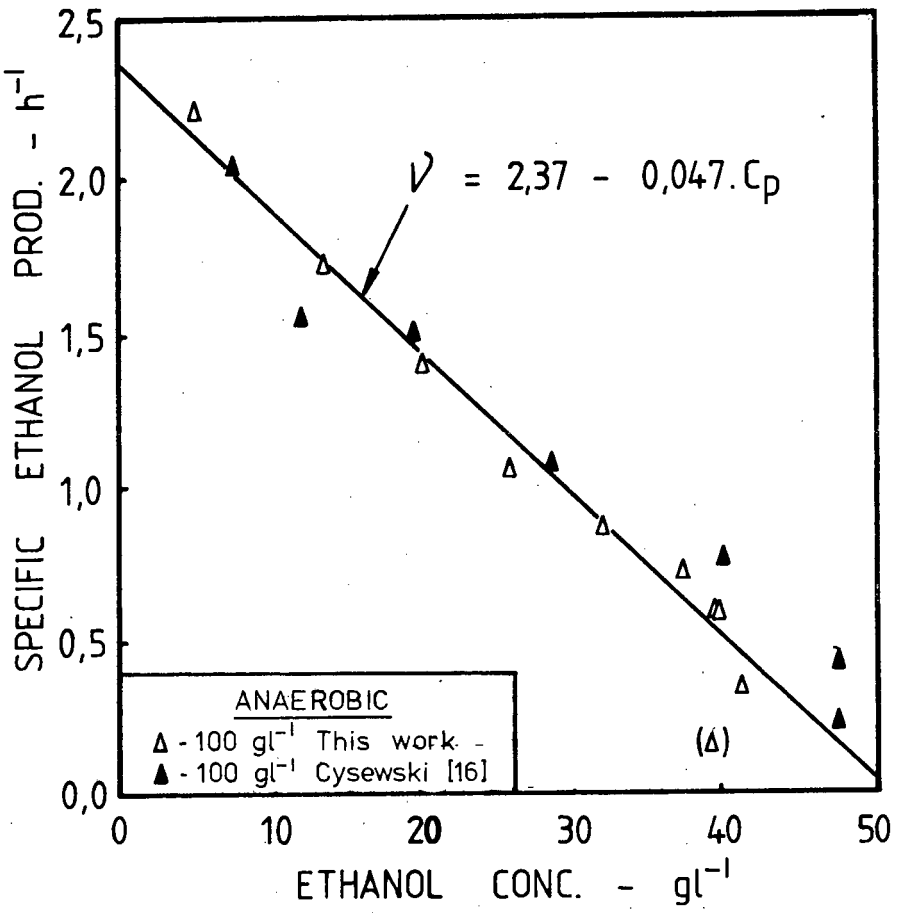

FIGURE 5.26 : SPECIFIC ETHANOL PRODUCTIVITY AS A FUNCTION OF THE ETHANOL CONCENTRATION

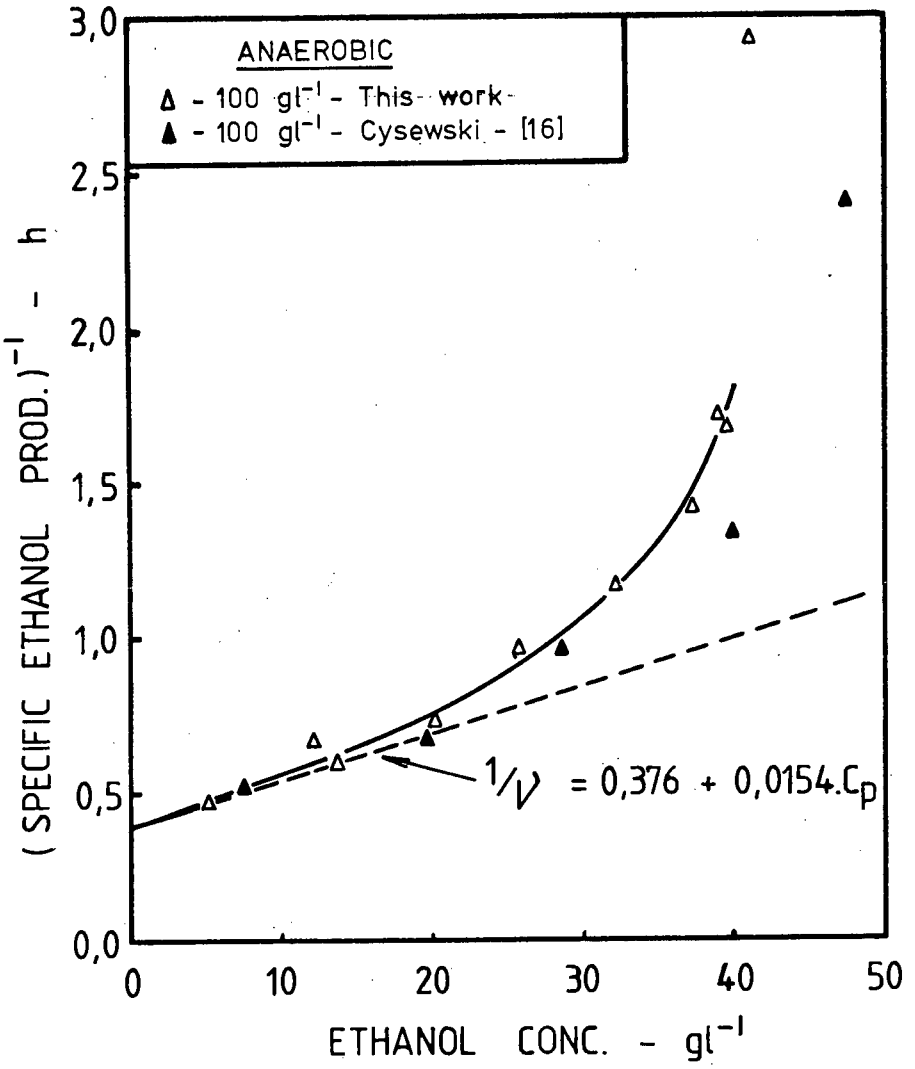

FIGURE 5.27 : INVERSE OF THE SPECIFIC ETHANOL PRODUCTIVITY AS A FUNCTION OF THE ETHANOL CONCENTRATION

$$\nu = \nu_{max} \cdot \frac{C_s}{C_s + K_s'} \cdot \frac{K_p'}{K_p' + C_p}$$

could be applied, so that the deviation was attributable to the value of K_s. From the figure K_s would appear to be considerably larger than K_s for the specific growth rate because a positive deviation was evident at ethanol concentrations of 20 gl^{-1} corresponding to glucose concentration levels of 50 gl^{-1}. Again the number of experimental values at the lower ethanol concentrations was limited, so that only the first two points were used. The following values were obtained:

ν_{max} = 2,66 h^{-1}

K_p' = 24,4 gl^{-1}

The maximum specific ethanol productivity was higher than the linear evaluation. K_p was very similar to the value, 27,6 gl^{-1}, obtained for the anaerobic experiments, so that the introduction of oxygen had reduced the ethanol inhibition on the growth of the organism but not on its ethanol production. However the oxygen may have only removed an apparent inhibition which was manifested by an actual growth factor limitation.

5.3 ANOMOLOUS BEHAVIOUR

The data used in Sections 5.1 and 5.2 represented the best estimates of the various concentrations at each steady state. But not all dilution rates showed only one steady state region or a "single step" change when approaching a particular steady state. No difficulties were experienced for the 20 gl^{-1} glucose feed concentration over the dilution rates measured (0,024 to 0,497 h^{-1}). Extensive observations were taken for the 100 gl^{-1} glucose feed concentration at a dilution rate of 0,02 h^{-1}. Experiment 10C gave many changes in the concentrations of the biomass and glucose (only these two variables were monitored). Several changes could not be related to leaks or stoppages in the system.

A repeat experiment, 12C (Figure 5.28), gave more consistent results. The "pseudo steady state" observed between 300 to 400 hours may have been the result of a dynamic oscillation, appearing so "gentle" because of the high residence time (50 hours) so that the latter steady state occurred after a process of adaptation. Adaptation seemed unlikely because of the rapid change from the first to second steady state, i.e. in approximately a residence time. The latter steady state was used in the calculations for Section 5.1.

Evaluation of the substrate utilisation rate (SUR) at the two steady conditions gave 1,24 and 1,04 h^{-1} respectively in order of occurrence. A maintenance rate of 1,3 h^{-1} was determined for this 100 gl^{-1}, anaerobic fermentation and this could therefore have favoured the first steady condition as the "truer" representative. The system could have returned to a similar value had it been observed for a longer period of time.

At low dilution rates (0,020 and 0,013 h^{-1}) for the 200 gl^{-1} glucose feed concentration, a very different but regular pattern was observed. Two cases resulted from the start-up of continuous fermentations after an initial period of batch growth. Figures 5.29 and 5.30 show that the final level of any one concentration variable was achieved in a series of steps. The reason for this is uncertain. Regan et al.[31] showed for S. cerevisiae, that when there is a step change in the dilution rate, the culture biomass came to a new steady state in a series of steps due to the inherent cyclic nature of budding and enzyme production. These steps occurred at intervals of the mean generation time. For the higher dilution rate the generation time would have been approximately 35 hours which is considerably below the times for each of the two steps namely 60 and 110 hours. For the lower dilution rate with a generation time of 54 hours, the steps occurred at intervals of 100 and 70 hours respectively and hence showed little

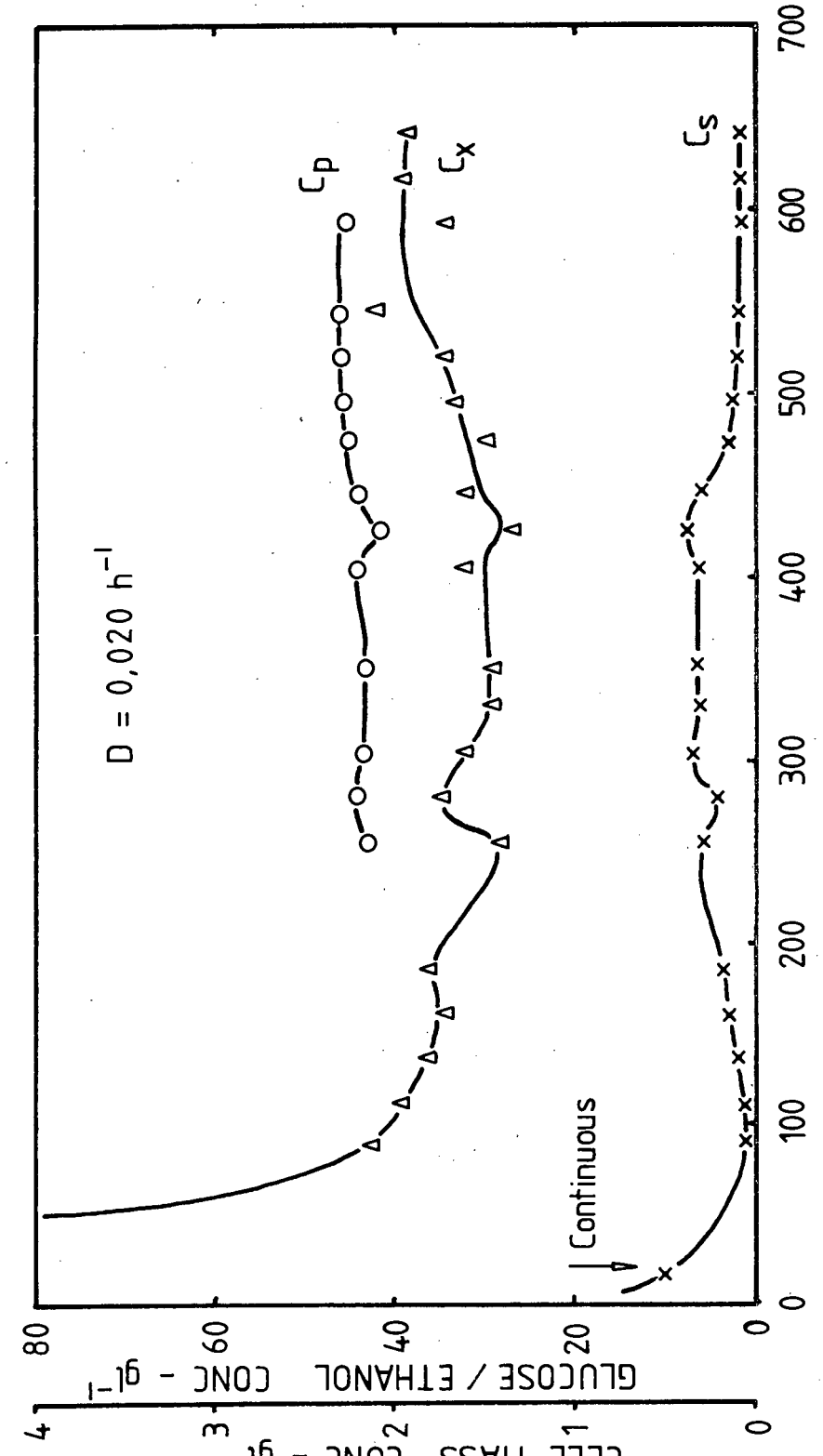

FIGURE 5.28 : OPERATING TIME COURSE FOR THE FERMENTATION GF-I2C-80 (I00 $g\ell^{-1}$ FEED GLUCOSE CONCENTRATION, ANAEROBIC)

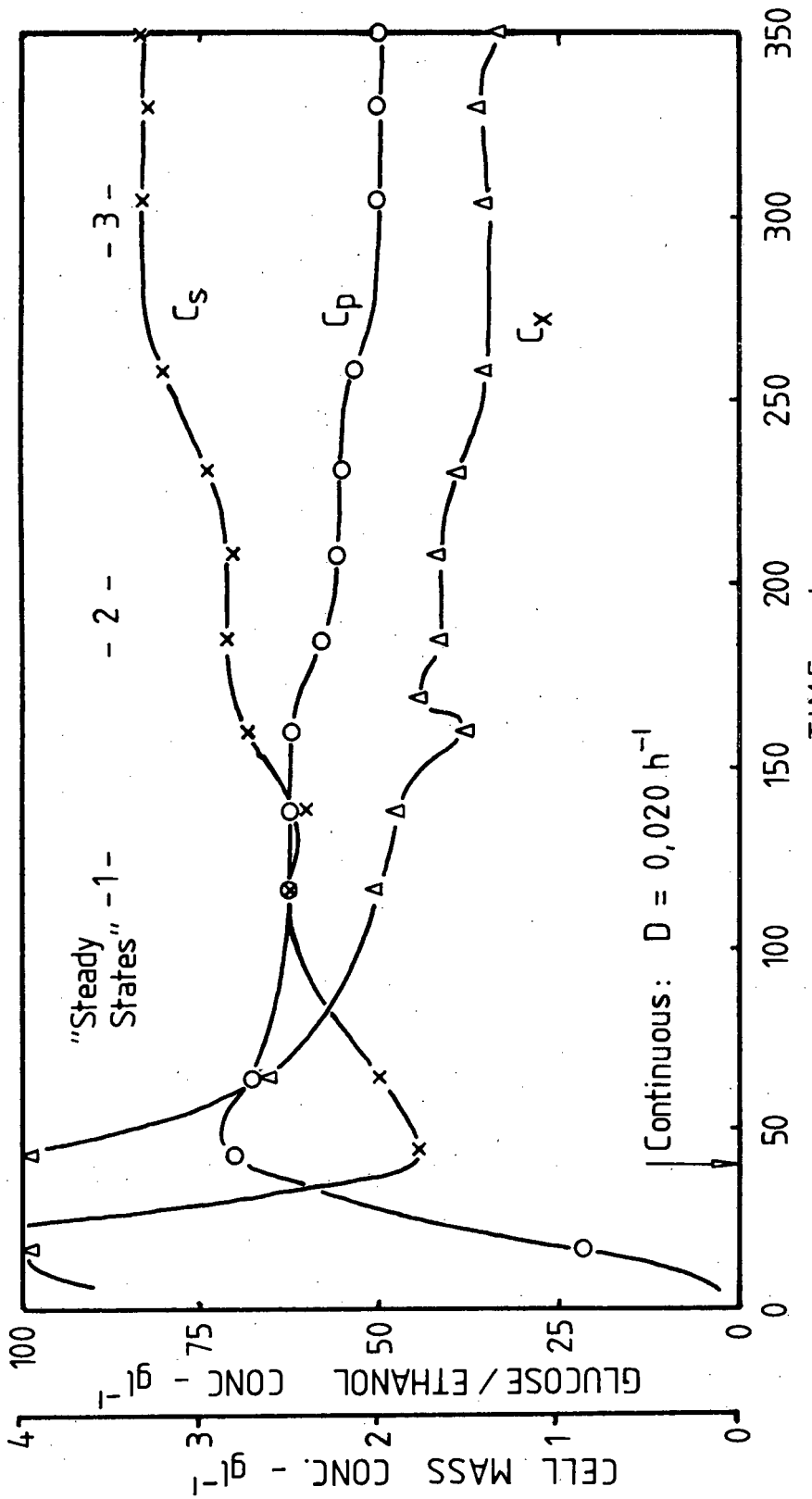

FIGURE 5.29 : OPERATING TIME COURSE FOR THE FERMENTATION GF-13C-80 (200 $g\ell^{-1}$ FEED GLUCOSE CONCENTRATION, ANAEROBIC)

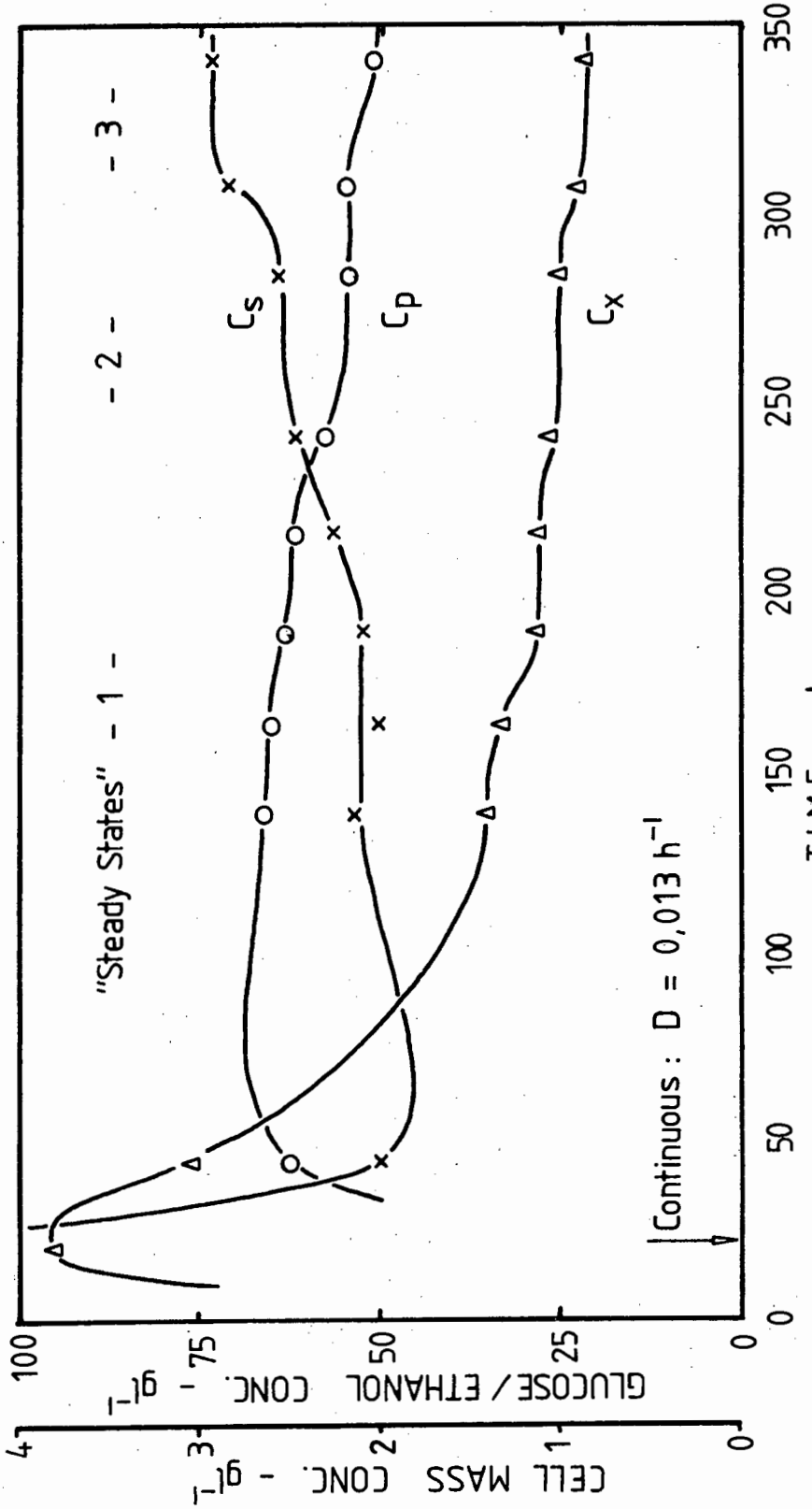

FIGURE 5.30 : OPERATING TIME COURSE FOR THE FERMENTATION GF-15C-80 (200 $g\ell^{-1}$ FEED GLUCOSE CONCENTRATION, ANAEROBIC)

correlation. By analysing the specific glucose uptake rate during each of the steps, it was found that these were less than the specific maintenance rate, increasing with each step until they exceeded the specific maintenance rate for the final steady state value. This is shown in Table 5.10. It therefore appeared, that when the glucose uptake rate was insufficient even for maintenance, the cell population decreased to a new value, probably related to the cyclic system mentioned by Regan et al., remained at this value for another cycle, found an insufficient glucose uptake rate and hence decreased further. On this basis, the steady state obtained on changing the dilution rate from 0,020 to 0,011 h^{-1} in experiment 13C, would be suspect because when the experiment was terminated, the specific glucose uptake rate was only 0,93 h^{-1}. Therefore the steady state obtained in experiment 15C for the dilution rate of 0,013 h^{-1} was taken as being representative, because the setting at a dilution rate of 0,011 h^{-1} may not have been held long enough.

Table 5.10 also showed a discrepency in the final level of the specific substrate uptake rate achieved for for the two dilution rates. This may have been due to insufficient holding time at the higher dilution rate.

TABLE 5.10: SPECIFIC GLUCOSE UPTAKE RATES FOR OBSERVED STEP CHANGES IN ATTAINING A STEADY STATE AT LOW DILUTION RATES

EXPERIMENT	GF-13C-80	GF-15C-80
DILUTION RATE - (h^{-1})	0,020	0,013
SPECIFIC GLUCOSE UPTAKE RATE - (h^{-1}) : Step 1	1,37	1,26
Step 2	1,55	1,60
Step 3	1,66	1,86
SPECIFIC MAINTENANCE RATE - (h^{-1})	1,68	1,68

NB: 1. Feed glucose concentration = 200 gl^{-1}.
2. Specific maintenance rates are given in Section 5.5.

5.4 SENSITIVITY OF THE MODEL PARAMETERS

The model in Section 5.1.4 used to describe the ethanol inhibited growth kinetics was also examined for its sensitivity to changes in the value of the constants $\hat{\mu}$, K_s and K_p. Changes in the maximum specific growth rate $\hat{\mu}$, will affect the growth rate proportionately and will therefore not be considered on its own.

5.4.1. Effect of K_s

An increase in K_s caused the growth curve as function of the substrate concentration to be depressed and visa versa. Variations in the value of K_s did not have a significant effect on the growth curve for the higher feed concentrations, namely 100 and 200 gl^{-1}. This was expected because substrate concentrations at higher dilution rates were very much higher than the value of K_s, even for variations of $\pm$ 50%. For the 20 gl^{-1} feed glucose concentration, the effect of K_s was pronounced and over the entire range of substrate concentrations. The effect of different values of K_s is shown in Figures 5.31 to 5.33.

5.4.2 Effect of K_p

An increase in K_p caused the growth curve to rise because a higher value for K_p represented a lower degree of inhibition. The reverse also applied. Changes in K_p affected the growth curve at all the different feed concentrations and over the whole range of the growth curve. The greatest percentage change occurred at the higher ethanol concentrations i.e. at low substrate concentrations and at low dilution rates, because here the growth rate becomes nearly directly proportional to the product saturation constant K_p

i.e. for $C_p \gg K_p$

$$\frac{K_p}{K_p + C_p} \longrightarrow \frac{K_p}{C_p}$$

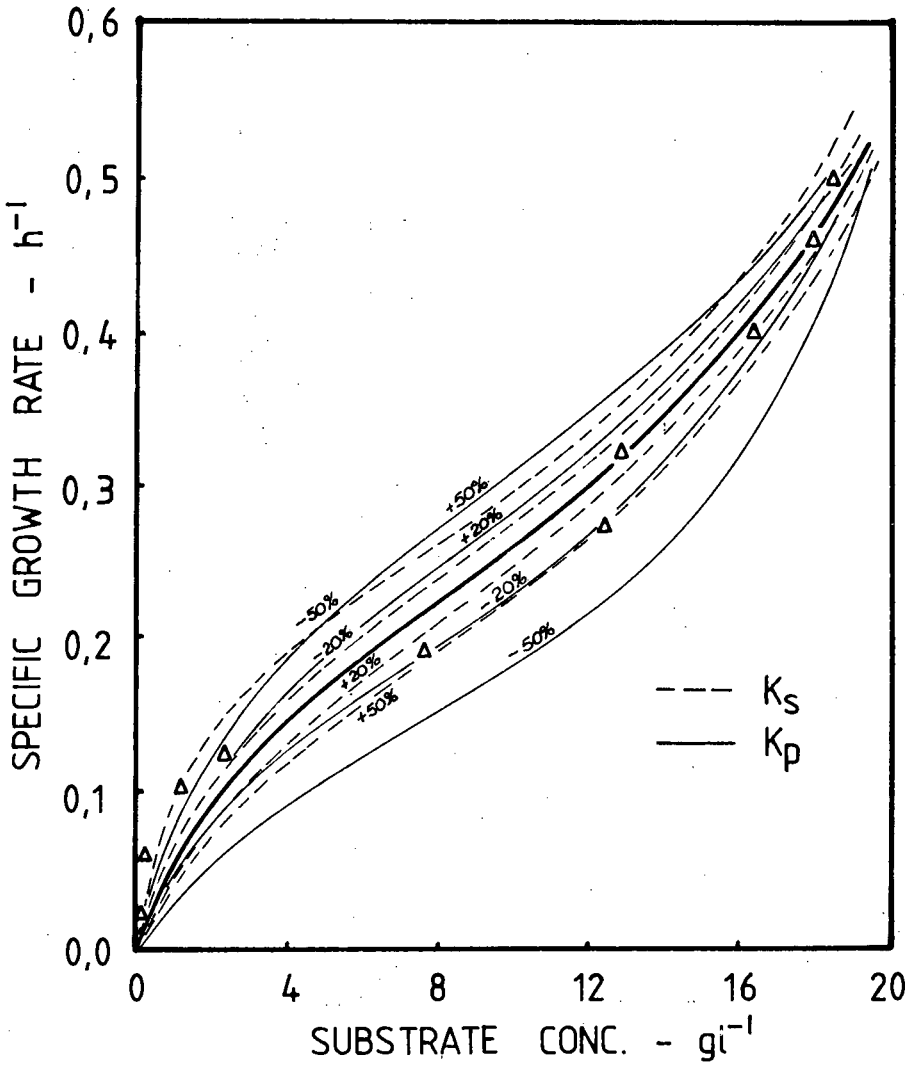

FIGURE 5.31 : EFFECT OF VARIATIONS IN K_s AND K_p ON GROWTH MODEL FOR THE 20 $g\ell^{-1}$ FEED CONCENTRATION - ANAEROBIC

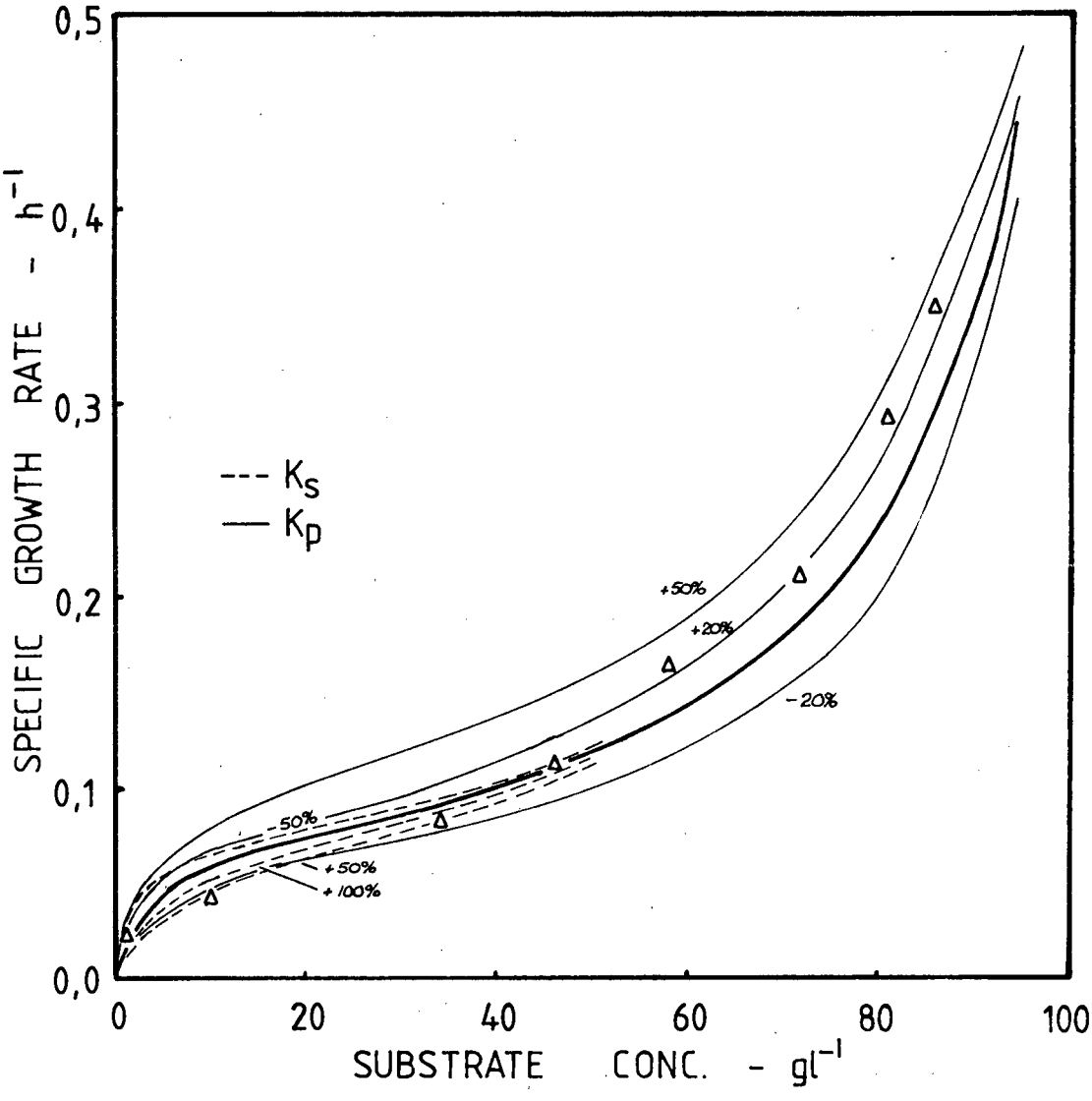

FIGURE 5.32 : EFFECT OF VARIATIONS IN K_S AND K_P ON GROWTH MODEL FOR THE 100 $g\ell^{-1}$ FEED CONCENTRATION - ANAEROBIC

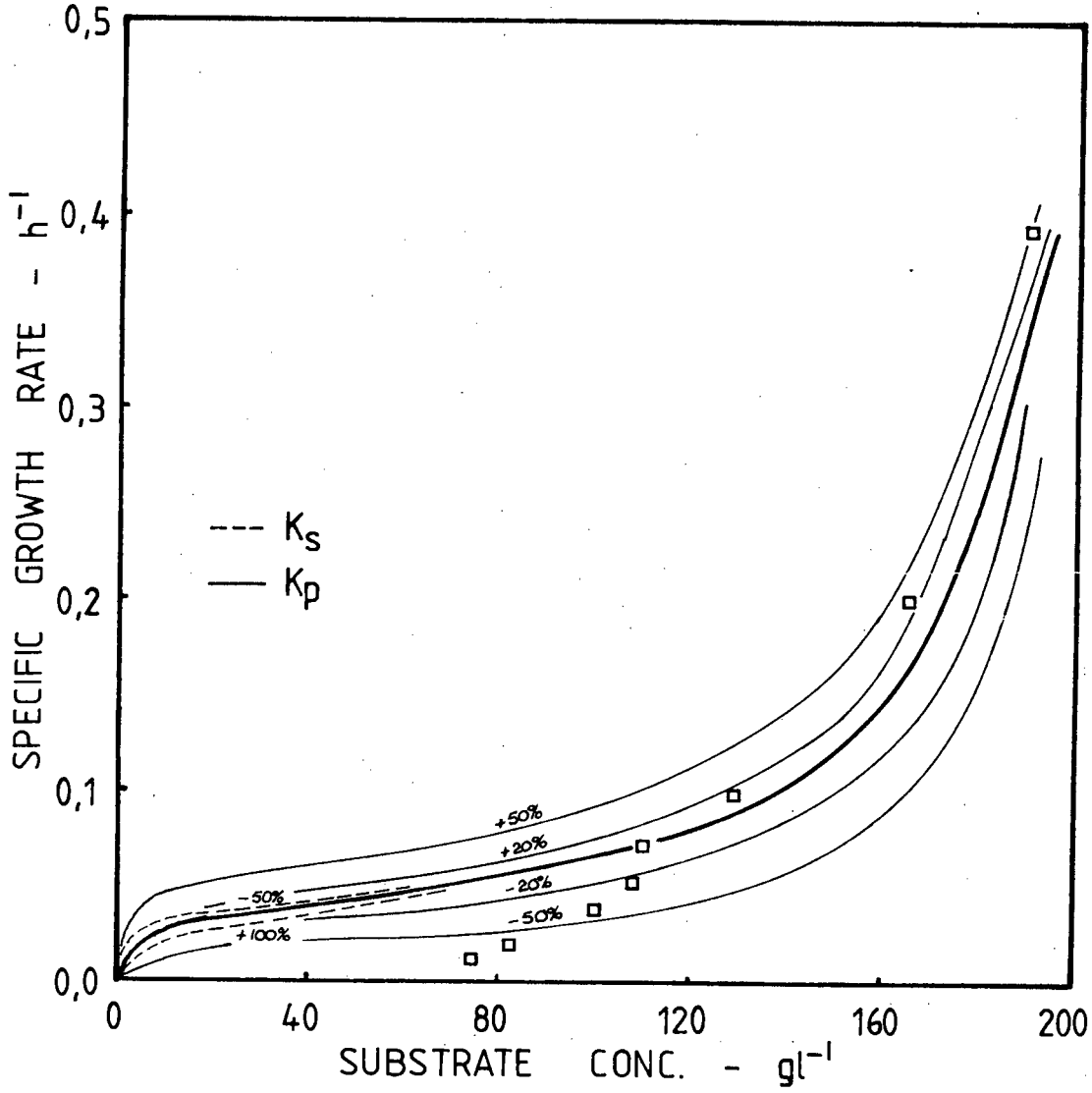

FIGURE 5.33 : EFFECT OF VARIATIONS IN K_s AND K_p ON GROWTH MODEL FOR THE 200 $g\ell^{-1}$ FEED CONCENTRATION - ANAEROBIC

The effect of Kp on the growth curve is also shown in Figures 5.31 to 5.33.

5.4.3 Combined effect of the Growth Constants

For the two higher feed concentrations, K_s is the least critical constant for modelling the growth curve. With insufficient data in the very low substrate concentration or dilution rate regions, K_s was also least accurately determinable. The model is therefore mainly dependent on the maximum specific growth rate and the ethanol inhibition constant. Although graphical analysis e.g. Figure 5.11, seems to point to a particular value for $\hat{\mu}$ and hence K_p, the model would not be able to account for sudden changes near the critical dilution rate as shown by the data of Cysewski [16] for the anaerobic, 100 gl^{-1} feed concentration fermentation i.e. the model could accurately determine the growth curve up to the critical dilution rate but would then overestimate the maximum possible dilution rate. A lower maximum specific growth rate would require a lower degree of ethanol inhibition (higher K_p value) for a similar predicted growth curve. e.g. reducing $\hat{\mu}$ to 0,45 h^{-1} and increasing K_p to 8,1 results in the same predicted curve up to a substrate concentration of 50 gl^{-1} at which stage it begins to underestimate the predicted model. This deviation in the preceeding example could not be eliminated, even if K_p were increased further and K_s were also increased to offset the positive deviation at the lower substrate concentrations. Therefore the model proposed in this work requires a maximum specific growth rate value in the region as predicted i.e. $\hat{\mu} = 0,64\ h^{-1}$.

For the low feed substrate concentration of 20 gl^{-1}. the values of K_p and K_s could be varied without significant change in the predicted curve. A 20% increase in K_p could be offset by a 20% increase in K_s and also the reverse could apply. This has already been shown in Section 5.1.4 in the individual model predictions for the 20 gl^{-1} feed substrate concentration.

5.5 MASS BALANCE AT THE STEADY STATES

Mass balances for each of the steady states at all the concentrations were performed to provide a check on the magnitude of the various flow streams, compare these to expected flow rates and hence point to critical areas. No mass balances were performed on the micro-aerobic data because the concentration of the carbon dioxide in the exit gas stream was not measured.

Mass balances performed on a "total mass flow" basis gave accountabilities greater than 99% for all steady states (see Appendix D). They were done by allowing for the variation in the specific gravity of the liquid streams due to different glucose and ethanol contents. The most probable reason for the high accountability was because the masses of sugar, yeast, ethanol and carbon dioxide were minor compared to the mass of water that was in conjunction with them. Therefore a more direct method was used to measure the changes in the concentrations of the important components - namely an elemental balance using carbon. The results have been summarised in Table 5.11 and were obtained by considering the inflow of carbon in the glucose and comparing it to the outflow of carbon in the exit glucose, ethanol, yeast and carbon dioxide. The results showed that the accountability increased as the dilution rate increased which was expected because it reflected the same case as above with the water now replaced by the glucose i.e. at high dilution rates most of the glucose was not fermented and hence inaccuracies in the determination of ethanol, yeast and carbon dioxide flows would be masked by the high exit glucose level.

Significant "losses" appeared at most of the lower dilution rates. These could have been due to incorrect measurements and significant levels of other products not measured e.g. glycerol. Glycerol can be formed to levels of 3 to 4% (Prescott and Dunn [32]) and hence could account for approximately a 2% decrease in the accountability.

TABLE 5.11: CARBON BALANCE AT THE VARIOUS STEADY STATES

FEED CONCENTRATION - gl^{-1}					
20		100		200	
D-h^{-1}	% ACC	D-h^{-1}	% ACC	D-h^{-1}	% ACC
0,024	94,0	0,020	86,6	0,013	83,1
0,063	84,5	0,040	95,0	0,020	89,5
0,105	77,7	0,078	92,5	0,037	88,1
0,128	92,3	0,081	92,2	0,053	91,0
0,191	100,7	0,112	91,0	0,073	91,5
0,276	97,8	0,162	89,1	0,101	92,3
0,320	93,1	0,208	95,1	0,201	97,5
0,400	99,5	0,289	97,9	0,397	97,8
0,461	101,2	0,347	95,5		
0,497	100,4				

Examination of the carbon dioxide mass term in the carbon balance showed this to be below that expected by a stoicheometric production with ethanol. The stoicheometric ratio for carbon in ethanol to carbon in carbon dioxide is 2.00, determined as follows

$$\frac{\text{C in } C_2H_5OH}{\text{C in } CO_2} = \frac{24/46}{12/44} \times \frac{92}{88}$$

$$= (\text{C in product}) \times (\text{product formation per 180 parts glucose})$$

$$= 2.00$$

For the second steady state in the 20 gl^{-1} feed glucose concentration fermentation, i.e. at D = 0,063 h^{-1}, the above mass ratio was 3,64, which showed the carbon dioxide level measured was too low. Using a mass ratio of 2 to predict the carbon dioxide carbon mass would have given an accountability of 97,9% which would be acceptable. Similarly the 77,7% accountability could have been increased to 88,1% which also showed that this

may not have been the only discrepancy.

The above procedure could also have been applied in reverse. For the 100 gl^{-1}, 0,162 h^{-1} steady state, the mass ratio for carbon in ethanol to carbon dioxide was 1,69, i.e. too low a value for the ethanol component. This was also shown by a correspondingly low ethanol yield coefficient for this steady state.

5.6 ERRORS AND LIMITATIONS

Fermentations, by their nature, will seldom allow exact repetition of experimental results but by keeping as many environmental factors as constant as possible, such as pH, temperature, agitation, and by adopting a consistent manner in operating and monitoring the fermentation, very similar results should be attainable. This scheme was strictly adhered to in this investigation. Also to minimise any process of adaption, dilution rates were chosen in a random way instead of in an increasing or decreasing sequence and more than one continuous fermentation was attempted within each of the three feed glucose concentrations. No noticable inconsistencies were found amoungst any of the experiments within one of the feed concentrations and hence the results were adopted with confidence.

Systematic errors could however have occurred and these will be discussed with particular reference to the experimental technique employed and the analyses performed.

5.6.1 Medium Preparation

The glucose component of the medium which was sterilised separately, had a light yellow colour after sterilisation, which could have represented a change in the nature of the glucose molecule, i.e. isomerisation, or the formation of higher sugar molecules. Such changes could have changed the medium from a single substrate to several different substrate components fermenting at different rates and/or times and

so creating a diauxic effect. This was attempted in Figure 5.34, and showed a possible effect at all three feed concentrations, increasing with increasing glucose concentration.

As has been mentioned before, the medium was not de-aerated and hence dissimilar amounts of oxygen were associated with each unit of glucose which could have resulted in different metabolic schemes. The effect of decreasing oxygen solubility for increasing component concentrations would have been minor to the above.

5.6.2 Fermenter Operation

Operational limits on temperature, pH and agitation have already been specified. These were sufficiently low to eliminate any effects due to them. The feed rate was subject to some fluctuation due to the decreasing head in the feed reservoir and a stretching of the tubing at the peristaltic pump. Regular checking and adjustment when necessary gave a maximum variation of ± 2% at all dilution rates. It was found that the various concentration variables were sensitive to the dilution rate and that a 2% variation could be detected, especially in the cell mass and glucose concentrations.

The withdrawal system did not provide a steady flow. This was because withdrawal was by a plain tube at a predetermined depth. Withdrawal continues to below the level of the tube because of surface tension so that when this was exceeded, a short lag period existed during which the level rose again to the tube height. These lag periods were very short because the uneven nature of the agitated broth surface, quickly allowed recontact to be made. The resultant fluctuations in the liquid depth in the fermenter or in the withdrawal rate were considered too small to have any significant effect on the steady state operation of the fermenter.

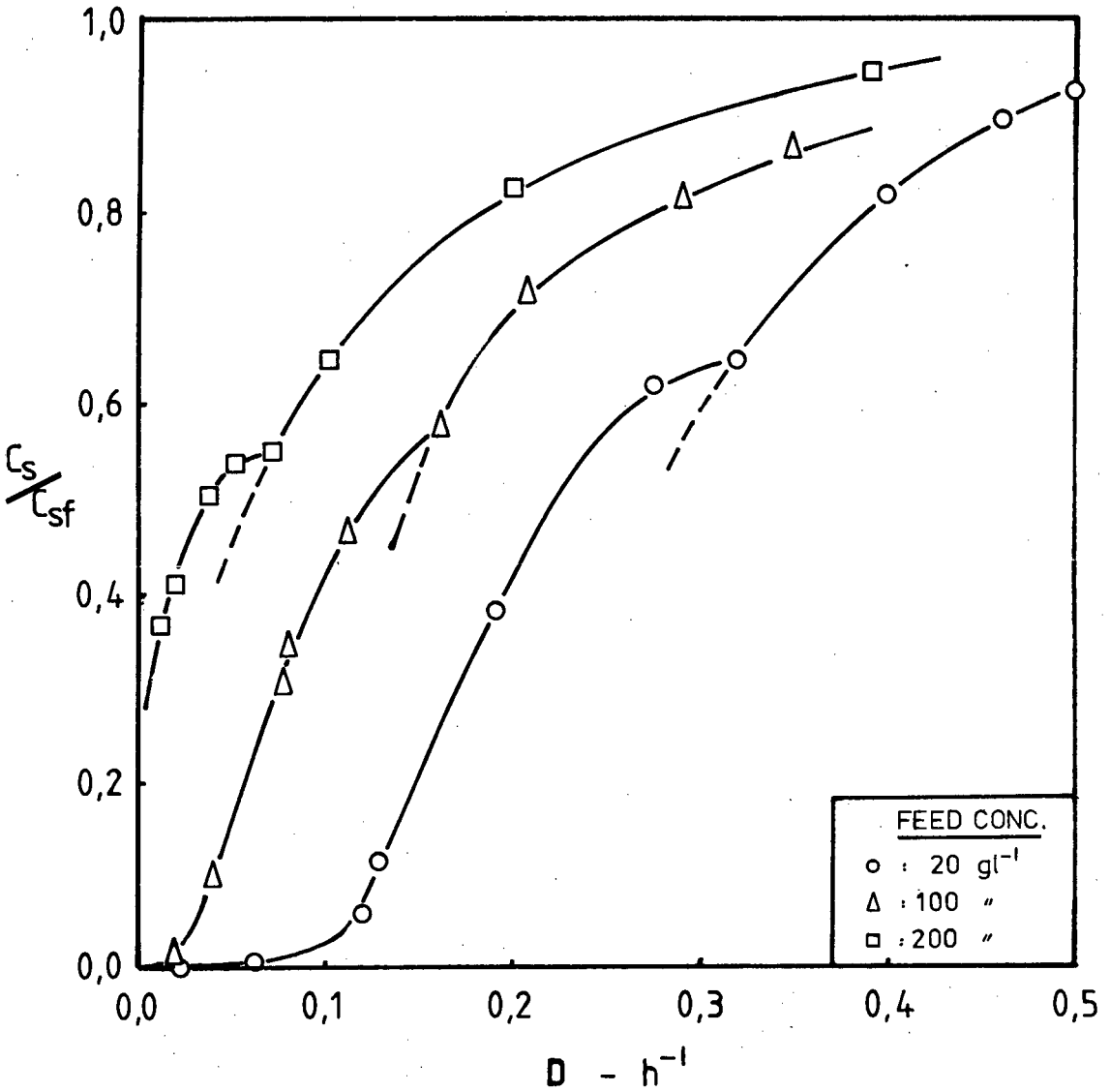

FIGURE 5.34 : FRACTION SUBSTRATE NOT CONSUMED AS A FUNCTION OF THE DILUTION RATE AND FOR DIFFERENT FEED CONCENTRATIONS (ANAEROBIC)

Wall growth was observed above the level of the broth in the fermenter. This occurred due to some intermittent foam formation which then left a cell deposit on the walls. This grew as it made contact with the medium and was also washed back into the medium by the uneven nature of the medium surface. No wall growth was visible below the surface of the culture, although it has been ovserved in the literature. Topiwala and Hamer [33] quantified the effect of this wall effect below the culture surface and the same analysis could have been applied above the surface. Wall growth increases the maximum dilution rate because of the greater difficulty by which these cells are dislodged and washed out. There was no appearance of this in these experiments, but maximum dilution rates used were also not close to the washout point.

5.6.3 Concentration Analyses

(a) Cell Mass: The determination of the cell mass concentration had a reproducibility of ±3%, as previously stated in Section 4.6.1. This applied to repeated sampling from a fermenter, working with different dilutions and the use of the calibration curve. The calibration curve itself was subject to an error of ± 2-3% in the 40 - 70% transmittance working range. At 20% transmittance an error of ±5% could be expected and therefore this end of the scale was not recommended for more accurate determinations. Determinations in the transient regions between steady states could have been done satisfactorily even outside the normal working range, because they were only for monitoring purposes.

Care needed to be exercised when preparing the calibration curve. Samples of cells were drawn from a growing sample culture and rapidly analysed for turbidity and dry cell mass content. Dry weight measurements were also performed at some of the steady states

as a check and good agreement was obtained.

Only the total cell mass was used to represent the cells in the culture and express their influence. No account was taken of changes in the physical (e.g. number and size) and chemical (e.g. DNA, RNA, protein content) properties of the cells as a function of the dilution rate or of the effect of prolonged continuous operation. This was done because it had been the aim to use a single and simple variable in classifying the yeast present in the fermentation.

No attempt had also been made to check the fraction of the cells which were viable. Pironti [19] had shown that at low dilution rates with a high feed glucose concentration, the fraction of non-viable cells began to increase significantly.

(b) Glucose: Again, as stated before, the reproducibility was better than ±2%. Best accuracy was obtained by working close to the calibration point of the Glucose Analyser. For good representation of the fermenter concentration, it was necessary to analyse immediately, especially in spinning out the yeast cells to minimise further reaction. The time for this preparation, approximately twenty minutes, was very small compared to any residence times used in the fermenter and therefore did not cause a significant change.

As mentioned in Section 5.6.1, the glucose in the medium may have undergone a change during sterilisation. This was also shown by different glucose analyses on the different glucose feed reservoirs.

This pehnomenon has not been examined further but has been taken into account by increasing the measured concentrations proportionately. The final values used represented a conservative value for the glucose concentration i.e. a lower limit, with a possible 5%

increase for the maximum limit. The effect was therefore most noticeable on the higher glucose concentrations, which would have also positively influenced the modelling i.e. a better fit between observed and predicted data would have resulted cf Figure 5.33.

(c) Ethanol: The ethanol concentration analysis was most susceptible to ethanol evaporation in each of the sample preparation steps: the transfer of sample from the syringe to the sample vial, subsequent dilution in a volumetric flask, transfer of a portion into centrifuge tubes and subsequent decantation into storage vials. With sufficient care these were held to a minimum. The analyses were initially performed without an internal standard, so that more reliance was placed on an accurate and consistent procedure. The chromatograms from the Hewlett Packard chromatograph were also analysed by hand using a planimeter. A linear calibration was obtained up to a concentration of 0,11 gl^{-1} ethanol and for the upper half of the calibration range, a reproducibility of better than $\pm$ 2% was obtained. The lower the concentration. the less reproducible was the analysis and hence most analyses were made to fall in the upper region. The introduction of the Varian chromatograph allowed a linear correlation to concentrations of 1,5 gl^{-1} and the use of an integrator and an internal standard, gave reproducibility to better than $\pm$ 1%.

6. CONCLUSIONS

From these foregoing experimental investigations, the following main conclusions were drawn:

(i) continuous laboratory fermentations on a 1ℓ scale, converting glucose to ethanol using a yeast, could be successfully operated for periods of up to 1500 hours without visible (under the microscope) signs of contamination,

(ii) the anaerobic fermentation of the pure substrate glucose by the yeast Saccharomyces cerevisiae, ATCC 4126, was strongly inhibited by the product ethanol,

(iii) a mathematical model based on non-competitive enzymic product inhibition was successfully used to describe the product inhibited growth kinetics of the yeast under continuous culture conditions; the growth model had the form

$$\mu = \hat{\mu} \cdot \frac{C_s}{C_s + K_s} \cdot \frac{K_p}{K_p + C_p} \cdot$$

where $C_p = 0{,}43\ (C_{sf} - C_s)$ gl^{-1}

$\hat{\mu} = 0{,}64$ h^{-1}

$K_s = 3{,}3$ gl^{-1}

$K_p = 5{,}2$ gl^{-1}

The values for the constants were derived using data obtained from three feed glucose concentrations, 20, 100 and 200 gl^{-1}.

(iv) the use of micro-aerobic conditions greatly enhanced the utilisation of substrate by increasing the ethanol tolerance of the yeast without any significant decrease in the ethanol yield per unit substrate consumed;

mathematically this was represented by the increase in the value of K_p to 16,0 gl^{-1}.

From these direct findings, several further implications can be drawn. For the present ethanol fermentation technology available, the substrate cost represents the major portion of the production costs. Therefore conditions close to complete utilisation of the glucose would be necessary and would therefore imply very low dilution rates. To increase the ethanol productivity, greater ethanol tolerance (lower ethanol inhibition), removal of ethanol during fermentation or increasing the cell concentration in the fermenter by separating and recycling the yeast from the effluent, would need to be incorporated into the fermentation system.

7. RECOMMENDATIONS

Some recommendations and suggestions during and for future work are as follows:

(a) During Future Work:

(i) When taking cell mass concentrations, to also determine the percentage viability of this cell mass and to perform a dry weight check at each steady state to allow for cells being in different states compared to the calibration curve.

(ii) Check and improve the reliability of the carbon dioxide measurement for a better mass balance

(iii) Analyse for the other main components, in the fermentation broth eg. glycerol, when operating at a steady state.

(iv) Operate at several steady states closer to the washout point or critical dilution rate.

(b) For Future Work:

(i) Incorporate several more intermediate feed glucose concentrations such as 50 and 150 gl^{-1} to give a more complete coverage over the feed concentration range.

(ii) Conduct continuous fermentations in larger fermenters (7 - 20 l which would allow better feed flow control) to obtain better low dilution rate ($< 0,01$ h^{-1}) steady state data. This could then be used to give a more accurate determination of K_s.

(iii) Optimise the fermentation temperature for cell growth and ethanol production.

(iv) Consider the effect of micro-aerobic conditions on the 200 gl^{-1} feed glucose concentration

(v) Improve the method of measurement and control of the dissolved oxygen content in the broth at the low levels attempted and envisaged for micro-aerobic fermentation.

(vi) Quantitatively determine the amount of oxygen that is being consumed in the micro-aerobic fermentations.

(vii) Attempt to improve the ethanol productivity using continuous cell recycle.

8. REFERENCES

1. Rahn O., "The Decreasing Rate of Fermentation", J. Bacteriol. 18, 207-226 (1929).
2. Holzberg I., Finn R.K. and Steinkraus K.H., "A Kinetic Study of the Alcoholic Fermentation of Grape Juice", Biotechnol. Bioeng., 9, 413-427 (1967).
3. Égamberdiev N.B., and Ierusalimskii N.D. "Effect of Ethanol Concentration on Rate of Growth of Saccharomyces vini (Race Pr-1)", Microbiologiya, 37(4). 686-690 (1968).
4. Aiba S. and Shoda M., "Reassessment of the Product Inhibition in Alcohol Fermentation", J. Ferment. Technol. 47, 12, 790-794 (1969).
5. Aiba S., Shoda M., and Nagatani M., "Kinetics of Product Inhibition in Alcohol Fermentation", Biotechnol. Bioeng. 10, 845-864 (1968).
6. Kunkee R.E., and Amerine M.A., "Yeasts in Wine-making", Chapter 2 in Vol 3, "The Yeasts" Ed. Rose A.H. and Harrison J.S., Academic Press 1970.
7. Bazua C.D., and Wilke C.R., "Ethanol Effects on the Kinetics of a Continuous Fermentation with Saccharomyces cerevisiae", Biotechnol. Bioeng. Symp. No 7. 105-118 (1977).
8. Ghose T.K., and Tyagi R.D., "Rapid Ethanol Fermentation of Cellulose Hydrolysate. II. Product and Substrate Inhibition and Optimisation of Fermentor Design", Biotechnol. Bioeng., 21, 1401-1420 (1979).
9. Nagodawithana T.W., and Steinkraus K.H., "Influence of the Rate of Ethanol Production and Accumulation on the Viability of Saccharomyces cerevisiae , in "Rapid Fermentation"", Appl. Environ. Microbiol., 31(2), 158-162 (1976).
10. Strehaiano P., Moreno M. and Goma G., "Alcoholic Fermentation : Influence of Glucose Concentration on the Rate of Production of Ethanol and the Growth Rate", C.R. Hebd. Seances Acad. Sci. Ser. D. Sci Nat., 286, 2, 225-228 (1978). (In French).

11. Yarovenko V.L., and Nakhmanovich B.M., "Kinetics of Product Synthesis in Continuous Alcohol Fermentation", Biotechnol. Bioeng. Symp. No. 4, 115-116 (1973).

12. Navarro J.M. and Durand G. "Alcoholic Fermentation; Influence of Temperature on the Accumulation of Alcohol in Yeast Cells." Ann. Microbiol. (Inst. Pasteur), 129b, 215-224 (1978). (In French).

13. Thomas D.S., Hossack J.A. and Rose A.H., "Plasma-Membrane Lipid Composition and Ethanol Tolerance in Saccharomyces cerevisiae", Arch. Microbiol, 117 239-245 (1978).

14. Andreasen A.A. and Stier T.J.B. "Anaerobic Nutrition of Saccharomyces cerevisiae. II. Unsaturated Fatty Acid Requirement for Growth in a Defined Medium." J. Cell. Comp. Physiol., 43, 271-281 (1954).

15. Larue F., Lafon-Lafourcade S. and Riberean-Gayon P., "Relationship Between the Sterol Content of Yeast Cells and Their Fermentation Activity in Grape Must", Appl. Environ. Microbiol., 39, 4, 808-811 (1980).

16. Cysewski, G.R., "Fermentation Kinetics and Process Economics for the Production of Ethanol", Ph.D. Thesis 1976, University of California, Berkeley.

17. Moss F.J., Rickard P.A.D., Bush F.E. and Caiger P., "The Response by Microorganisms to Steady-State Growth in Controlled Concentrations of Oxygen and Glucose. II. Saccharomyces carlsbergensis." Biotechnol. Bioeng., 13, 63-75 (1971).

18. Ough C.S., "Fermentation Rates of Grape Juice. III. Effects of Initial Ethyl Alcohol, pH and Fermentation Temperature", Am. J. Enol. Vitic., 17, 74-81 (1966).

19. Pironti F.F., "Kinetics of Alcoholic Fermentation" Ph.D. Thesis, Cornell University (1971).

20. Jackson J.V. and Edwards V.H., "Kinetics of Substrate Inhibition of Exponential Yeast Growth", Biotechnol. Bioeng., 17, 943-964 (1975).

21. Aiba S., Humphrey A.E., and Millis N.F. "Biochemical Engineering" 2nd Edition, Academic Press. (1973).

22. Pirt S.J., "The Maintenance Energy of Bacteria in Growing Cultures." Proc. Roy. Soc. (Lond). B163, 224-231 (1965).

23. Aijar A.S., and Leudeking R. "A Kinetic Study of the Alcoholic Fermentation of Glucose by Saccharomyces cerevisiae." Chem. Eng. Prog. Symp. Series, 62(69), 55-59 (1969).

24. Phaff H.F., Miller M.W. and Mrak E.M., "The Life of Yeasts", Harvard University Press (1966).

25. Nelder, J.A. and Mead R. "A Simplex Method for Function Minimisation." The Computer Journal, 5, 308-313 (1965).

26. Leuenberger H.G.W., "Cultivation of Saccharomyces cerevisiae in Continuous Culture", Arch. Mikrobiol., 79, 176-186 (1971).

27. Pirt S.J., "Principles of Microbe and Cell Cultivation", Blackwell Scientific Publications (1975).

28. Djavan A. and James A.M., "Determination of the Maintenance Energy of Klebsiella aerogenes growing in Continuous Culture." Biotechnol. Lett., 2(7), 303-308 (1980).

29. Luedeking R. and Piret E.L., "A Kinetic Study of the Lactic Acid Fermentation Batch Process at Controlled pH." J. Biochem. Microbiol. Tech. Eng. 1(4), 393-412 (1959).

30. Schatzmann H., "Anaerobes Wachstum von Saccharomyces cerevisiae", Ph.D. Thesis, Eidgenössischen Technischen Hochschule, Zurich (1975).

31. Regan D.L., Roper G.H. and Moss F.J., "Response of Continuous Cultures to Stimuli in Glucose Feed Rate and Dilution Rate", Biotechnol. Bioeng, 13, 815-824 (1971).

32. Prescott, S.C. and Dunn C.G., "Industrial Microbiology", International Student Edition, 3rd Edition, McGraw Hill (1959).

33. Topiwala H.H. and Hamer G., "Effect of Wall Growth in Steady-State Continuous Cultures", Biotechnol. Bioeng, 13, 919-922 (1971).

APPENDIX A:

EXPERIMENT GF-8C-79 : ANAEROBIC AND AEROBIC 100 gl^{-1} FEED

ELAP TIME (h)	FEED RATE ($mlmin^{-1}$)	CO_2 (tot l)	CO_2 - ($lmin^{-1}$)	C_x (mgl^{-1})	C_s (gl^{-1})	C_{p_1} (gl^{-1})
0	-	-				
0,17	-	0,00	-	215	85,0	-
1,5	-	0,07	0,001	275	84,5	-
3,5	-	0,37	0,003	615	85,0	3,7
5,0	-	1,12	0,008	1030	80,0	-
6,5	-	2,77	0,018	1625	67,0	10,2
9,0	-	7,04	0,029	2775	51,0	18,0
10,5	-	9,91	0,032	3150	40,5	20,7
14,5	-	17,08	0,030	4550	20,3	35,7
16,0	-	19,24	0,025	4700	10,4	39,0
17,5	-	21,11	0,021	5600	4,3	42,7
18,5	-	22,00	0,015	6300	1,1	41,2
20,0	-	22,53	0,006	5365	-	41,1
21,5	-	22,59	0,001	4475	-	42,5
22,0	1,25					
24,5	1,23/1,28	24,08	0,012	4140	11,5	37,9
26,5	1,25	26,13	0,017	3500	12,6	-
					C_{sf}=88,0	
29,0	1,23/1,33	28,86	0,018	3000	16,5	40,4
34,5	1,30	35,22	0,019	2700	22,5	35,7
40,0	1,30	41,60	0,019	2310	27,8	33,9
45,0	1,30	47,29	0,019	2250	28,3	32,0
50,0	1,29	52,83	0,019	2360	29,8	32,8
55,5	1,29	58,39	0,018	2250	32.0	28,8
61,0	1,28/1,30	64,87	0,018	2335	33,3	30,2
66,5	1,30	70,86	0,018	2620	28,8	32,5
72,5	1,30	77,17	0,018	2250	31,0	27,3
78,5	1,26/1,29	83,36	0,017	2450	31.0	28,4
84,75	1,30	89,86	0,017	2400	32,3	28,0
89,5	1,29	94,73	0,017	2525	32,8	28,2
95,0	1,32	100,36	0,017	2400	32,5	27,0
100,5	1.32/2,56	106,01	0,017	2150	31,8	25,0

EXPERIMENT GF-8C-79 : (Continued)

ELAP TIME (h)	FEED RATE ($ml\,min^{-1}$)	CO_2 (tot l)	CO_2 - ($l\,min^{-1}$)	C_x ($mg\,l^{-1}$)	C_s ($g\,l^{-1}$)	C_p ($g\,l^{-1}$)
108,5	2,59/2,54	112,94	0,014	1825	50,5	16,3
114,5	2,46/2,52	118,84	0,016	1625	52,0	12,4
121,0	2,44/2,5+	125,71	0,018	1875	53,0	14,3
122,1	2,61		NEW FEED		C_{sf}=85,5	
127,0	2,50/2,59	132,57	0,019	1825	52,5	13,9
132,75	2,56	139,37	0,020	2050	52,5	13,5
138,0	2,50/4,62	145,68	0,020	1770	52,0	13,0
141,0	4,62	147,74	0,011	1500	63,5	9,8
144,0	4,58/4,66	148,84	0,006	1115	71,0	6,9
147,0	4,62	149,73	0,005	1015	74,5	7,0
150,0	4,54/4,66	150,53	0,004	1250	75,5	7,9
155,0	4,58/4,70	151,69	0,004	1275	75,0	5,1
					C_{sf}=91,0	
159,5	4,62/1,80	152,67	0,004	1310	76,0	7,1
165,0	1,79	158,24	0,017	2375	59,5	15,5
170,0	1,79	164,83	0,022	2300	50,5	16,7
175,0	1,63/1,78	170,71	0,020	2115	45,0	24,1
180,0	1,78	176,14	0,018	1920	45,5	21,7
185,0	1,75	181,39	0,018	2100	44,3	22,8
190,0	1,71/1,79	186,62	0,017	2175	44,8	21,4
195,0	1,72/1,81	191,67	0,017	2010	44,3	21,3
200,0	1,81/3,30	196,68	0,017	2125	46,8	22,7
208,0	3,25/3,36	201,74	0,011	1325	63,0	14,5
213,0	3,30	204,48	0,009	1340	66,0	11,0
224,25	3,30	211,09	0,010	1440	68,0	11,0
232,0	3,30	216,02	0,011	1540	65,5	11,3
235,0	3,3/5,5	217,97	0,011	1585	65,5	13,2
239,0	5,32/5,69	220,16	0,010	1320	70,0	8,8
241,5	5,59	220,60	0,003	1150	74,0	6,7
248,75	5,32/5,69	220,74	0,000	1050	79,5	4,9
256,0	5,45			990	79,0	4,6
258,3	0,61				C_{sf}=85,0	

EXPERIMENT GF-8C-79 : (Continued)

ELAP TIME (h)	FEED RATE ($ml min^{-1}$)	CO_2 (tot l)	CO_2 ($l min^{-1}$)	C_x ($mg l^{-1}$)	C_s ($g l^{-1}$)	C_p ($g l^{-1}$)
261,5	0,63	224,31	0,011	2225	71,0	10,5
268,0	0,63	225,09	0,028	2815	38,5	27,3
279,5	0,62/0,64	238,64	0,020	2555	15,8	41,0
289,25	0,63	250,79	0,021	2015	13,3	42,4
298,5	0,63	258,15	0,013	1675	12,3	44,9
306,0	0/0,63	260,77	0,006	2425	0,6	48,8
315,0	0,62/0,64	263,81	0,006	1885	8,5	46.2
323,0	0,64	269,03	0,011	1850	12,3	42,5
324,5	0,63	NEW FEED			C_{sf}=85,0	
329,0	0,63	273,782	0,013	2063	11,5	41,8
333,5	0,62/0,64	277,52	0,014	2350	10,5	42,4
340,0	0,63	283,02	0,014	2450	10,0	41,7
346,5	0,64	285,54	0,014	2285	9,5	39,3
352,5	0,62/0,64	290,40	0,014	2235	9,4	42,0
355,5	0,64	298,67		START AERATION		
357,5	0,65	32,15*	0,357	2450	6,7	41,0
401,25	low	873,8	0,333	11125	0,02	39,3
402,75	0,68	LINE TO FLOW PIPETTE CLEANED				
473,25	0,64/1,32	1442,1	0,334	11375	0,04	38,4
477,5	1,34	90,63	0,355	9790	-	42,8
555,5	1,23	1646,95	0,350	8690	0,11	41,4
568,75	1,25	267,92	0,337	8420	0,03	43,0
618,75	1,20/1,25	1103,10	0,368	9250	0,03	43,0
633,5	1,25	332,70	0,376	9125	-	40,4
641,75	1,23/1,25	183,2	0,370	9000	0,11	36,9
647,1	1,25	119,75	0,374	8565	0,05	40,8
652,25	1,23/1,25	117,75	0,380	9025	-	42,2
653,0	INCREASED AIR RATE O_2 : 0,0 → 0,5% saturation					
663,5	1,23/1,25	344,0	0,546	9065	0,06	41,5
668,5	1,23	170,0	0,567	9400	-	40,9
669,75	2,50	NEW FEED			C_{sf}=89,5	-
673,5	2,44/2.54	167,75	0,559	6940	18,5	32,6

EXPERIMENT GF-8C-79 : (Continued)

ELAP TIME (h)	FEED RATE ($ml\,min^{-1}$)	CO_2 (tot l)	CO_2 ($l\,min^{-1}$)	C_x ($mg\,l^{-1}$)	C_s ($g\,l^{-1}$)	C_p ($g\,l^{-1}$)
688,75	2,44/2,50	513,50	0,561	6300	26,9	26,3
704,25	2,38/2,56		-	5500	24,8	31,5
711,5	2,50/2,54	187,5	0,474	5825	24,3	31,5
718,0	2,50/4,00	85,75	0,476	5800	24,3	32,3
724,5	3,81/4,07	181,00	0,464	4150	44,5	20,9
730,75	4,14	173,5	0,463	3900	48,5	20,7
731,75	4,14		NEW FEED		C_{sf}=83,5	
737,0	3,87/4,00	178,25	0,475	3785	49,5	18,6
743,0	3,93/4,00	170,25	0,473	3750	49,5	21,8
750,75	3,93	211,00	0,454	3625	49,0	19,8
751,75	5,59					
759,0	5,59	223,25	0,451	2775	66,5	13,6
765,0	5,59	149,50	0,415	2775	65,5	13,0
					C_{sf}=88,5	
771,25	5,41/1,79	158,50	0,423	2800	64,5	13,8
786,0	1,78	378,25	0,427	6000	6,8	34,6
791,5	1,81	150,75	0,454	6625	4,9	39,4
809,75	1,75/1,78	470,75	0,430	7050	7,0	41,0
816,5	1,78	188,75	0,449	7370	6,5	39,0
833,0	1,74	421,00	0,425	7330	5,6	38,5
835,0	2,02		NEW FEED		C_{sf}=97,5	
840,0	1,97/2,05	183,00	0,436	7125	9,6	42,9
856,5	2,00	415,50	0,420	6000	13,1	39,3
864,75	2,00	230,75	0,466	6500	9,5	37,7
881,5	2,05	447,75	0,446	6560	13,0	34,9
887,25	2,03	161,00	0,467	6650	11,5	36,6
905,0	1,90/3,05	470,50	0,442	6560	10,2	37,8
912,0	2,95	188,50	0,449	5025	32,5	29,7
912,2	3,10		NEW FEED			
929,5	2,90/+	472,50	0,450	4700	27,3	25,8
933,0	3,05	93,50	0,445	4600	28,0	25,6
937,1	2,95/3,16	108,50	0,441	4670	29,3	25,6

EXPERIMENT GF-8C-79 : (Continued)

ELAP TIME (h)	FEED RATE ($ml min^{-1}$)	CO_2 (tot l)	CO_2 - ($l min^{-1}$)	C_x ($mg l^{-1}$)	C_s ($g l^{-1}$)	C_p ($g l^{-1}$)
953,75	3,16	441,00	0,441	4250	32,8	25,8
954,5	7,5				C_{sf}=86,5	
959,0	7,38/+	135,00	0,429	2000	66,0	9,8
962,0	7,38/+	74,00	0,411	1585	71,0	8,2
964,5	7,63	61,00	0,407	1440	74,5	7,4
976,75	7,50	290,50	0,395	1050	78,0	5,6
979,75	7,38	47,50	0,264	1075	77,0	5,2
983,75	7,38	24,65	0,103	1065	77,5	5,0
1080,0	pH = 4,00					
	HOLD UP = 950 ml					

* From here onwards, total l represent the CO_2 produced between consecutive readings.

EXPERIMENT GF-10C-80 : ANAEROBIC - 100 $g l^{-1}$ FEED

ELAP TIME (h)	FEED RATE ($ml min^{-1}$)	CO_2 (Total)	CO_2 - (1 h^{-1})	C_x ($g l^{-1}$)	C_s ($g l^{-1}$)	C_p ($g l^{-1}$)
0	-	0		215	82,0	-
2,20	-	0,11		440	-	-
4,50	-	20,40		995	79,0	-
18,60	0/1,90	20,51		7210	0,1	-
21,40	1,90/1,35	0,39	-	7100	3,9	-
26,92	1,29	7,57	1,306	4700	10,8	-
46,67	1,29	32,52	1,106	3325	17,4	-
65,67	1,29	51,64	1,006	2675	25,0	-
74,67	1,27/1,31	59,81	0,908	2600	28,5	-
97,50	1,30	79,956	0,882	2290	32,9	-
122,58	1,20/1,29	100,160	0,806	2235	34,5	-
138,00	1,29	111,43	0,731	1935	37,5	-
145,75	1,29	117,44	0,775	2000	33,7	-
163,00	1,29	132,46	0,871	2325	33,7	-
185,50	-	150,76	0,813	2140	35,0	-
191,33	-	-	-	2290	34,5	-
214,00	-	173,66	0,804	2065	36,3	-
217,50		NEW FEED				-
235,00	1,31	192,66	0,905	2750	39,9	-
242,50	1,30	200,66	1,067	2875	35,9	-
290,00	0,86/Incr.	231,26	0,644	4440	7,2	-
307,17	Incr.	248,41	0,999	3320	11,5	-
329,50	-	269,41	0,940	3075	27,2	-
340,25	1,29	280,41	1,023	2965	30,1	-
353,42	-	294,01	1,033	2965	28,5	-
	1,29	NEW FEED				
362,00	1,27/1,31	303,06	1,054	2990	29,5	-
377,67	1,29	320,09	1,087	2965	31,5	-
384,42	-	328,11	1,094	2925	31,3	-
385,67				2825	30,5	30,5
401,33	1,29	345,81	1,046	2840	30,3	-
404,33		349,06	0,975	2855	30,0	30,5

EXPERIMENT GF-10C-80 : (Continued)

ELAP TIME (h)	FEED RATE (ml min^{-1})	CO_2 (Total)	CO_2 (l h^{-1})	C_x (g l^{-1})	C_s (g l^{-1})	C_p (g l^{-1})
473,67	1,34/0,25	417,910	0,998	2695	30,5	-
499,33	0,26	433,11	0,570	2965	2,5	-
523,16	0,31	440,41	0,306	1920	1,0	-
548,50	0,31	448,31	0,312	1690	2,0	-
571,00	0,31	454,91	0,293	1640	3,1	-
644,25	0,30	475,75	0,284	1440	2,4	-
665,83	0,29	471,51	0,001	3125	0,1	46,0
		(LEAKAGE AT HEAD PLATE)				
674,00	0,32			4070		-
689,75	0,33/0,32	484,16	0,343	4650	0,2	-
697,75				4450		-
714,00	0,32	492,86	0,359	3610	0,8	-
738,67	0,32	501,68	0,358	2325	1,7	-
810,42	0,32	520,81	0,253	1055	14,8	-
834,92				1070	11,2	-
858,75	0,31	533,51	0,263	1265	13,4	-
883,75	0,32	541,11	0,304	1225	14,3	-
906,50	0,32	547,84	0,295	1225	13,1	-
977,50	0,33/Decr.	569,69	0,308	1250	11,8	-
1004,33	0,31	577,16	0,278	1225	11,3	-
1029,00	0,30	583,16	0,244	1150	13,9	-
					C_{sf}=97,5	-
1049,67	0,30	592,62	0,459	2750	2,6	-
1073,67	0,30	601,05	0,351	3550	0,7	-
1145,67	0,28/0,31	627,36	0,365	1525		-
1169,67	0,34/0,32	637,01	0,402	2025		-
1193,67	0,35/0,30	648,01	0,459	2065		-
1217,67	0,27	661,15	0,547	2425	C_{sf}=92,5	-
1241,67	0,28	670,75	0,400	2240	1,7	-
1274,42	0,30	681,24	0,320	1700	4,8	-
1315,00	0,30	692,04	0,266	1325	13,8	-
1337,67	0,29	697,61	0,257	1240	15,3	-

EXPERIMENT GF-10C-80 : (Continued)

ELAP TIME (h)	FEED RATE ($ml min^{-1}$)	CO_2 (Total)	CO_2 ($l\ h^{-1}$)	C_x ($g l^{-1}$)	C_s ($g l^{-1}$)	C_p ($g l^{-1}$)
1361,67	0,28/0,30	703,69	0,253	1265	15,7	
1385,67	0,31	709,46	0,240	1265	18,3	
1409,67	0,31	716,02	0,273	1315	19,0	
1481,67	0,28	736,29	0,281	1315	17,4	
1505,67	0,35	743,65	0,307	1550	20,0	
1529,67	0,36	751,02	0,307	1440	19,8	
	STOPPED					
		HOLD UP :	940 ml			

EXPERIMENT GF-11C-80 : ANAEROBIC - 200 gl^{-1} FEED

ELAP TIME (h)	FEED RATE ($ml min^{-1}$)	CO_2 (tot l) - (l h^{-1})		C_x (gl^{-1})	C_s (gl^{-1})	C_p (gl^{-1})
0,00	-	0	-			
	(INOCULUM:)	0	-	5000	38,5	-
16,75	-	15,30	0,914	6000	89,5	-
20,25	-	22,31	2,010	5865	67,0	-
21,00	0/0,92					
24,50	0,92	25,60	0,940	4615	72,0	-
40,25	0,92	34,95	0,543	1875	105,0	-
112,25	0,82	86,40	0,715	2150	106,0	-
136,25	0,83	107,83	0,892	2250	99,5	-
160,25	0,83	130,06	0,927	2100	106,5	-
163,75	0,83	-	-	2450	107,4	35,7
170,25	0,83	139,25	0,919	1925	105,5	-
184,25	0,81	152,35	0,936	2100	106,0	-
187,25	0,81	-	-	2450	108,0	36,6
208,25	1,27	175,93	0,982	2585	125,0	-
216,25	1,25/1,67	-	-	2500	128,0	-
241,00	1,64	212,32	1,111	2325	132,0	-
281,50	1,60	258,47	1,140	2350	129,0	-
304,25	1,60	284,85	1,213	2400	135,0	-
328,25	1,58/1,64	312,90	1,168	2480	126,0	-
352,25	1,62	341,35	1,185	2425	133,0	-
376,25	1,58	370,38	1,210	2490	125,0	-
401,00	1,56	400,90	1,233	2480	134,0	-
401,75	-/3,23	-	-	2540	129,0	27,1
428,25	3,23	428,06	0,997	1850	167,0	-
448,25	3,23	448,85	1,040	1860	168,0	-
451,75	-	-	-	1900	165,0	14,3
452,25	-/3,5	-				
455,25	3,5/5,36	455,40	0,936	1410	170,0	-
458,25	5,33/6,67	456,82	0,473	1160	173,0	-
					C_{sf}=195,0	
472,25	6,21	460,43	0,258	665	184,0	-

EXPERIMENT GF-11C-80 : (Continued)

ELAP TIME (h)	FEED RATE ($ml\,min^{-1}$)	CO_2 (tot l)	CO_2 ($l\,h^{-1}$)	C_x ($g\,l^{-1}$)	C_s ($g\,l^{-1}$)	C_p ($g\,l^{-1}$)
475,25	6,21/1,09	460,83	0,133	665	189,0	2,8
496,25	1,05	487,05	1,249	2325	126,0	-
520,25	0 /1,20	NEW FEED				
522,75	1,15	519,63	1,230	2650	108,0	-
528,75	1,15	527,50	1,312	2660	110,0	-
544,25	-	547,80	1,310	2610	-	-
550,75	-	556,15	1,285	2700	-	35,0
616,25	0,59	600,93	0,684	1800	99,5	-
624,25	0,59	606,07	0,605	1700	101,0	39,7
640,25	0,58	614,91	0,571	1695	98,0	38,7
647,50	-	618,95	0,557	-	-	-
664,50	0,58	629,68	0,632	1625	104,5	37,7
688,25	0,58	644,95	0,642	1600	101,0	38,4
713,50	0,56	661,00	0,635	1500	101,5	37,6
720,75	0,59	665,32	0,596	1540	101,0	-
785,25	-	703,37	0,590	1375	112,0	34,0
	STOPPED					

HOLD UP : 950 ml

EXPERIMENT GF-12C-80 : ANAEROBIC - 100 gl^{-1} FEED

ELAP TIME (h)	FEED RATE ($ml min^{-1}$)	CO_2 (tot l) - (l h^{-1})		C_x (gl^{-1})	C_s (gl^{-1})	C_p (gl^{-1})
16,00	0	18,09	-	5550	9,9	-
22,00	0 /0,66	20,65	-			
88,00	0,32	42,77	0,335	2120	1,5	-
112,00	0,32	49,960	0,300	1950	1,8	-
136,25	0,32	56,980	0,289	1800	2,3	-
160,00	0,32	63,75	0,285	1700	2,8	-
185,25	0,32	71,07	0,290	1800	3,5	-
257,00	0,32	92,07	0,293	1400	5,9	43,2
280,00	0,32	98,96	0,300	1735	3,8	43,9
304,25	0,32	106,26	0,304	1600	7,0	43,3
330,75	0,315	113,54	0,275	1460	6,4	-
351,75	0,33	119,46	0,282	1440	6,7	43,2
405,00	0,33	134,54	0,283	1600	6,4	44,0
425,00	0,32	139,93	0,269	1310	7,7	41,5
448,00	0,32	147,39	0,324	1600	6,1	44,1
					C_{sf}=99,0	
473,00	0,325	157,16	0,390	1465	3,1	44,9
496,00	0,315/0,32	165,24	0,352	1650	2,6	45,4
520,00	0,32	173,48	0,343	1700	1,9	45,4
545,50	0,32	182,24	0,343	2085	1,4	45,9
		NEW FEED				
593,00	0,32	196,97	0,310	1700	1,3	45,2
618,50	0,315	205,64	0,339	1950	1,3	45,2
641,00	0,31	213,14	0,333	1910	1,2	45,2
643,00						

EXPERIMENT GF-13C-80 : ANAEROBIC - 200 $g1^{-1}$ FEED

ELAP TIME (h)	FEED RATE ($ml min^{-1}$)	CO_2 (tot l)	CO_2 - (1 h^{-1})	C_x ($g1^{-1}$)	C_s ($g1^{-1}$)	C_p ($g1^{-1}$)
0,00	0	0	-	-	-	-
16,75	/0,33	12,57	-	4000	130,0	22,5
43,50	0,33	51,22	1,445	4120	44,0	69,9
64,25	0,32	64,69	0,641	2650	50,5	67,8
117,50	0,31	92,84	0,528	2000	62,5	62,4
137,50	0,31/0,34	104,47	0,581	1670	60,0	62,5
160,50	0,32/0,34	116,14	0,507	1460	68,0	61,6
168,00	-	-	-	1790	C_{sf}=195,0	-
185,50	0,32/0,34	128,67	0,500	1650	71,0	58,3
208,00	0,34	140,52	0,515	1650	70,0	56,3
232,00	0,35	152,17	0,485	1550	74,0	54,7
257,50	0,34	164,28	0,474	1385	80,0	52,7
305,00	0,33	185,22	0,441	1425	83,0	49,8
330,50	0,33	197,07	0,465	1450	81,5	49,7
353,00	0,33	206,92	0,437	1275	83,0	49,9
377,50	0,19	216,91	0,404	1340	71,0	55,5
401,75	0,16	225,52	0,353	1175	63,0	60,3
473,0	0,21	252,52	0,379	1325	54,5	65,0
497,50	0,17	261,81	0,379	1450	54,5	54,6
521,00	0,17/0,21	270,07	0,351	1300	53,5	65,5
546,00	0,21	279,33	0,370	1550	54,0	65,0
567,75	-	287,35	0,368	1550	50,5	65,5
574,75	-	289,78	0,347	1520	52,5	67,5
	STOPPED					

HOLD-UP : 985 ml

EXPERIMENT GF-14C-80 : ANAEROBIC - 20 gl^{-1} FEED

ELAP TIME (h)	FEED RATE ($mlmin^{-1}$)	CO_2 (tot l)	CO_2 - (1 h^{-1})	C_x (gl^{-1})	C_s (gl^{-1})	C_p (gl^{-1})
0,00	CONTINUATION OF 12C BUT 20 gl^{-1} FEED					
5,00				1460	0,4	
22,50	0,98	0	-	1380	0,33	18,50
28,75	0,98	0,26	-	1100	0,35	15,70
46,50	0,97	1,16	0,051	1075	0,36	11,20
53,00	0,97	1,57	0,063	1090	0,38	10,70
118,00	0,90/0,95	6,66	0,078	665	0,18	9,47
124,60	0,95	7,24	0,087	690	0,19	9,33
142,35	0,92	8,63	0,079	1250	0,05	10,75
148,50	0,98	9,00	0,060	1290	0,18	9,09
					C_{sf}=19,4	
166,0	0,98	10,31	0,074	1200	0,18	9,13
173,50	0,98	10,88	0,079	1275	0,22	9,11
191,00	0,97	12,21	0,076	1275	0,19	9,03
196,75	-	12,74	0,098	1275	0,04	9,03
212,75	-	10,59	LEAK	790	12,2	3,09
213,75	-	10,48				
215,75	4,62	10,62	0,038	790	12,0	3,25
219,00	4,29/4,41	10,74	0,035	810	11,8	3,25
222,08	4,29/4,29	10,93	0,065	825	12,1	3,41
225,60	4,29	11,10	0,053	810	12,0	3,41
226,50	1,33	NEW FEED				
285,00	1,38/1,74	23,27	0,208	1290	0,37	8,22
291,33	1,71	24,22	0,150	1175	1,06	7,65
308,75	1,64	27,42	0,184	1156	1,30	7,55
317,00	1,66	28,85	0,191	1156	1,43	7,50
332,75	1,64	31,58	0,173	1180	1,20	7,63
340,75	1,61/Incr	32,76	0,149	1180	1,10	7,66
356,75	1,64	35,24	0,151	1180	1,14	7,64
364,50	5,56	-	-	-	11,00	-
380,75	5,08	35,88	0,039	675	12,00	2,50
384,50	5,08	35,98	0,028	710	12,50	2,64

EXPERIMENT GF-14C-80 : (Continued)

ELAP TIME (h)	FEED RATE ($ml\,min^{-1}$)	CO_2 (tot l)	CO_2 - ($l\,h^{-1}$)	C_x ($g\,l^{-1}$)	C_s ($g\,l^{-1}$)	C_p ($g\,l^{-1}$)
387,75	5,00	36,11	0,038	710	12,00	2,77
389,75	0,36	36,71				
476,75	0,38	44,87	0,094	1625	0,03	9,14
500,75	0,37	46,53	0,069	1495	0,03	9,30
526,00	0,36/Incr	48,08	0,061	1375	0,04	9,33
550,60	0,40/0,36	49,75	0,068	1390	0,03	9,36
579,00	0,43/0,38	51,69	0,068	1420	0,05	9,41
620,75	0,39	54,30	0,062	1415	0,12	9,38
629,33	3,56/3,10	54,82	0,061	700	11,60	3,45
646,00	3,00	60,69	0,035	1090	7,20	5,65
649,50	3,00	62,09	0,040	1150	7,80	5,71
653,00	2,95	63,38	0,037	1135	7,25	5,67
	6,98				C_{sf}=18,8	
668,75	6,32	63,90	0,023	415	15,40	1,53
672,00	6,19/6,38	-		435	15,80	1,57
674,75	6,32	-		440	15,60	1,63
677,00	6,19/7,50	-		450	15,30	1,67
679,00	7,50	-		430	15,90	-
693,00	STOPPED					

HOLD UP : 940 ml

EXPERIMENT GF-15C-80 : ANAEROBIC - 200 $g1^{-1}$ FEED

ELAP TIME (h)	FEED RATE ($ml min^{-1}$)	CO_2 (tot l)	CO_2 - ($l h^{-1}$)	C_x ($g1^{-1}$)	C_s ($g1^{-1}$)	C_p ($g1^{-1}$)
0,00	-	0	-			
3,25	-	0,05	-	60	180,0	0,2
19,75	0,0/0,204	13,98	-	3900	115,0	-
43,75	0,208	40,15	1,090	3020	49,8	62,9
130,75	0,191	75,88	0,372	1425	54,0	66,1
163,75	0,197	84,15	0,345	1310	50,5	65,7
189,00	0,197	91,91	0,307	1135	52,5	63,2
213,60	0,197	98,81	0,280	1125	57,0	62,1
242,00	0,202	106,42	0,268	1055	62,0	57,8
283,75	0,203	116,26	0,235	1000	64,5	53,8
309,00	-	122,23	0,237	915	71,5	54,1
331,75	0,205	127,60	0,236	875	73,5	51,3
	STOPPED					

EXPERIMENT GF-16C-80 : ANAEROBIC - 20 gl^{-1} FEED

ELAP TIME (h)	FEED RATE ($mlmin^{-1}$)	CO_2 (tot l)	CO_2 - (l h^{-1})	C_x (gl^{-1})	C_s (gl^{-1})	C_p (gl^{-1})
0,00	0	0	-	-	-	-
20,00	2,50					
65,75	2,00	23,76	0,361	1290	2,11	7,28
69,00	2,00	25,07	0,404	1260	2,01	7,07
71,67	8,33	26,28	0,450	-	-	-
89,75	7,23	-	-	270	16,20	0,88
		NEW FEED			Csf=18,0	
95,00	8,33	-	-	290	16,6	-
99,50	8,33	-	-	230	17,0	0,76
113,75	7,79	-	-	200	17,0	0,68

HOLD UP : 940 ml

O_2 IN FEED : 63% SATURATION

PENDIX B:

TABLE A9 : 20 gl^{-1} FEED CONCENTRATION - ANAEROBIC - STEADY STATE DATA

D	C_s	C_x	C_p	CO_2	Y_{xs}	Y_{ps}	DC_p	DC_p/C_x	SUR	D^{-1}	$(DC_p/C_x)^{-1}$
h^{-1}	gl^{-1}	gl^{-1}	gl^{-1}	lh^{-1}			$gl^{-1}h^{-1}$	h^{-1}	$gl^{-1}h^{-1}$	h	h
,024	0,08	1,42	9,40	0,073	0,071	0,472	0,226	0,159	0,337	41,67	6,293
,063	0,18	1,28	9,10	0,120	0,065	0,459	0,573	0,448	0,976	15,87	2,232
,105	1,20	1,18	7,65	0,171	0,063	0,407	0,803	0,681	1,673	9,52	1,469
,128*	2,30	1,29	7,28	0,426	0,073	0,411	0,932	0,722	1,756	7,81	1,384
,191	7,67	1,14	5,68	0,421	0,093	0,461	1,085	0,952	2,066	5,24	1,051
,276	12,38	0,81	3,40	0,251	0,106	0,446	0,938	1,159	2,596	3,62	0,863
,320	12,90	0,71	2,77	0,092	0,100	0,390	0,886	1,249	3,335	3,13	0,801
,400	16,30	0,45	1,67	-	0,122	0,451	0,668	1,484	3,289	2,50	0,674
,461*	17,90	0,27	0,88	-	0,129	0,419	0,406	1,503	3,586	2,17	0,666
,497*	18,50	0,20	0,68	-	0,133	0,453	0,338	1,690	3,728	2,01	0,592

* From Experiment GF-16C-80, others all from GF-14C-80.

TABLE A 10 : 100 gl^{-1} FEED CONCENTRATION - ANAEROBIC - STEADY STATE DATA

D	C_s	C_x	C_p	CO_2	Y_{xs}	Y_{ps}	DC_p	DC_p/C_x	SUR	D^{-1}	$(DC_p/C_x)^{-1}$
h^{-1}	gl^{-1}	gl^{-1}	gl^{-1}	lh^{-1}			$gl^{-1}h^{-1}$	h^{-1}	$gl^{-1}h^{-1}$	h	h
020*	1,3	1,90	45,2	0,366	0,019	0,458	0,904	0,476	1,039	50,00	1,724
040	10,0	2,26	42,0	0,840	0,025	0,467	1,680	0,743	1,593	25,00	1,346
078+	30,6	2,67	30,5	1,105	0,039	0,439	2,379	0,891	2,027	12,82	1,122
081	34,6	2,45	28,2	1,080	0,038	0,431	2,284	0,932	2,162	12,35	1,073
112	46,3	2,18	22,1	1,094	0,041	0,412	2,475	1,135	2,759	8,93	0,881
162	57,5	1,85	14,1	1,288	0,044	0,332	2,284	1,235	3,722	6,17	0,810
208	71,5	1,56	12,3	0,780	0,055	0,432	2,558	1,640	3,800	4,81	0,610
289	81,0	1,28	7,9	0,430	0,067	0,416	2,283	1,784	4,290	3,46	0,501
347	86,2	1,05	4,8	0,231	0,076	0,348	1,666	1,586	4,561	2,88	0,631

From * Experiment GF-12C-80

\+ Experiment GF-10C-80

TABLE A11 : 200 $g1^{-1}$ FEED CONCENTRATION - ANAEROBIC - STEADY STATE DATA

D	C_s	C_x	C_p	CO_2	Y_{xs}	Y_{ps}	DC_p	DC_p/C_x	SUR	D^{-1}	$(DC_p/C_x)^{-1}$
h^{-1}	$g1^{-1}$	$g1^{-1}$	$g1^{-1}$	$1h^{-1}$			$g1^{-1}h^{-1}$	h^{-1}	$g1^{-1}h^{-1}$	h	h
,013*	73,5	0,87	51,3	0,239	0,007	0,406	0,667	0,767	1,890	76,92	1,304
,020*	82,0	1,45	49,8	0,449	0,012	0,422	0,996	0,687	1,628	50,00	1,456
,037	101,0	1,70	38,3	0,649	0,017	0,387	1,417	0,834	2,155	27,03	1,199
,053	108,0	2,45	36,1	0,965	0,027	0,392	1,913	0,781	1,990	18,87	1,280
,073	110,0	2,70	35,0	1,337	0,030	0,389	2,555	0,946	2,433	13,70	1,057
,101	129,0	2,54	27,1	1,291	0,036	0,382	2,737	1,078	2,823	9,90	0,928
,201	165,0	1,90	14,3	1,295	0,054	0,409	2,874	1,513	3,703	4,98	0,661
,392	189,0	0,80	2,8	0,336	0,073	0,255	1,098	1,372	5,390	2,55	0,729

* From Experiment GF-13C-80, otherwise GF-11C-80.

TABLE A12 : 100 $g1^{-1}$ FEED CONCENTRATION - AEROBIC - STEADY STATE DATA

D	C_s	C_x	C_p	CO_2	Y_{xs}	Y_{ps}	DC_p	DC_p/C_x	SUR	D^{-1}	$(DC_p/C_x)^{-1}$
h^{-1}	$g1^{-1}$	$g1^{-1}$	$g1^{-1}$	$1h^{-1}$			$g1^{-1}h^{-1}$	h^{-1}	$g1^{-1}h^{-1}$	h	h
,042	0,03	11,25	38,9	20,06	0,113	0,389	1,634	0,145	0,373	23,81	6,897
,079	0,06	9,50	41,2	33,41	0,095	0,412	3,255	0,343	0,831	12,66	2,915
,110	4,20	7,30	38,9	20,93	0,076	0,406	4,279	0,586	1,444	9,09	1,706
,112	5,90	7,35	39,5	26,94	0,078	0,420	4,424	0,602	1,434	8,93	1,661
,128	12,40	6,60	37,2	28,54	0,075	0,425	4,762	0,721	1,699	7,81	1,387
,158	25,90	5,80	31,9	28,61	0,078	0,430	5,040	0,869	2,019	6,33	1,151
,193	31,20	4,70	25,7	27,20	0,068	0,374	4,960	1,055	2,825	5,18	0,948
,253	52,70	3,65	20,1	28,55	0,077	0,425	5,085	1,393	3,279	3,95	0,718
,353	69,80	2,78	13,5	25,59	0,092	0,447	4,766	1,714	3,835	2,83	0,583
,466	82,60	1,08	5,1	-	0,062	0,293	2,377	2,201	7,508	2,15	0,454

TABLE A 13 : 100 $g1^{-1}$ FEED CONCENTRATION - ANAEROBIC - STEADY STATE DATA - CYSEWSKI [16]

D	C_s	C_x	C_p	CO_2	Y_{xs}	Y_{ps}	DC_p	DC_p/C_x	SUR	D^{-1}	$(DC_p/C_x)^{-1}$
h^{-1}	$g1^{-1}$	$g1^{-1}$	$g1^{-1}$	$1h^{-1}$			$g1^{-1}h^{-1}$	h^{-1}	$g1^{-1}h^{-1}$	h	h
0,040	27,8	3,07	40,0	-	0,034	0,554	1,600	0,521	0,941	25,00	-
0,119	51,6	2,62	21,1	-	0,054	0,436	2,511	0,958	2,197	8,40	-
0,181	65,6	2,20	15,3	-	0,064	0,445	2,769	1,259	2,830	5,53	-
0,231	73,0	1,96	12,0	-	0,073	0,444	2,772	1,414	3,189	4,33	-
0,295	78,6	1,71	9,6	-	0,080	0,449	2,813	1,645	3,665	3,41	-
0,354	80,0	1,47	8,2	-	0,074	0,410	2,903	1,975	4,826	2,83	-
0,428	88,8	1,17	4,9	-	0,105	0,438	2,097	1,792	4,100	2,34	-
0,441	94,0	0,84	2,6	-	0,140	0,433	1,147	1,365	3,315	2,27	-

TABLE A14 : 100 gl^{-1} FEED CONCENTRATION PLUS 10 mgl^{-1} ERGOSTEROL - STEADY STATE DATA - CYSEWSKI[16]

D	C_s	C_x	C_p	CO_2	Y_{xs}	Y_{ps}	DC_p	DC_p/C_x	SUR	D^{-1}	$(DC_p/C_x)^{-1}$
h^{-1}	gl^{-1}	gl^{-1}	gl^{-1}	lh^{-1}			$gl^{-1}h^{-1}$	h^{-1}	$gl^{-1}h^{-1}$	h	h
0,035	0,5	7,42	47,6	-	0,075	0,478	1,666	0,225	0,469	28,57	4,454
0,075	1,0	8,54	47,6	-	0,086	0,481	3,570	0,418	0,869	13,33	2,392
0,135	18,9	7,14	40,2	-	0,088	0,497	5,427	0,760	1,533	7,41	1,316
0,210	41,6	5,62	28,6	-	0,096	0,490	6,006	1,069	2,182	4,76	0,935
0,310	60,5	4,05	19,5	-	0,103	0,494	6,045	1,493	3,023	3,23	0,670
0,385	72,4	2,97	11,9	-	0,108	0,431	4,582	1,543	3,578	2,60	0,648
0,475	83,2	1,73	7,4	-	0,103	0,440	3,515	2,032	4,613	2,11	0,492

BLE A15 : 20, 90, 180 $g1^{-1}$ FEED CONCENTRATIONS - STEADY STATE DATA - PIRONTI [19]

D	C_s	C_x	C_p	CO_2	Y_{xs}	Y_{ps}	DC_p	DC_p/C_x	SUR	D^{-1}	$(DC_p/C_x)^{-1}$
h^{-1}	$g1^{-1}$	$g1^{-1}$	$g1^{-1}$	$1h^{-1}$			$g1^{-1}h^{-1}$	h^{-1}	$g1^{-1}h^{-1}$	h	h
0,027	0,05	2,60	9,3	-	0,128	0,445	0,251	0,097	0,207	-	-
0,050	0,05	2,83	9,3	-	0,142	0,445	0,465	0,373	0,353	-	-
0,215	0,05	2,61	9,35	-	0,130	0,445	2,01	0,770	1,648	-	-
0,048	0,07	5,90	40,0	-	0,066	0,445	1,900	0,322	0,724	-	-
0,068	2,45	6,15	40,5	-	0,070	0,465	2,754	0,448	0,968	-	-
0,122	34,0	3,46	25,0	-	0,066	0,450	3,050	0,882	1,975	-	-
0,140	36,0	3,51	25,1	-	0,067	0,470	3,570	1,000	2,154	-	-
0,215	64,5	2,18	12,6	-	0,065	0,495	2,709	1,243	2,515	-	-
0,013	9,0	8,16	78,0	-	0,048	0,455	1,014	0,248	0,272	-	-
0,026	26,5	6,65	71,0	-	0,044	0,460	1,846	0,392	0,600	-	-
0,048	67,0	4,15	50.8	-	0,037	0,450	2,413	0,680	1,293	-	-
0,114	154,0	1,77	14,2	-	0,068	0,550	1,619	0,915	1,675	-	-
0,215	176,5	0,28	1,5	-	0,080	0,430	0.322	1,170	2,688	-	-

TABLE A 16 : 9.4 $g1^{-1}$ FEED CONCENTRATION - STEADY STATE DATA - BAZUA AND WILKE [7]

D	C_s	C_x	C_p	CO_2	Y_{xs}	Y_{ps}	DC_p	DC_p/C_x	SUR	D^{-1}	$(DC_p/C_x)^{-1}$
h^{-1}	$g1^{-1}$	$g1^{-1}$	$g1^{-1}$	$1h^{-1}$			$g1^{-1}h^{-1}$	h^{-1}	$g1^{-1}h^{-1}$	h	h
0,072	0,05	1,50	4,75	-	0,160	0,508	0,342	0,228	0,449	13,89	-
0,192	0,23	1,40	4,60	-	0,153	0,502	0,883	0,631	1,258	5,21	-
0,264	0,38	1,27	4,75	-	0,141	0,527	1,254	0,987	1,875	3,79	-
0,270	0,40	1,28	4,75	-	0,142	0,528	1,283	1,002	1,898	3,70	-
0,420	4,50	0,69	3,00	-	0,141	0,612	1,260	1,826	2,983	2,38	-

TABLE A17 : 30 $g1^{-1}$ FEED CONCENTRATION - STEADY STATE DATA - SCHATZMANN [30]

D	C_s	C_x	C_p	CO_2	Y_{xs}	Y_{ps}	DC_p	DC_p/C_x	SUR	D^{-1}	$(DC_p/C_x)^{-1}$
h^{-1}	$g1^{-1}$	$g1^{-1}$	$g1^{-1}$	$1h^{-1}$			$g1^{-1}h^{-1}$	h^{-1}	$g1^{-1}h^{-1}$	h	h
0,030	0,05	2,91	10,04	-	0,097	0,335	0,301	0,104	0,309	33,33	-
0,100	0,10	3,00	10,66	-	0,100	0,357	1,066	0,355	0,997	10,00	-
0,150	0,38	2,93	9,75	-	0,099	0,329	1,463	0,500	1,516	6,67	-
0,230	1,31	2,78	8,80	-	0,097	0,307	2,024	0,759	2,374	4,37	-
0,270	3,00	2,57	8,55	-	0,095	0,317	2,308	0,897	2,837	3,72	-
0,310	8,44	1,91	6,39	-	0,089	0,296	1,979	1,035	3,499	3,22	-
0,320	11,06	1,73	5,77	-	0,091	0,305	1,845	1,070	3,503	3,13	-

APPENDIX C

SENSITIVITY OF THE KINETIC MODEL TO CHANGES IN THE CONSTANTS

MODEL: $$\mu = \hat{\mu} \cdot \frac{C_s}{C_s + K_s} \cdot \frac{K_p}{K_p + C_p}$$

where

$C_p = Y_{ps} (C_{sf} - C_s)$ $g l^{-1}$

$\hat{\mu} = 0,64$ h^{-1}

$K_s = 3,3$ $g l^{-1}$

$K_p = 5,2$ $g l^{-1}$

TABLE A 18: $C_{sf} = 20\ g l^{-1}$, VARIATION OF K_s

C_s ($g l^{-1}$)	K_s - $g l^{-1}$				
	1,65	2,64	3,30	3,96	4,95
1	0,094	0,068	0,058	0,050	0,042
4	0,195	0,166	0,151	0,138	0,123
8	0,266	0,242	0,227	0,215	0,198
13	0,360	0,337	0,323	0,311	0,294
19	0,544	0,519	0,504	0,489	0,469

TABLE A 19: C_{sf} = 20 $g1^{-1}$, VARIATION OF K_p

C_s ($g1^{-1}$)	K_p - $g1^{-1}$				
	2,60	4,16	5,20	6,24	7,80
1	0,036	0,050	0,058	0,064	0,073
4	0,096	0,132	0,151	0,167	0,186
8	0,152	0,202	0,227	0,248	0,273
13	0,237	0,296	0,323	0,344	0,368
19	0,468	0,494	0,504	0,510	0,517

TABLE A 20: C_{sf} = 100 $g1^{-1}$, VARIATION OF K_s

C_s ($g1^{-1}$)	K_s - $g1^{-1}$				
	1,65	2,64	3,30	4,95	6,60
2	0,039	0,030	0,027	0,020	0,016
12	0,068	0,063	0,061	0,055	0,050
48	0,117	0,114	0,113	0,109	0,106
95	0,445	0,441	0,438	0,430	0,423

TABLE A 21: C_{sf} = 100 $g1^{-1}$, VARIATION OF K_p

C_s ($g1^{-1}$)	K_p - $g1^{-1}$				
	2,60	4,16	5,20	6,24	7,80
2	0,014	0,022	0,027	0,031	0,038
12	0,032	0,050	0,061	0,071	0,086
48	0,062	0,094	0,113	0,131	0,155
70	0,103	0,149	0,176	0,199	0,230
95	0,339	0,408	0,438	0,460	0,485

TABLE A 22: C_{sf} = 200 gl^{-1}, VARIATION OF K_s

C_s (gl^{-1})	K_s - (gl^{-1})			
	1,65	3,30	3,96	6,60
10	0,033	0,029	0,027	0,023
40	0,043	0,042	0,041	0,039
120	0,083	0,082	0,081	0,079
190	0,347	0,344	0,343	0,339

TABLE A 23: C_{sf} = 200 gl^{-1}, VARIATION OF K_p

C_s (gl^{-1})	K_p - gl^{-1}				
	2,60	4,16	5,20	6,24	7,80
5	0,012	0,018	0,023	0,027	0,033
20	0,018	0,028	0,035	0,041	0,050
80	0,029	0,046	0,056	0,066	0,081
120	0,044	0,067	0,082	0,096	0,115
160	0,082	0,122	0,146	0,167	0,196
190	0,237	0,309	0,344	0,372	0,406

APPENDIX D

MASS BALANCES

A. OVERALL MASS BALANCE:

An overall mass balance over the fermenter gives

$$\text{Mass in} = \text{Mass out}$$

$$\text{Feed stream} + \text{Base addtn} = \text{Exit stream} + \text{Gas stream}$$

Now the base addition was very minimal compared to the main stream and was therefore neglected

Hence

$$(\text{Vol. flowrate in}) \times SG_{mix} = (\text{Vol flowrate out}) \times SG + \text{Gas exit rate}$$

$$F \times SG_{in} = F \times SG_{out} + (\text{Gas flowrate adj. to STP}) \times \frac{g(g\ \text{mole})^{-1}}{22{,}41\ 1(g\ \text{mole})^{-1}}$$

The specific gravity of the feed and exit streams is dependent on the components of the streams. The controlling components will be the glucose and ethanol concentrations and only these will be considered. The dissolved carbon dioxide in the exit stream will also have a negligible effect.

Using [1] p 3.83

Ethanol Conc.	Density (at 30°C)
0 $g1^{-1}$	0,9957 $g(ml)^{-1}$
20	0,9919
40	0,9884
60	0,9851

$$\therefore \text{Density} = 0{,}9957\ (1 - 1{,}75 \times 10^{-4}\ C_p)\ g(ml)^{-1}$$

From [2] p D-230

Glucose Conc.	SG
20,1 gl^{-1}	1,0076
50,9	1,0193
103,7	1,0393
147,6	1,0559
192,8	1,0729
204,3	1,0772

$$\therefore \quad SG = 1 + (3{,}78 \times 10^{-4} C_s)$$

Now density of water @ 30°C is 995,68 gl^{-1} ([1] p 3.70) so that the density of a solution containing glucose and ethanol is given by

$$\text{Density} = 995{,}68 \left[1 + (3{,}78 \times 10^{-4} \times C_s) - (1{,}75 \times 10^{-4} C_p) \right] gl^{-1}.$$

A Mass Balance for the entry and exit streams is given in Table A 24.

TABLE A24 : OVERALL MASS BALANCE FOR 20 gl^{-1} FEED GLUCOSE CONCENTRATION

D	LIQUID STREAMS FEED	EXIT	CO_2	TOT EXIT	ACCOUNTABILITY
(h^{-1})	$(gl^{-1}h^{-1})$		$(gl^{-1}h^{-1})$	$(gl^{-1}h^{-1})$	%
0,024	24,14	23,92	0,14	24,06	99,7
0,063	63,36	62,79	0,22	63,01	99,4
0,105	105,60	104,72	0,32	105,04	99,5
0,128	128,74	127,72	0,79	128,51	99,8
0,191	192,10	190,74	0,78	191,52	99,7
0,276	277,59	276,63	0,46	277,09	99,8
0,320	321,84	320,82	0,17	320,99	99,7
0,400	402,30	401,62	-	401,62	99,8
0,461	463,65	463,21	-	463,21	99,9
0,497	499,86	499,51	-	499,51	99,9

B: COMPONENT MASS BALANCE:

Consider a carbon balance where the carbon "In" is in the glucose (yeast extract does not contain fermentable carbohydrates [3]) and the carbon "Out" is found in the glucose remaining, the ethanol, carbon dioxide and the yeast. The fraction carbon in each of the compounds is given in Table A25.

TABLE A 25 : CARBON CONTENT OF FERMENTATION PRODUCTS

COMPOUND	FORMULA	C FRACTION
Glucose	$C_6H_{12}O_6$	0,4
Ethanol	C_2H_5OH	0,5217
Carbon Dioxide	CO_2	0,2727
Yeast	$C_6H_{10}NO_3$	0,5

For any compound, "carbon flow" is given by

(conc. of compound) x (dilution rate) x (C fraction)

For the carbon dioxide, the excess flow in the extra gas volume of the exit stream must also be included (see Appendix J for the pumping capacities as a function of the tube size on the peristaltic pumps).

$\therefore$ total CO_2 flow = flow registered on the gas meter
+ excess pumping flow
+ CO_2 dissolved in the exit liquid
($1{,}257\ g\,l^{-1}$ at $30^{\circ}C$ [1] p3.92)

The carbon balances for the three feed concentrations (anaerobic) are given in Tables A26 to A28.

ETHANOL (E) LOSS IN VAPOUR:

@ $30^{\circ}C$, vapour pressure of ethanol, P_E = 80 mm Hg

by Raoult's Law $P_E^* = P_E$. (mole fraction ethanol in broth)

$= 80 \times x_E$

Now x_E = (E conc in broth) $\frac{g}{1} \times \frac{1 \text{ mole E}}{46\ g\ E} \times \frac{18\ g\ H_2O}{1 \text{ mole } H_2O} \times \frac{1\ l\ H_2O}{995{,}7\ g\ H_2O}$

$= C_p \times 0{,}0004$

hence Y_E = mole fraction ethanol in vapour
= PE*/760 mm Hg
= $x_E \times 0{,}00004$

For the ethanol concentrations encountered here, the loss in ethanol is very small.

TABLE A26 : CARBON BALANCE FOR 20 $g l^{-1}$ GLUCOSE FEED CONCENTRATION (ANAEROBIC)

D (h^{-1})	C 'IN' Glucose ($g l^{-1} h^{-1}$)	C 'OUT' ($g l^{-1} h^{-1}$)						OUT/IN (%)
		Glucose	Yeast	Ethanol	CO_2	total	Ethanol/CO_2	
0,024	0,1920	0,0008	0,0170	0,1177	0,0450	0,1805	2,62	94,0
0,063	0,5040	0,0045	0,0403	0,2992	0,0821	0,4261	3,64	84,5
0,105	0,8400	0,0496	0,0620	0,4191	0,1223	0,6530	3,43	77,7
0,128	1,0240	0,1178	0,0826	0,4862	0,2586	0,9452	1,88	92,3
0,191	1,5280	0,5860	0,1089	0,5660	0,2780	1,5389	2,04	100,7
0,276	2,2080	1,3368	0,1118	0,4896	0,2214	2,1596	2,21	97,8
0,320	2,5600	1,6512	0,1136	0,4625	0,1562	2,3835	2,96	93,1
0,400	3,2000	2,6080	0,0900	0,3485	0,1373	3,1838	2,54	99,5
0,461	3,6880	3,3008	0,0622	0,2117	0,1136	3,6883	1,86	100,0
0,497	3,9760	3,6778	0,0497	0,1763	0,0874	3,9912	2,02	100,4

TABLE A27 : CARBON BALANCE FOR 100 $g1^{-1}$ GLUCOSE FEED CONCENTRATION (ANAEROBIC)

D (h^{-1})	C 'IN' Glucose ($g1^{-1}h^{-1}$)	C 'OUT' ($g1^{-1}h^{-1}$)						$\frac{OUT}{IN}$ (%)
		Glucose	Yeast	Ethanol	CO_2	total	$\frac{Ethanol}{CO_2}$	
0,020	0,800	0,010	0,019	0,472	0,192	0,693	2,46	86,6
0,040	1,600	0,160	0,045	0,877	0,438	1,520	2,00	95,0
0,078	3,120	0,955	0,104	1,242	0,586	2,887	2,20	92,5
0,081	3,240	1,121	0,099	1,192	0,574	2,986	2,08	92,2
0,112	4,480	2,074	0,122	1,292	0,591	4,079	2,19	91,0
0,162	6,480	3,726	0,155	1,192	0,707	5,775	1,69	89,1
0,208	8,320	5,949	0,162	1,335	0,465	7,911	2,87	95,1
0,289	11,560	9,634	0,185	1,192	0,312	11,323	3,82	97,9
0,347	13,880	11,965	0,182	0,869	0,236	13,252	3,68	95,5

TABLE A 28 : CARBON BALANCE FOR 200 $g l^{-1}$ FEED GLUCOSE CONCENTRATION (ANAEROBIC)

D (h^{-1})	C 'IN' Glucose ($g l^{-1} h^{-1}$)	C 'OUT' ($g l^{-1} h^{-1}$)						
		Glucose	Yeast	Ethanol	CO_2	Total	$\frac{\text{Ethanol}}{CO_2}$	$\frac{\text{OUT}}{\text{IN}}$ (%)
0,013	1,040	0,382	0,005	0,348	0,125	0,860	2,78	82,7
0,020	1,600	0,656	0,015	0,520	0,234	1,435	2,22	89,7
0,037	2,960	1,495	0,031	0,740	0,341	2,607	2,17	88,1
0,053	4,240	2,290	0,065	0,999	0,503	3,857	1,99	91,0
0,073	5,840	3,212	0,099	1,334	0,700	5,345	1,91	91,5
0,101	8,080	5,212	0,128	1,429	0,687	7,456	2,08	92,3
0,201	16,080	13,266	0,191	1,500	0,723	15,680	2,07	97,5
0,392	31,360	29,635	0,157	0,573	0,304	30,669	1,88	97,8

APPENDIX E:

CELL MASS CALIBRATION CURVE

The cell mass calibration data determined below was used for all the experiments. The broth was obtained from the effluent of experiment GF-10C-80. Dry weight determinations from various steady states during different experiments are also shown, see Figure A.

Experimental Procedure:

(a) Dry three millipore, 0,45μ, filter papers at 105°C for 24 hours.

(b) Cool to room temperature in a dessicator and weigh.

(c) Filter a known amount, 25 ml, of the cell solution through each filter.

(d) Redry at 105°C and 24 hours, cool and reweigh.

(e) Prepare serial dilutions of the cell solution and read the transmittance of each at 580 nm on a Beckman Photometer 1211.

Results: TABLE A29

Dilution	% Transmittance Reading			Avge	Concentration* mg/l
0,0100	75,0	75,0		75,0	41,3
0,0125	69,5	69,3	69,4	69,4	51,7
0,015	66,0	66,3		66,2	62,0
0,020	56,3	56,7		56,5	82,7
0,025	50,8	51,4		51,1	103,4
0,030	47,4	46,3	46,8	46,8	124,0
0,040	38,3	38,0		38,2	165,4
0,050	28,4	28,3		28,4	206,8

* Calculated from an initial solution of cell mass concentration of 0,1034 g $(25\ ml)^{-1}$ or 4,136 mg ml^{-1}.

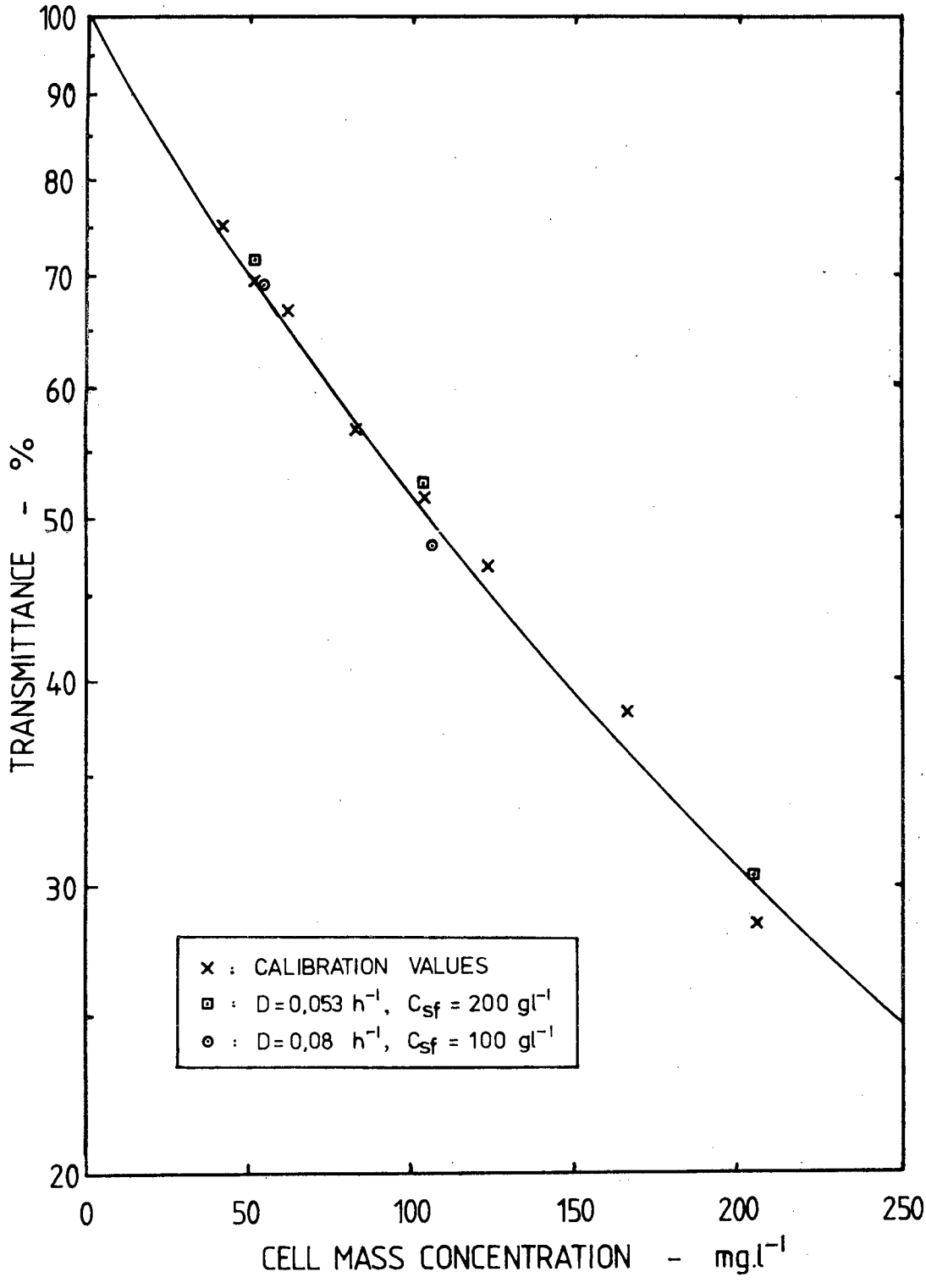

FIGURE E1: CELL MASS CALIBRATION CURVE.

APPENDIX F

TABLE A 30 : INORGANIC CONTENT OF YEAST EXTRACT [4]

ELEMENT	RANGE OF 5 BATCHES (µg/g dry wt)	MEAN
Al	2,1 - 3,8	3,1
Ba	1,0 - 1,7	1,3
Cd	1,2 - 2,0	1,5
Co	1,0 - 6,1	3,5
Cr	9,4 - 17,4	12,0
Cu	41,6 - 101,0	71,3
Fe	121 - 185	150
Ga	0,01 - 0,20	0,09
Mg	980 - 1580	1270
Mn	1,4 - 3,2	2,3
Mo	2,6 - 9,1	5,9
Ni	6,3 - 32,9	18,2
Pb	2,6 - 12,0	6,8
Sn	0,03 - 0,18	0,09
Sr	0,84 - 1,4	1,1
Ti	1,4 - 4,8	3,0
V	31,2 - 66,1	43,7
Zn	46,2 - 104,0	74,0
Ash		12,87%

APPENDIX G:

TABLE A 31: ANALYSES OF 'TAP' WATER

COMPONENT ION	CONCENTRATION - ppm	
	SEPT '79	JULY '80
Chloride	15,5	18,8
Hydrogen	0	
Sodium	8,7	12,0
Magnesium	1,3	1,5
Calcium	17,6	18,0
Nitrate	0	
Ammonia	1,8	0,0
Sulphate	14,8	
COD	5,6	

APPENDIX H:

SUBSTRATE CONCENTRATION, C_s, AS FUNCTION OF THE DILUTION RATE, D

$$\mu = \hat{\mu} \cdot \frac{C_s}{K_s + C_s} \cdot \frac{K_p}{K_p + C_p}$$

replacing $\mu = D$

and $C_p = Y_{ps} (C_{sf} - C_s)$

substituting

$$D = \hat{\mu} \cdot \frac{C_s}{C_s + K_s} \cdot \frac{K_p}{K_p + Y_{ps} (C_{sf} - C_s)}$$

$$\hat{\mu} K_p C_s = D(C_s + K_s) [K_p + Y_{ps}(C_{sf} - C_s)]$$

$$= D[C_s K_p + C_s Y_{ps} C_{sf} - C_s^2 Y_{ps} + K_s K_p + Y_{ps} K_s C_{sf} - K_s Y_{ps} C_s]$$

$$\frac{\hat{\mu} K_p}{D} \cdot C_s = C_s(K_p + C_{sf} Y_{ps} - K_s Y_{ps}) + C_s^2(-Y_{ps}) + (K_s K_p + Y_{ps} K_s C_{sf})$$

Rearranging

$$C_s^2 + C_s(K_s - C_{sf} + \frac{K_p}{Y_{ps}} (\frac{\hat{\mu}}{D} - 1)) - (\frac{K_s K_p}{Y_{ps}} + K_s C_{sf}) = 0$$

$$\therefore \quad C_s = \frac{- b \pm \sqrt{4 \text{ a.c.} - b^2}}{2a}$$

where

$a = 1$

$b = (K_s - C_{sf} + (K_p / Y_{ps})(\hat{\mu}/D - 1))$

$c = - (K_s K_p / Y_{ps} + K_s C_{sf})$

APPENDIX I:

ETHANOL INHIBITION MODELS - TAYLOR SERIES EXPANSION [5]

1. $$\frac{K_p}{K_p + C_p} = \frac{1}{1 + C_p/K_p} = (1 + C_p/K_p)^{-1}$$

$$= 1 + (-1)\frac{C_p}{K_p} + \frac{(-1)(-2)}{2!}\left(\frac{C_p}{K_p}\right)^2 + \ldots$$

$$\simeq 1 - (1/K_p) \cdot C_p$$

2. $$e^{-kC_p} = 1 - kC_p + \frac{(kC_p)^2}{2!} - \ldots$$

$$\simeq 1 - (k).C_p$$

3. $$1 - \frac{C_p}{C_{pm}} = (1 - C_p/C_{pm})^1 = 1 - 1\left(\frac{C_p}{C_{pm}}\right)^1 + \frac{1.0.}{2!}\left(\frac{C_p}{C_{pm}}\right)^2 \ldots$$

$$= 1 - \left(\frac{1}{C_{pm}}\right) \cdot C_p$$

4. $$(1-a(C_p-b)) = (1+ba) - aC_p$$

$$= 1 - \left(\frac{a}{1+a.b}\right) \cdot C_p$$

APPENDIX J:

A. MAGNETIC STIRRER - CALIBRATION

The Gallenkamp magnetic stirrer module was calibrated for the agitation rate by measuring the rotational speed of the magnetic drive unit. Results are presented in TABLE A32.

TABLE A 32: ROTATIONAL SPEED OF MAGNETIC STIRRER MODULE AS A FUNCTION OF THE DIAL SETTING.

DIAL SETTING	MAGNETIC DRIVE - rpm
2	100
3	290
4	475
5	680
6	890
8	1370
9	1665

B. PUMPING RATIO AS A FUNCTION OF TUBE SIZE

Four different sizes of thin-walled, silicone tubing were used in conjunction with the Gallenkamp peristaltic pumping module. One size greater was used on the exit stream. The flow ratios are given in Table A 33.

TABLE A.33 PUMPING RATIO AS A FUNCTION OF THE TUBE SIZE.

TUBE SIZES		PUMPING RATIO
TUBE NO.	TUBE ID	
1	2 mm	] 2,8
2	3 mm	] 1,7
3	4 mm	] 1,5
4	5 mm	

APPENDIX K:

REFERENCES

1. Perry J.H., Editor "Chemical Engineers' Handbook", 4th Edition McGraw-Hill (1963).
2. Weast R.C., Editor "CRC Handbook of Chemistry and Physics", 58th Edition, CRC Press Inc. (1978).
3. Handbook of Microbiology - Merck Publishers.
4. Grant G.L. and Pramer D., "Minor Element Composition of Yeast Extract" J. Bacteriol., 84, 869-870 (1962).
5. Protter M.H., Morrey Jr., C.B. "Modern Mathematical Analysis", Addison-Wesley Publishing Co. Inc., (1969).